HAWASSA UNIVERSITY

INSTITUTE OF TECHNOLOGY

FACULTY OF ELECTRICAL ENGINEERING

DEPARMENT OF ELECTRICAL AND COMPUTER

ENGINEERING

Comparative Analysis and Calibration of Empirical Path loss models at 1800 and 2100 MHz frequency Bands for Hawassa City

By: Robel Getachew

Advisor: Yihenew Wondie (PhD)

Co-Advisor: Tamirat Yenealem (MSC)

Thesis Submitted to the Department of Electrical and Computer Engineering, in

Partial Fulfillment of the requirements for the Degree of Masters of Science in

Communication Engineering and Networking

September, 2021

Hawassa, Ethiopia

HAWASSA UNIVERSITY

INSTITUTE OF TECHNOLOGY

FACULTY OF ELECTRICAL ENGINEERING

DEPARMENT OF ELECTRICAL AND COMPUTER ENGINEERING

Comparative Analysis and Calibration of Empirical Path loss models at 1800 and 2100 MHz frequency Bands for Hawassa City

By: Robel Getachew

Approval by Board of Examiners

Mr. Samson Alemayehu (MSc.)	_____
Chair Person	Signature

Committee

Dr. Ing. Yihenew Wondie	_____
Advisor	Signature
Mr. Tamirat Yenealem (MSc.)	_____
Co-Advisor	Signature
Mr. Bayisa Fufa (MSc.)	_____
Internal Examiner	Signature
Dr. Muluneh	_____
External Examiner	Signature

Acknowledgment

First of all, I would like to praise GOD Almighty who gave me the opportunity and guidance to achieve my goal and to be successful in this part of my life's journey so far.

Then, I could not express my adequate thanks to my advisor Dr. Yihenew Wondie for his unreserved support, invaluable comments, corrections and encouragement and to my co-advisor Mr. Tamirat Yenealem, for his meaningful and constructive feedbacks, and unreserved support. Their advice and help were absolutely invaluable for the successful completion of this thesis. I also would like to thank Mr. Fitsum Zerfu for his help and support in completion of this thesis.

To my caring, loving, and supportive wife, Melat Alemayehu: my deepest gratitude. Your encouragement when the times got rough are much appreciated and duly noted. It was a great comfort and relief to know that you were willing to provide management of our household activities while I completed my work. My heartfelt thanks.

Finally, the completion of this project could not have been accomplished without the support of my Family members, classmates, coworkers and everybody who supported and encouraged me through this journey.

Declaration

I hereby declare that this M.Sc. this thesis is my original work and has not yet been submitted for a degree in Hawassa University and other institution, and all sources of materials used for the thesis have been duly acknowledged.

Robel Getachew	_____
Name	Signature

This thesis has been submitted for examination with my approval as an advisor.

Dr. Ing. Yihenew Wondie	_____
Advisor	Signature

Mr. Tamirat Yenealem (MSc).	_____
Co-Advisor	Signature

Date of Submission: __/__/2021

Place: Hawassa University, Hawassa Ethiopia

Abstract

Due to recent years' fast development of mobile communication technologies, the demand for high capacity network and excellent quality of service with thorough coverage has become essential. And the basic criteria in planning this type of network is the concept of Path loss. Path loss models estimates the average path loss a signal encounter at a certain distance from a transmitter. But, each kind of path loss propagation model intended to forecast path loss in a specific environment which might be wrong in another environment. Incorrect propagation model might cause low data throughput, poor coverage, poor quality of service, high investment cost and call drops which is clearly being observed in Hawassa City. Therefore, one of the root cause of these problems is the usage of un-calibrated path loss model during the network planning stage.

This thesis presents a comparative study of five empirical path loss models according to the measured data collected from selected sites in Hawassa city at 1800 and 2100 MHz frequency bands. The preferred five models for investigation are COST- 231, ECC-33, Hata, SUI, and Ericsson model. A drive test approach was used for data collection and Nemo Handy and Nemo Outdoor were used as measuring a tools for the test. And the measured data were analyzed and extracted to suitable excel form for further analysis using ACTIX analyzer. Error measuring tools such as RMSE, Standard Deviation (SD), Mean Absolute Percentage Error (MAPE), and Mean Absolute Error (MAE) were used to evaluate the closeness of actual measured path loss with the path loss calculated from the listed empirical models in all area types. Then the best suited models were statistically calibrated using the Least Square algorithm to enhance the estimation accuracy.

The result shows that, at 1800 Mhz band ECC-33 was the best fit model for Hawassa Urban areas with RMSE of 4.18 and 2.46 before and after calibration respectively whereas Hata was the finest for Sub-urban with RMSE of 7.86 and 5.18 before and after calibration respectively. And at 2100 Mhz band ECC-33 was once again the best fit model for Urban areas with RMSE of 6.15 and 5.28 before and after calibration respectively while Hata model found to be the best model for sub-urban areas with RMSE of 6.11 and 2.86 before and after calibration respectively. Thus, the optimized models are recommended for better deployment and gives an accurate path loss prediction.

Keywords: Path Loss models, Urban, Sub-Urban, RMSE, MAPE, Least Square

Content

List of Tables

List of Figures

Acronyms

2G	Second Generations
3G	Third Generations
3GPP	3rd Generation Partnership Project
4G	Fourth Generations
AP	Access Pont
BCCH	Broadcast control channel
BTS	Base Transceiver Station
BS	Base Station
CDMA	Code Division Multiple Access
COST	Cooperation for Science and Technology
CPE	Customer Peripheral Equipment
dB	Decibel
dBm	Decibel-mill watt
DT	Drive Test
ECC	European communication committee
FDMA	Frequency Division Multiple Access
GSM	Global System for Mobile Communication
Ho	Hand Over
HSPA	High Speed Packet Access
IEEE	Institute of Electrical and Electronics Engineers
IP	Internet Protocol
LOS	Line of sight
LLSM	Linear Least Square method
LTE	Long Term Evolution
MAPE	Mean absolute percentage error
MAE	Mean Absolute Error
MHz	Mega Hertz
MIMO	Multiple Input Multiple Output

MMDS	Multipoint Microwave Distribution System
MRSP	Measured Received Signal Power
MS	Mobile Station
NLOS	None line of sight
PL	Path Loss
PSC	Pilot Scrambling Code
QoE	Quality of Experience
QoS	Quality of Service
RAN	Radio Access Network
RF	Radio Frequency
RMSE	Root mean square error
RSSL	Received Signal Strength Level
Rx	Receiver
SD	Standard Deviation
TCO	Total cost of ownership
Tx	Transmitter
UE	User Equipment
UMTS	Universal Mobile Telecommunications System
VHF	Very High Frequency
VoIP	Voice over IP
VoLTE	Voice over Long-Term Evolution
WCDMA	Wideband Code Division Multiple Access

Chapter One

1. Introduction

All wireless communications mainly involve transmission of data in the form of electromagnetic (EM) waves. And the transmitted data experiences a path loss when the electromagnetic wave travels from the transmitter to the receiver. Path loss refers to electromagnetic wave power density reduction (attenuation) or degradation in its signal strength as it travels between transmitter and receiver [1]. Radio wave propagation, particularly in urban environment, is a complex scenario since diffracted and reflected waves which are caused by multipath propagation are included. In general, radio wave propagation can be seen as three different main modes:

(a) Reflection: It's when a radio wave propagation in one medium impinges on a different medium with dissimilar electromagnetics characteristics. After the Collison, some portion of the radio wave energy could be absorbed or transmitted through the reflecting medium causing some kind of attenuated reflected wave [3].

(b) Diffraction: Occurs when a radio wave passing through two different mediums or through a gradual variation in a medium alters its direction to bend or diverge in the neighborhood of obstacles [3].

(c) Scattering: It occurs when radio a wave hits an irregular surface or a body having a size much smaller relative to the signal wave length [3].

Besides the above main characteristics of radio waves; Terrain contours, environment (rural or urban, foliage and vegetation), propagation medium (moist air or dry), and the location and height of antennas also influence the path loss [4]. Signal strength degradations like this will cause call drop and other cellular network quality of service degradation.

Hence, we can say that path loss forecasting is a significant element in the designing phase of any communication system. A reliable propagation model is a model which can estimate the path loss with minimum standard deviation. And to achieve that the proper models should be selected for path loss, field strength and other parameters measurements. A precise and reliable forecasting methods helps for coverage area and transmitter power optimization, realization of highest quality of service

and eliminating interference problems of another radio transmitter as well. This will help planners and network engineers to improve the coverage area and to apply the accurate transmitted power.

As we know Cities have the most changing environment because of fast increasing of a high rising and highly dense buildings. Besides, cities also have different environment types (i.e. morphology types) across its region. Hence, propagation models tuned to each environment type should be considered when planning cellular networks.

Therefore, numerous path loss models which can estimate path losses that could be encountered by wireless signal propagation at different frequencies and landscapes have been developed and used. And this path loss models are categorized in 3 groups, which are empirical models, deterministic models and non-deterministic models [10]. Empirical models like Hata model and Okumura model uses measurement data and statistical properties. Semi-deterministic models like Cost-231 are based upon empirical model and deterministic aspects. Whereas, Deterministic models are site-specific and need large number of the city's geometrical information.

Because of their simplicity, the Wireless communication industry have been using empirical models intensively which has made them most popular [13]. Nevertheless, the original empirical model parameters have to be tuned or adjusted to reduce the estimation error when they are deployed in some other terrain than the one they were developed.

In the case of Hawassa city, Although the network is designed to have a full coverage in the city, it is not difficult to observe that there are areas with almost null coverage. That is why Coverage problems are issues in Hawassa that demand daily focus. This problem is caused because of the fact that coverage planning was not done with an appropriate path loss model for the terrain, environmental aspects (buildings, foliage and vegetation) and propagation medium (moist air or dry) of Hawassa city.

Therefore, it is necessary to find the best path loss model that fit Hawassa city's terrain, environmental aspects and propagation medium and calibrate it by using the actual measured path loss data as an input. And this would benefit Ethio-telecom by saving of an investment cost and delivering quality of service. Hence, this thesis focuses on selecting the right propagation model and calibrate it based on the measurement data taken from some selected sites in different areas of Hawassa.

1.1 Statement of the Problem

Coverage planning is one of the key tasks in network dimensioning. And the reliability of radio network planning for optimum network coverage principally depends upon the precision of the path loss prediction models implemented for the network planning. This indicates the non-linear correlation between the Received Signal Strength Level (RSSL) and the distant between the mobile station and the BTS, while the essential radio network parameters provided. Ethio-Telecom used the original (un calibrated) COST-231 model to make coverage planning for both GSM and WCDMA networks in Hawassa City. Because this original model is not calibrated for the specific nature of Hawassa, it is one of the root causes for the coverage problems, poor quality of services and poor quality of experiences in both GSM and WCDMA networks with many other factors. Therefore, since a propagation model goals to characterize some parameters which varies with the environment at hand and their property might alter according to the system that models will be applied for, the existing path prediction model has to be calibrated to accurately fit the actual measurements collected over the part of the network already deployed. This process aims to improve the degree of precision of the model so that it could represent the actual signal propagation behavior of Hawassa city. This can as well save investment cost beside solving the problems stated above.

1.2 Objective

This thesis aims to achieve the following general and specific objectives.

1.2.1 General Objective

The general objective of the thesis is to compare COST- 231, ECC-33, Hata, SUI, and Ericsson models for different selected areas of Hawassa city at 1800 and 2100 MHz and calibrate the best performing models so that they could fit the city terrain, propagation medium and environmental aspect.

1.2.2 Specific Objective

The specific objectives of the thesis are listed below:

- Find the best theoretical propagation models for 900, 1800 and 2100 MHz frequency bands from the selected five propagation models.
- Calculate the actual path loss of Awassa city using the measured signal strength data of the selected sites.
- Examine the performance of the models using Root Mean Square Error (RMSE), Mean Absolute Error (MAE), Standard Deviation (SD), and Mean Absolute Percentage Error (MAPE).
- Calibrate the models for all morphological areas and evaluate their performance.
- Propose the calibrated model that best fit Hawassa's terrain, propagation medium and environmental aspects.

1.3 Methodology

As mentioned in the objective section of this thesis the aim of the thesis is to compare different path loss models for different selected areas of Hawassa city and calibrate the best performing models so that they could fit the city terrain, propagation medium and environmental aspect. And to accomplish the objective the thesis was divided in different phases and different procedures were used in each phase.

The first phase was pre-planning and preparation. In this phase detailed information was collected about the existing cellular coverage and network quality of Hawassa city, Sites distribution, path loss model and cellular network planning parameters. And with this information different works written on path loss model comparison and optimization were reviewed.

The Second phase of the thesis was Site Selection and data collection. Site selection was one of the crucial parts of the thesis so sites which represent all types of environment, building distribution and population density were chosen. And then measurement data were collected from the live network using Drive Test methodology. In this step, a high number of data which would be enough for analysis were collected. Data was collected by drive test using tools such as laptop, mobile equipment, Nemo software (Licensed) and GPS.

The Next phase was data analysis. Here selected sites were classified into different area types and the actual measured path loss data was compared with the path loss calculated from empirical models base on different error measurement tools such as RMSE, Standard Deviation (SD), Mean Absolute Percentage Error (MAPE) and Mean Absolute Error (MAE). In this step MATLAB and excel were used as data analysis and result displaying tools.

The final phase of this thesis was model tuning and result discussion. In the last phase of the thesis the best fit original path loss models were calibrated using LLSM. And the calibrated models path loss values were compared with the original model's and the measured path loss values to show how successful the thesis was.

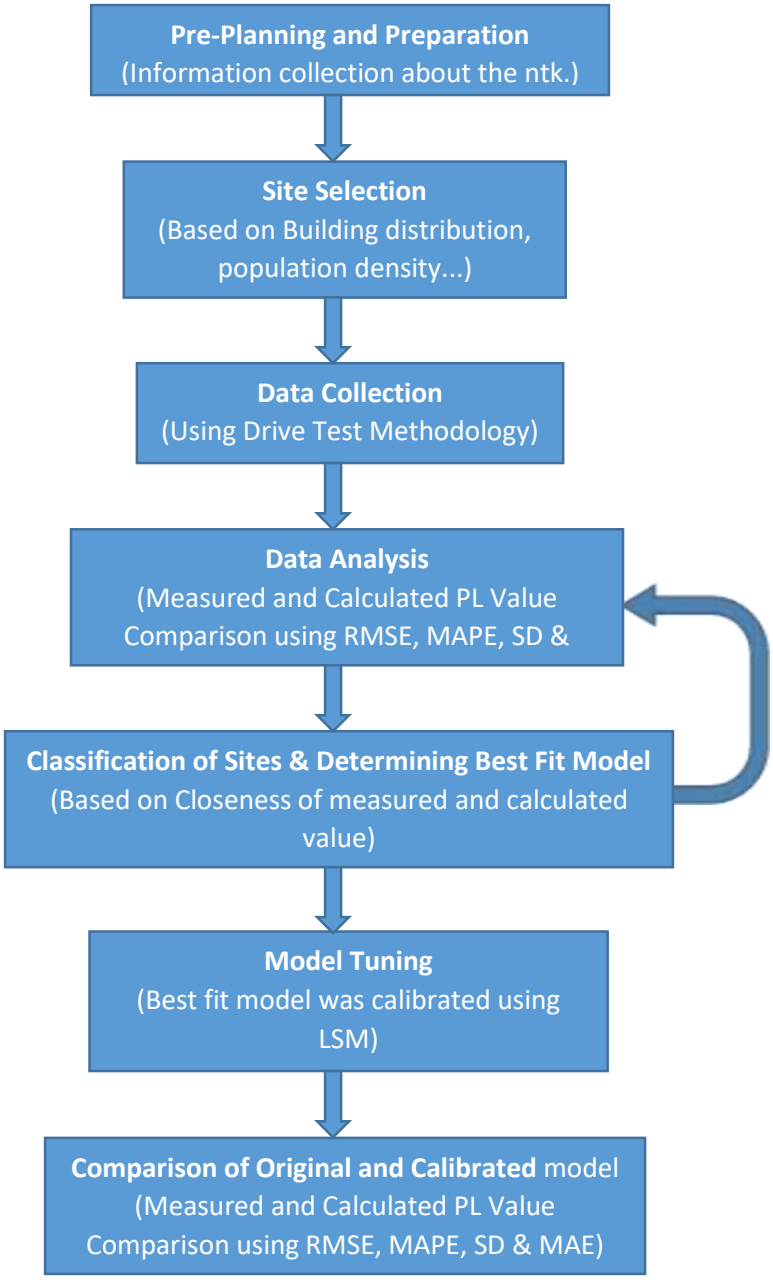

Figure 1.1 Methodology Flow Chart

1.4 Literature Review

There are Several studies which are done in the fields of path loss propagation model where many obtained good results. Many researches tried to choose a certain propagation model and optimize it to fit a specific area. In this thesis some researches which are which are more related to my title were reviewed.

Authors in [4] compared three propagation models; COST 231-Hata, Okumura-Hata, and Egli models by comparing the relative outcomes attained from each models with their Measured Received Signal Power (MRSP). 2100 MHz radio communication RSS was measured in Egbu-Abba Road, Owerri suburban area. And finally, the thesis found COST 231-Hata to give the closest prediction so it was tuned by using Least Square method (LSM). The thesis has considered three propagations models but took measurement data at only 2100 MHZ.

In [5], Okumura, Cost231 and Egli propagation models were studied. The comparison was based upon the original data of each models and field measurements in the frequency range of 400MHz to 1800MHz. The field measurement was conducted in Cyberjaya, Malaysia. The thesis found Cost231 and Egli model to accomplish a better result than Okumura for sub-urban areas of Malaysia. And calibrated model was found to be a best fit to the Malaysia suburban areas, so it was suggested to estimate the signal strength of mobile stations from the base stations.

In [6], Hata model was modified at frequency bands of 900, 1800 and 2100 MHz to match the environment of Tripoli area. Measurements were taken from five area types (Rural, Suburban, Dense Suburban, Urban and Dense Urban). And regression method and neural network approaches were used to edit Hata model parameters so that they could coincide with the real measured RSS figures within an agreeable range of precision. Finally, the calibrated module gives 3.62 to 20.29 dB enhancement in the accuracy of estimating the path loss. In this thesis, even if the authors studied the path loss at 3 different frequency bands, it only considers one path loss model.

In [7], the performance of three path loss models (COST231, SUI and ECC-33) were investigated against field data measurement from the three possible area type (i.e. Urban, Suburban and Open areas) at 1800MHZ and 2100MHZ. The research was done to modify a path loss model that best

fit Addis Ababa city. The Author used RMSE to measure the error between the predicted path loss values and the measured values. And after the analysis, the author concludes COST231 to be the most fitting path loss model for urban and sub urban areas and SUI model for open areas in Addis Ababa at 1800MHZ. While SUI was the best path loss model in all the three morphology types at 2100MHZ band. Generally, in this thesis, the author tries to compare the three path loss models for Addis Ababa city and tune the best model but he only collect data at 1800 and 2100 MHz frequency bands.

In [8], Calibration of COST-231 Hata model was done based upon experiment at 2.3 GHz WiMAX transmission carried out in western India. The authors tried take measurement records from seventeen sites so that they could make accurate predication. In the thesis a linear iterative tuning method was used to adjust the parameter of the COST-231 model. And the path loss estimation of calibrated model were compared versus the theoretical COST-231 Hata model. Finally, the authors have concluded the adjusted model offers high precision and is able to estimate path loss with minimum standard deviation relative to the theoretical COST-231 Hata model.

In [9], different propagation models Hata Model, ECC-33 Model, Cost-231 Model and Ericson Model) were analyzed and compared using the collected data. The author takes measured data from two different sites operating at 800 MHz frequency band using a drive test. Finally results of the comparison concludes that the Hata Model and Ericsson model were better in predicting the urban environments. And in rural environment Hata model generally provides better estimation. In this thesis, even if the comparison of four path loss models was done it only considers measured data from only two sites at only single frequency band.

While [10], forecasts path loss using the following five models, ECC-33 model, Stanford University Interim (SUI) model, COST-231 Hata model, Hata-Okumura model and Ericsson model. In this thesis, received power experimental measurements for 900 MHz GSM system were made in rural, suburban, and urban areas of Dar es Salaam, Tanzania. The authors compared the results of the original models with the measured data from the field. And the results show the ECC-33 model provides better estimation for sub-urban environment. In this thesis, five path loss models were compared but the best performed model was not modified to fit the city and the experiment was done only at 900 MHz frequency band.

In the above listed reviewed and many other thesis, we can see that COST-231, SUI and ECC-33 models showed a best result at different environment types and frequency band. So, we cannot conclude that a particular propagation model is best for all the environment types and for all frequency ranges. Different Propagation models can be best for different environment areas or for the same area with varying morphology types and frequency range. Therefore, it is necessary to perform a research so that we could know which propagation model could fit the environment of Hawassa city and calibrate the model for a good coverage, high data throughput, minimum call drops, good quality of service and low investment cost.

Chapter Two

2. Radio Wave Propagation

Radio propagation is the way radio waves travels from one point (transmitter) to another (receiver) and how the medium of transmission affects them and specifically the way the waves propagate around the Earth in different parts of the atmosphere. And the transmission path in which the wave propagate can be a simple line of site(LOS) where there is only air between the transmitter and the receiver or heavily congested by mountains, foliage, buildings or moving objects. Depending on the barriers the radio wave propagating in the NON line of site medium may exhibit diffraction, reflection and refraction. The resultant radio signal might also be the combination of numerous signals which might have propagated through different paths. These signals might be added together or subtracted from each other, and furthermore the signals propagating through different paths might be delayed resulting resultant signal distortion. This is known as propagation path loss. Hence, it is important to recognize the potential radio propagation characteristics which probably prevails [21].

Thus, Radio propagation is extremely site-specific and it varies depending on the terrain, interference, how fast the mobile device is moving, operating frequency and other dynamic factors [21]. Therefore, accurate classification of the radio channels via basic parameters and mathematical model is essential for the predicting signal coverage, different systems' interference analysis and base station antennas optimal location selection.

As mention above received signal in wireless communication is affected by path loss and fading during the propagation process. And mobile radio propagation creates a small-scale effects and large-scale effects on the received signal. The small-scale propagation effect is when the power strength of received signals varies rapidly in a relatively short distance. It may occur due to multipath or Doppler spread (when the frequency of received signals differs from the frequency of the transmitted signal.). In other hand, Large-scale propagation effect is when the power strength of received signals varies slowly in a relatively longer distance and it occur due to shadowing and path loss. Therefore, Large scale and small scale (fading) propagation effects

should be studied carefully to get a complete picture of the channel in a particular environment [21,22].

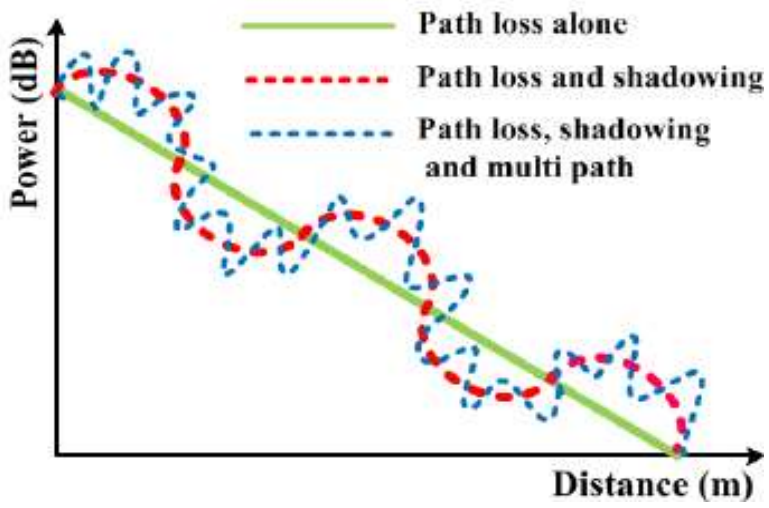

Figure 2.1 Characterization of Path Loss, Multipath and Shadowing versus Distance [25]

2.1 Propagation Mechanisms

Propagation of radio waves in space may go through different physical mechanisms: line-of-sight or free space propagation, scattering, diffraction, reflection and wave guiding. The free space propagation model is the most simple scenario for the propagation of radio signals. Here radio wave travels out of the source where they are radiated by the antenna without encountering any obstacle.

Reflection is the phenomenon which occurs when radio waves encounter transmission medium change and some of them propagates into the new medium whereas the remainder is reflected. For shorter range signals like cellular communication the signals undergo numerous reflections and these multiple reflections may direct the signal reaching to the receiver through several paths. So, radio wave reflections usually rise to multi-path effects. And the multiple reflections and multi-path effects will distort the signal and cause fading [21,22].

Refraction occurs when radio waves impinges upon a sharper and more like a "knife edge" obstacles. As a results wave disturbance will occur which affect the propagation of the radio waves like bending of the path around obstacles or beam divergences. And the radio wave

propagates behind the blockade arriving at the receiver even if there is no LOS. For radio signals the level of a knife edge depend on the frequency and the wavelength of the signal. For instance, low frequency signals may found a mountain ridge sufficiently sharp edge and more rounded hill may not result a noticeable effect.

Scattering is when the energy of the radio wave is dispersed in the propagation medium in several directions after the signal hits an irregular surface or heterogeneities with small dimensions compared to the signal's wavelength [21,22].

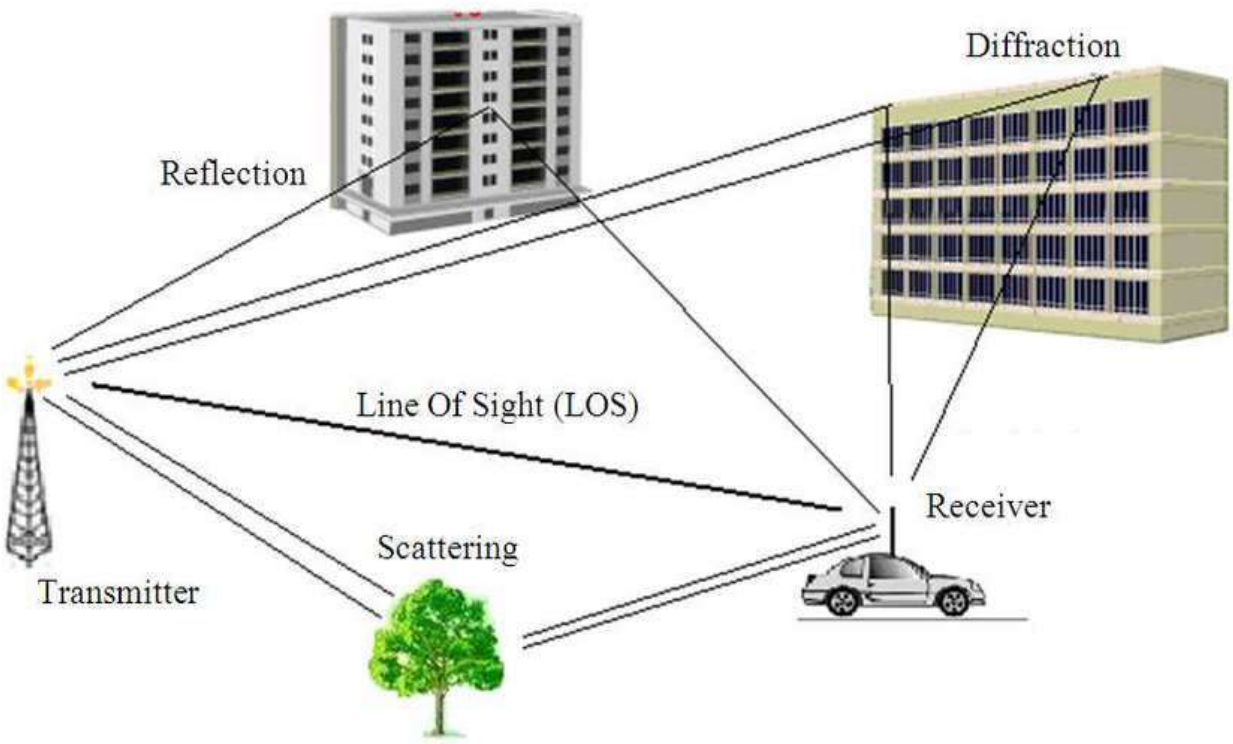

Figure 2.2 Propagation Mechanisms [23]

2.2 Small Scale Effect

Small Scale effect refers to the quick alteration of the amplitude and phase of a radio wave signal in a small period of time (a matter of seconds) or a small distance (few wavelengths). This may be caused when a radio waves hit small objects with sharper edges which make the signal scattered, reflected or absorbed. Beside this small scale effect may occur due to Doppler shift,

multipath propagation and transmission bandwidth of the signal [24]. In a mobile-radio environment, every path has its own time delay, Doppler shift, multipath propagation, and path attenuation which causes a time-varying signal when the mobile changes position. And this makes it suitable for small scale fading. Depending on the correlation between signals parameters (symbol period and bandwidth) and channel parameters (Doppler spread, delay spread, coherence time and coherence bandwidth) small scale fading can have two forms. For example, Flat fading is caused when the channel coherence bandwidth is greater than the signal's bandwidth and delay spread is less than the symbol period Flat fading will arise. And frequency-selective fading results when the reverse case happens. Coherence bandwidth can be defined as the frequency gap over which two frequencies are expected to experience equivalent fading. While, Fast fading is caused when there is a high Doppler spread and when the coherence time is less than symbol period and the channel variations is faster than base band signal variations. Similarly, the reverse case results in slow fading. Coherence time can be defined as the time duration over which impulse response is considered to be not varying [24].

2.3 Large Scale Effect

Large Scale effect is used to describe the average signal-power reduction or path loss because of propagation of radio waves in a larger area. The landscape pattern between the transmitter and receiver impacts large scale effect, and power will also be steadily attenuated over a very long distance (several hundreds or thousands of meters). The measurement of large-scale fading, defined in terms of a mean-path loss (n^{th} -power law) and a log-normally distributed variation about the mean, will help for path loss estimation as a function of distance. And Experiments prove that log-normal distribution obeys the large scale fading [24].

$$f(x) = \frac{1}{\sqrt{2\pi}\sigma x} e^{-(\ln(x)-\mu)^2 / 2\sigma^2} \quad (2.1)$$

The below figure illustrates the received signal strength variance in fast and slow fading over the distance from the transmitter. As shown in the middle graph we can find slow fading or shadowing curve by taking a small segment from the path loss curve and magnifies it. And by taking a small segment from the slow fading curve and examines it in detail we could find the fast fading or short-term fading curve as shown in the first graph.

Large-scale effect can also be briefly defined in the concepts of path loss and shadowing.

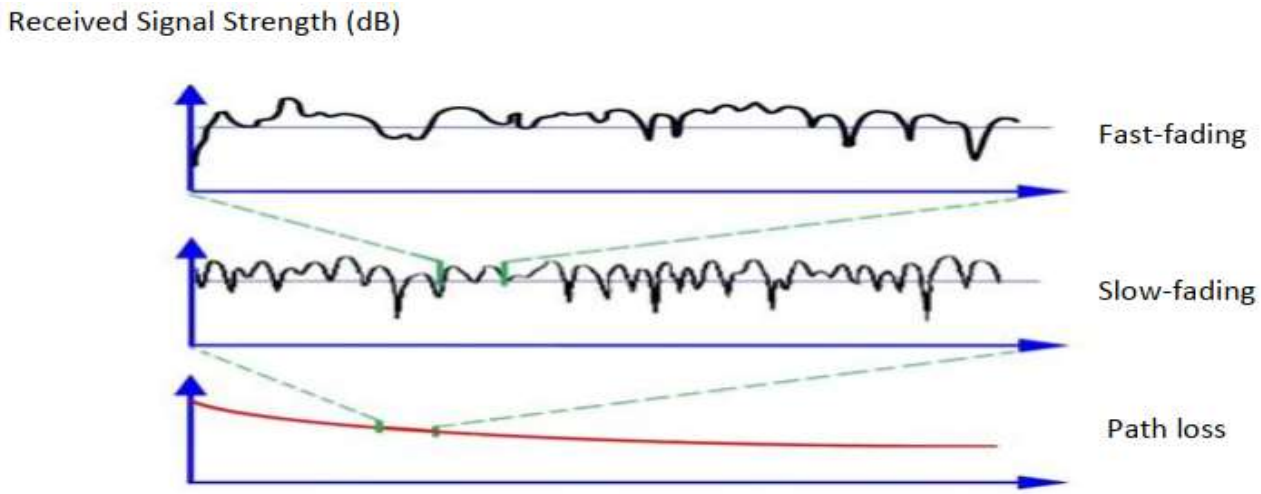

Figure 2.3 Path loss Vs Slow Fading Vs Fast fading characteristics [26]

2.3.2 Path Loss

As described in Large scale effect, path loss is the first type of large scale fading and it is defined as the dissipation of the power which is emitted from the transmitter as the radio wave propagates from source to destination. Path loss can be caused by numerous reasons; like natural expansion of the radio wave, due to obstruction which causes diffraction path-loss or due to the presence of non-transparent medium to electromagnetic waves which causes absorption path loss. As illustrated below Path loss is frequently expressed as a received power $P_r(d)$ as a function of the distance (d) between the transmitter and receiver:

$$P_r(d) \propto \frac{\lambda^2}{4\pi d^2}(P_t) \tag{2.2}$$

Where, $P_r(d)$ is the received signal power, λ is the wavelength, P_t is the transmitted signal power and d is the distance between transmitter and receiver [21].

2.3.3 Shadowing

Shadowing is the other type of large scale effect which refers to the fluctuation or degradation of the received signal power due to large object obstructions like buildings, mountains and vegetation between the transmitter and receiver. This means, the signal variations because of the shadowing mostly originate from reflection and scattering during propagation. Wave lights bending is also another outcome of the shadowing effect, this means the transmission will not follow a straight line. In addition to large-scale fading, sometimes shadowing is also described as the small-scale fading [22] [25].

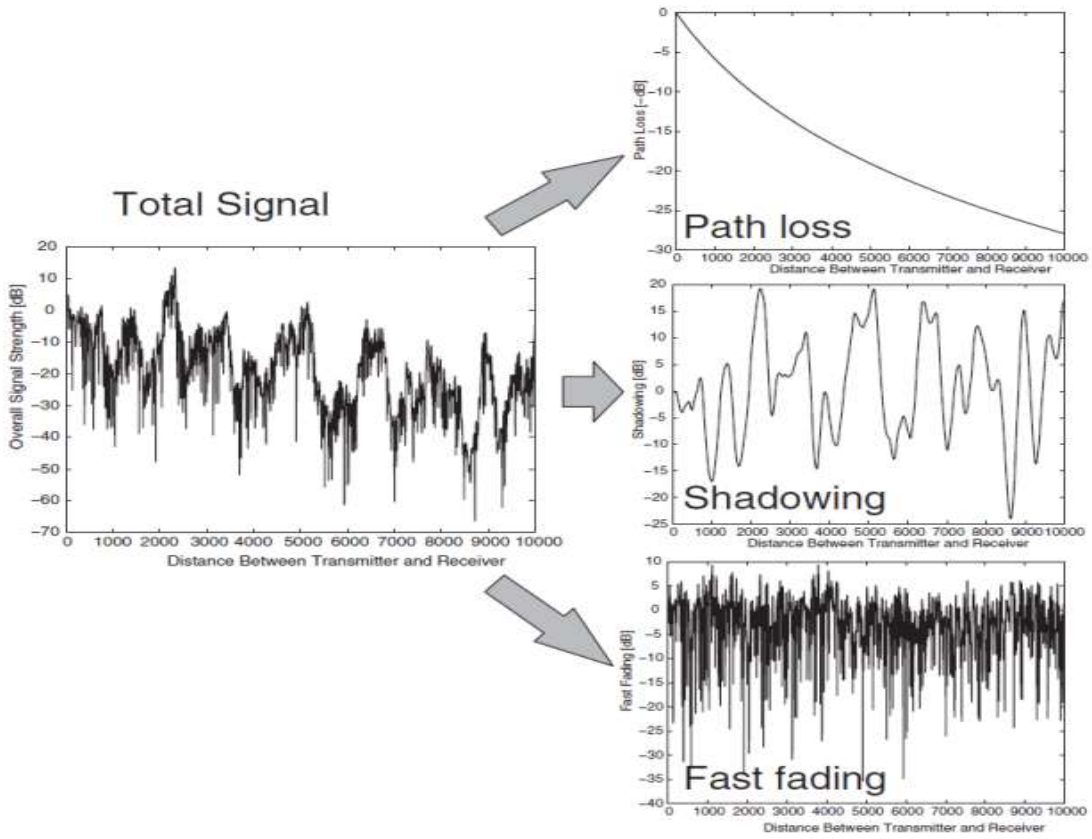

Figure 2.4 Path loss, shadowing and fast fading Characteristics versus distance [22]

Commonly radio coverage is believed to be the most significant measurements to ensure network quality. In GSM network planning, radio coverage planning takes the vital role since it sets coverage area range, mobility, speech quality, and customer satisfaction. Different forms of customer's inputs and limitations in terms of frequency planning, local wireless regulations,

network dimensions, network growth, spectrum availability, and the RF environment itself plays a significant role in coverage planning. The coverage planning approach should also be well described, since it needs to accommodate, several phases of network growth across time without compromising any service quality target. In areas with limited network coverage the coverage planning phase is necessary to find the least possible amount of cell sites with optimal locations which delivers the requested coverage for the target area. Coverage planning is usually performed with forecasting modules on digital map database. Coverage region's, coverage threshold values (outdoor, in-car, indoor), antenna (tower height limitation), preferred antenna line system specification and preferred BTS specifications are the key input information for coverage planning. Activities like propagation modeling, field strength forecasts and measurements are commonly denoted as coverage planning.

Chapter Three

3. Propagation Models

3.1 Cellular Network Coverage Planning processes

Mobile communication has vital role in our daily life. The fast growing mobile technology is enabling us to use it beyond voice application. Data usage, Location applications, financial transactions and many others are emerging in the new mobile communication technology [11]. All these applications are possible if and only if the mobile network is properly designed, implemented and managed. The two key activities in designing a mobile network are capacity planning and coverage planning. The main objective of planning is to minimize Total Cost of Ownership (TCO), maximize coverage, maximize capacity, optimize Handover (HO) zones and minimize power consumption while achieving the maximum quality of service. The planning work is done in three phases: Dimensioning, Detail Planning and Optimization [12]. The main output of dimensioning is to forecast the number of base stations required to cover the required area. The locations and the estimated number of BS stations are determined in the detailed planning. Once the network is deployed and running, adjustments are made in the optimization phase.

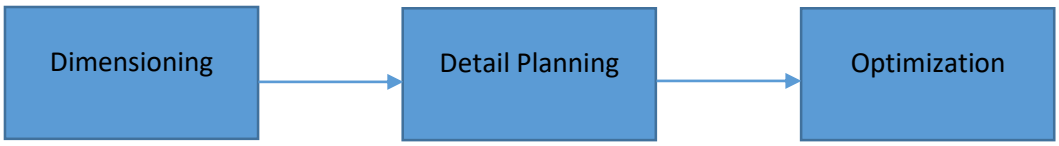

Figure 3.1 The three phases of planning cellular networks [12]

The following steps are followed in detailed planning of cellular networks: Capacity Planning, Coverage Planning and Parameter Planning [11]. The practical processes followed in capacity and coverage planning in different technologies are shown below and they are elaborated further.

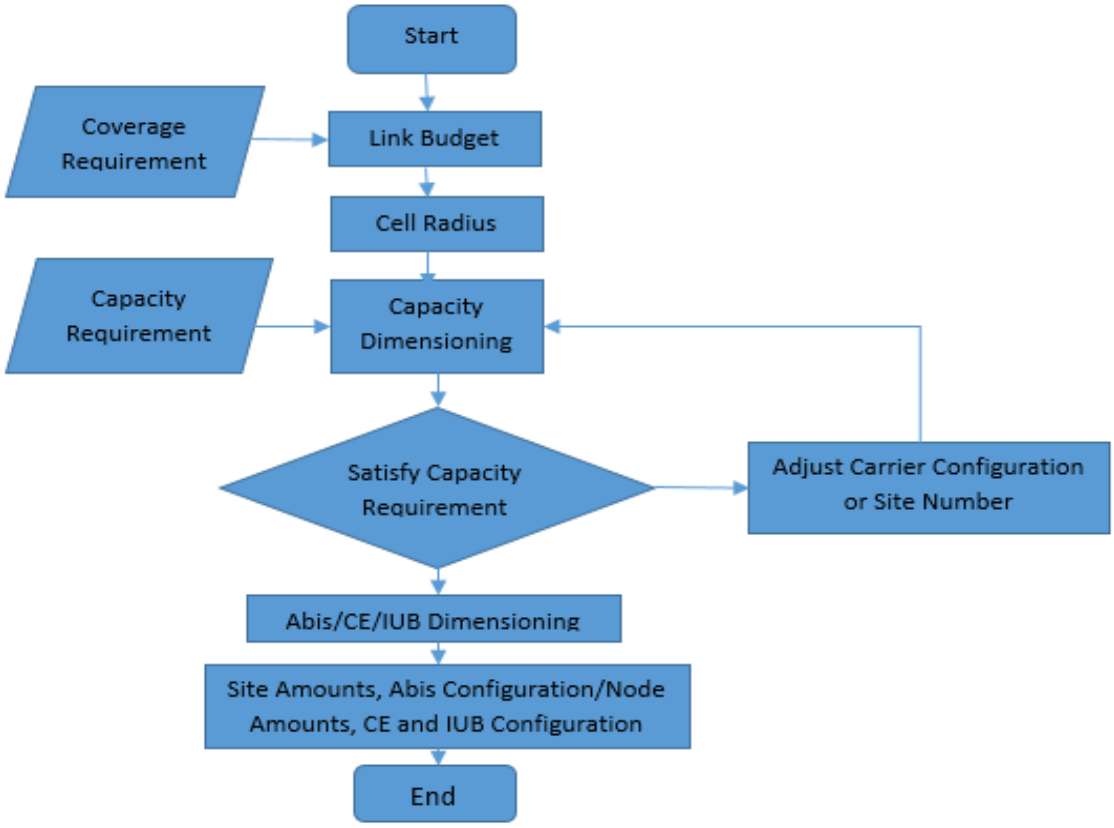

Figure 3.2 GSM and UMTS Planning Process [7]

As shown in the planning process above, link budget is done with the coverage requirement as an input. The coverage requirement is stated as the coverage probability of, for example, 95% which is the total area the radio signal should cover with acceptable signal strength. Link budget is performed to get the cell radius and the distance between sites. The link budget in any cellular technologies is calculated with the formula below. The value of P_{rx} is highly dependent on the value of P_{tx} and P_L. P_{tx} is obtained by measuring the transmitter output signal strength whereas the value of PL is determined with only a best estimation through path loss models. The value of PL at a point obtained from one path loss model is different from the one obtained from the other. This will vary the value of the received signals power (P_{rx}) which will lead to a conclusion that a point which is actually in the acceptable signal strength range to be considered as out of the range or a point which is not actually in the acceptable signal strength range to be considered as in the range. This will either reduce the coverage area of the BS or enlarge the coverage area of the base station beyond the actual one, leading to either incurring higher cost or bad quality of service.

$$P_{rx} = P_{tx} + G_{tx} + G_{rx} - L_{tx} - L_{rx} - PL \quad (3.1)$$

Where,

P_{rx} - the received power (dBm).

P_{tx} - the transmitter output power (dBm).

G_{tx} - the transmitter antenna gains (dBi).

G_{rx} - the receiver antenna gains (dBi).

L_{tx} - cable and other transmitter loss.

L_{rx} - receiver side losses.

PL - Path Loss

3.2 Radio Propagation Path loss Model

Path loss is the reduction in Electromagnetic signal received power when it travels through space. Path loss happens because of many reasons like is diffraction, absorption, reflection, free space path loss, coupling and cable loss, and refraction. And it depends on depends on numerous variables like distant between transmitter and receiver, propagation environments, location and height of antennas. It is calculated by subtracting the transmitted power to the received power as shown in the equation below.

$$PL = P_{tx} - P_{rx} \quad (3.2)$$

In wireless network design stage estimating signal strength in terms of separation distant between receiver and transmitter is the fundamental objective, which affects cellular network cell coverage radius.

In network planning, propagation models are broadly used to study feasibility and in the initial deployment. Similarly, as the deployment proceeds they are helpful to perform interference studies. Generalizing the models to different types of environment, either to specific areas (rural, suburban, and urban), or to a particular cell radius (macro cell, microcell, Pico cell) based on the

environment diversity where mobile communications take place is necessary. Generally, there is a correlation between the models and the type of environment where they are suitable.

The models could be divided into 3 types; empirical, deterministic and semi-empirical [10].

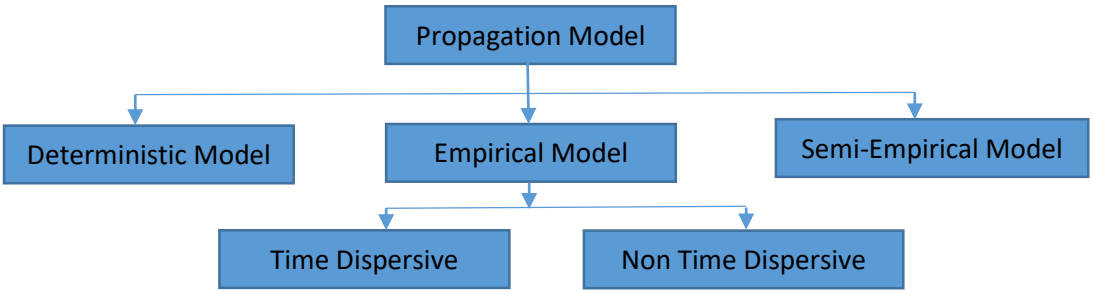

Figure 3.3 Classification of Propagation model [10]

3.2.1 Empirical Models

Empirical path loss models are used to study the main behaviors of system-level theories or to assist a rough prediction of required amount of sites in large areas. These models do not need site-specific terrain data. Their input parameters are effective antenna heights, path loss decay exponents, or average clutter loss factors describing the average propagation environment and the likes [15]. Empirical path loss models are subdivided into time dispersive and non-time dispersive. Time dispersive models are formulated to deliver data related to the time dispersive properties of the channel i.e. the multipath delay spread of the channel whereas non time dispersive models estimates mean path loss from the function as distant, antenna height, and so on. SUI is a best example of time dispersive model whereas Okumura and Hata models are examples for non-time dispersive [16].

3.2.2 Semi-empirical Models

The extensive obtainability of digital terrain data like terrain height, building data, and land use information resulted the development of site-specific propagation model and its inclusion into radio planning tools. They depend on the complete terrain properties which exists along the individual propagation paths between transmitter and receiver. Semi-empirical models are the first site-specific models used for cellular planning tasks. Here the path loss computation is based

upon the combination of empirical models and deterministic approaches. These models use Low Resolution (LR) geographic data. They give realistically good outcomes for the coverage estimation of large macro cell sites even when implemented in urban areas, but because of their limited resolution these models have their limits in estimating. For instance, indoor coverage difficulties in dense urban areas. Okumura-Hata model and its extensions are the commonly used semi-empirical macro-cell path loss models in commercial radio planning tools [15].

3.2.3 Deterministic Models

Deterministic path loss models depend on a terrain description (altitude, building layout, clutter types, building contours, etc.) and accurate terminal locations. And they take advantage of these terrain descriptions to simulate part of the shadow fading, to approximate the effect of propagation physical mechanisms, then provides realistic and correlated spatial variations of the path loss.

Two families of deterministic models are commonly incorporated in the radio-planning tools: vertical-plane (VP) models depend on multiple knife-edge diffraction and they are bi dimensional models that analyze the direct path only whereas ray-based (RB) models compute the lateral multipath contributions and may be bi- or three-dimensional [15].

3.3 Empirical Models

As explained on the above section empirical models are models based on the practical measurement data. Under these model the COST- 231, ECC-33, SUI, Hata, and Ericsson models are discussed respectively.

3.3.1 COST-231 Model

This model is the most extensively used path loss estimating model in mobile wireless system [16]. The model is designed to work in the frequency range of 500 MHz to 2000 MHz, BS antenna height from 30m to 200m and MS antenna height from 1m to 10m. It also contains corrections for rural (flat), sub-urban, and urban environments. Even if the measured data is out of its frequency range, its simplicity and the prepared correction factor has make it broadly used for path loss forecasting at this frequency band.

The main equation of the path loss in dB is [17],

$$PL = 46.3 + 33.9\log_{10} f - 13.82\log_{10} h_b - a_{hm} + (44.9 - 6.55\log_{10} h_b)\log_{10} d + C_m \quad (3.3)$$

where, f is frequency in Mhz, d is the distant between MS and BS in km, and h_b is the MS antenna height above ground level in meter. The parameter C_m is defined as 0 dB for sub-urban or open environment and 3 dB for urban environment.

The parameter a_{hm} for urban environment is given as:

$$a_{hm} = 3.2\,(\log_{10} 11.75h_r)^2 - 4.97 \quad \text{for } f > 400 \text{ MHz} \quad (3.4)$$

And for suburban or rural (flat) environments,

$$a_{hm} = (1.1\log_{10} f - 0.7)h_r - (1.56\log_{10} f - 0.8) \quad (3.5)$$

where, h_r is the BS antenna height above ground level.

The following simulated graphs shows how cost-231 path loss model performs to the variation of different parameters like distance, base station height and frequency.

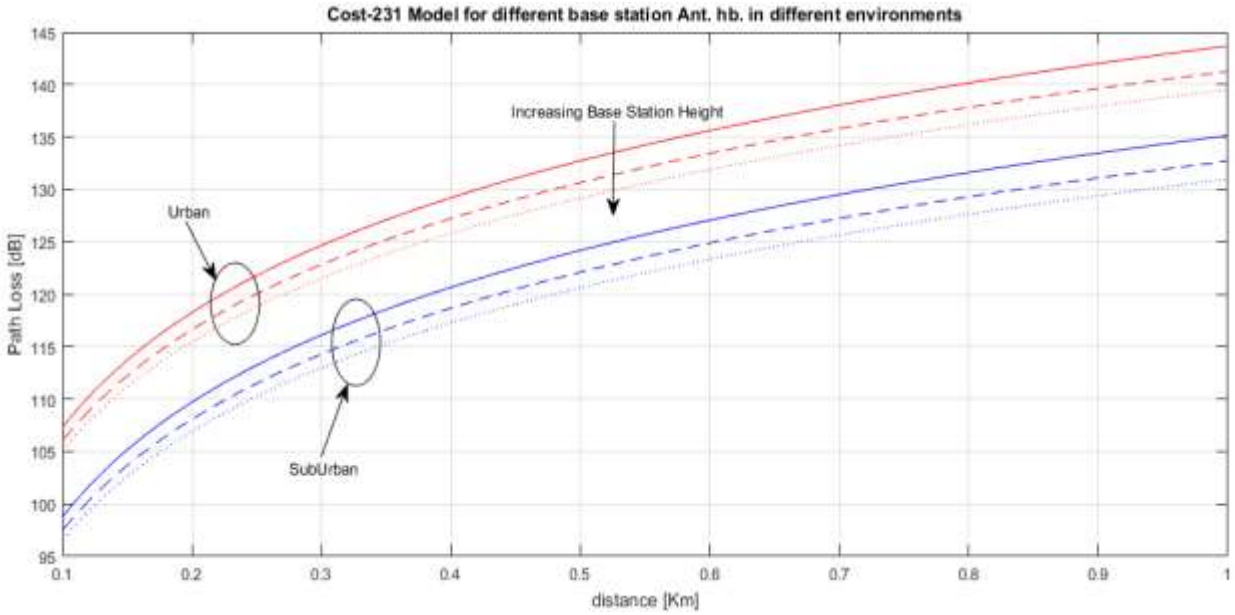

Figure 3.4. Cost-231 model path loss performance with the variation of base station height

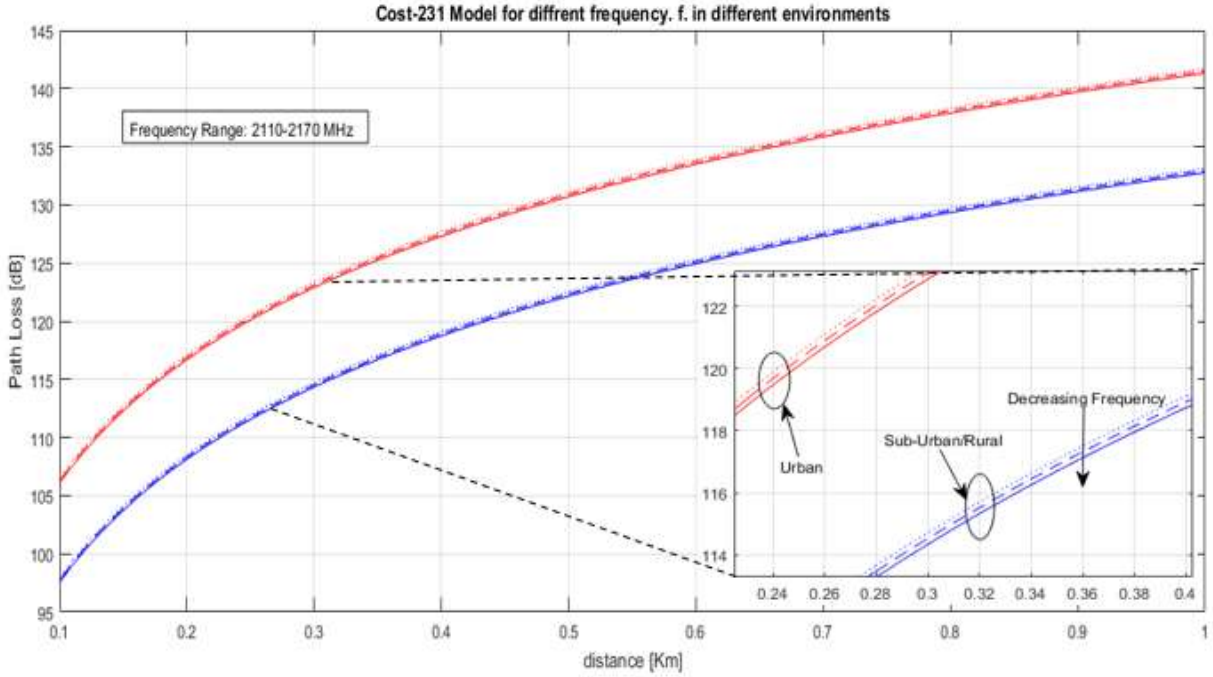

Figure 3.5 Cost-231 model path loss performance with the variation of frequency

The above figures show the characteristics of COST-231 path loss model respect to distance. As shown in both graph the path loss near to the base station in Urban areas is higher than Sub-urban areas. And as expected the path loss also increases as we go further away from the base station.

Figure 3.4 displays how the path loss responds when we vary base station heights in all area types. And as we increase the base station height the path loss decreases. Similarly, figure 3.5 shows the relation between frequency and Cost-231 path loss model where path loss decreases with decreasing operational frequency.

3.3.2 ECC-33 Model

The ECC−33 path loss model is developed by the Electronic Communication (ECC). It was derived out of the original measurement by Okumura and its assumptions were modified [18]. The initial experiments of Okumura model were implemented at the suburban areas of Tokyo. Okumura model divides urban areas into large city and medium city types and gives correction factors to sub-urban and open areas [19]. The ECC−33 path loss model is empirical model formulated from four terms [20] and it defined in dB as:

$$PL = A_{fS} + A_{bm} - G_b - G_r \tag{3.6}$$

where, G_b, A_{fS}, G_r and A_{bm} are BS height gain factor, free space attenuation, the MS height gain factor and, the basic median path loss. They are independently described as [10].

$$A_{fS} = 92.4 + 20\log_{10} d + \log_{10} f \tag{3.7}$$

$$A_{bm} = 20.41 + 9.83\log_{10} d + 7.894\log_{10} f + 9.56[\log_{10} f]^2 \tag{3.8}$$

$$G_b = \log_{10}(\frac{h_b}{200})\{13.958 + 5.8[\log_{10} f]^2\} \tag{3.9}$$

for medium city environments.

$$G_r = [42.57 + 13.7\log_{10} f][\log_{10} h_r - 0.585] \tag{3.10}$$

and for the large city.

$$G_r = 0.759h_r - 1.862 \tag{3.11}$$

where, f is frequency (GHz) , d is the distant between mobile antenna and base station(BS) in km, h_b is height of the BS in meters and h_r is height of the mobile antenna in meters. The medium city model is more applicable for European cities while large city environments must only be

considered for cities with tall building. It is interesting to note that the estimation generated by the ECC-33 model do not lie on straight lines when plotted against distant having a log scale.

The following simulated graphs shows how ECC-33 path loss model performs to the variation of different parameters like distance, base station height and frequency.

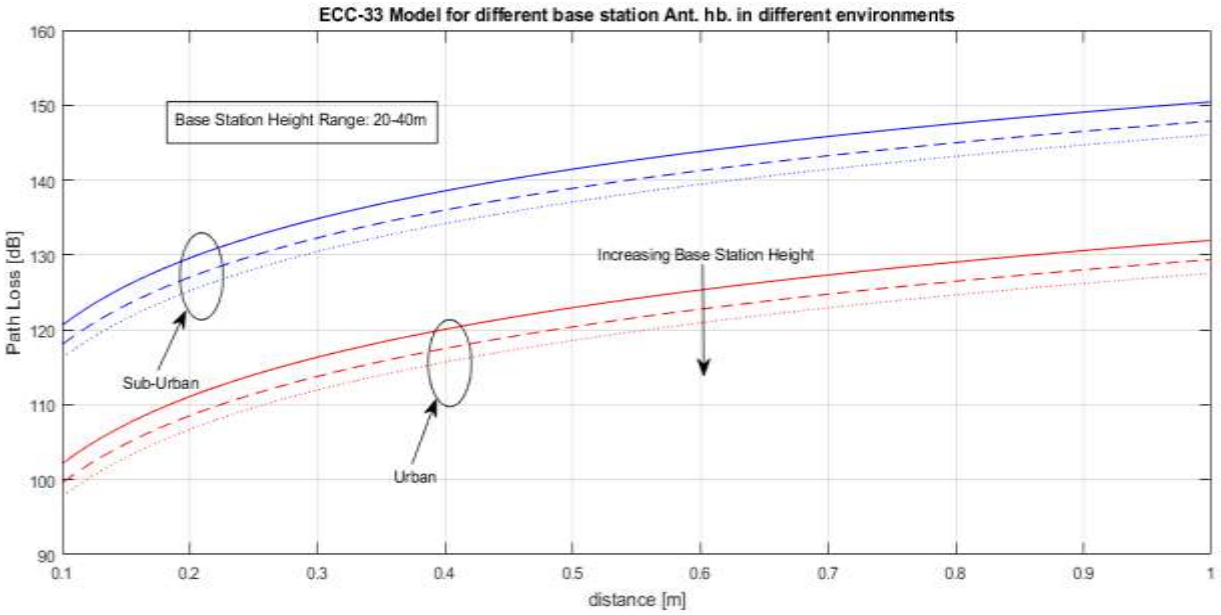

Figure 3.6 ECC-33 model path loss performance with the variation of base station height

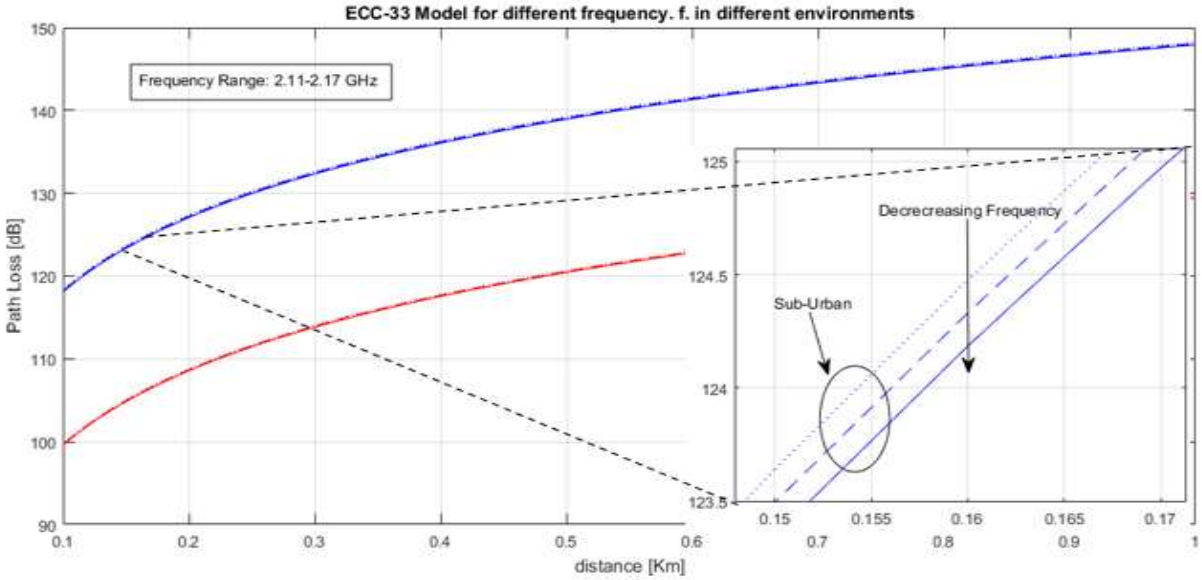

Figure 3.7 ECC-33 model path loss performance with the variation of frequency

The above figures show the characteristics of ECC-33 path loss model with respect to distance. As shown in both graph the path loss nearby the base station in sub-urban areas is higher than Urban areas. And as expected the path loss also increases as we go further far to the base station. Figure 3.6 displays how the path loss responds when we vary base station heights in all area types. And as the base station height increases the path loss decreases. Similarly, figure 3.13 shows the relation between ECC-33 path loss model and frequency where path loss decreases with decreasing operational frequency.

3.3.3 Stanford University Interim (SUI) Model

This model was developed by the Institute of Electrical and Electronics Engineers (IEEE) 802.16 working group for estimation of path loss in rural, sub-urban and urban environments. This model is defined for the Multipoint Microwave Distribution System (MMDS) frequency band ranging from 2.5 to 2.7 GHz. The functionality of this model within the range of 800 and 1900MHz band is not validated. But, since there is a correction factor for this frequency, the model has been selected. The SUI model is categorized into 3 types of terrains, namely, A, B, and C. Type A is linked with maximum path loss and it is preferable for hilly landscape with heavy to moderate to foliage densities. Whereas, Type C is linked with minimum path loss and it is applied to flat landscape with slight tree densities. Finally, Type B is linked with either mostly flat landscapes with heavy to moderate to heavy tree density or hilly terrain with slight tree densities. The fundamental path loss equation with the correction factors is presented in [10]:

$$PL = A + 10\gamma \log_{10}(\frac{d}{d_o}) + X_f + X_h + s \quad \text{for } d > d_o \tag{3.12}$$

where d is the distant between the mobile station (MS) and Access Point (AP) in meters, $d_o = 100m$ and s is log normal distributed factor which is necessary to account for the shadow fading owning to tree and other cluster and its value is between 8.2 dB and 10.6dB . The rest of the parameters are described as [10]:

$$A = 20 \log_{10}(\frac{4\pi d_o}{\lambda}) \tag{3.13}$$

$$\gamma = a - bh_b + \frac{c}{h_b} \tag{3.14}$$

where h_b is the height of the base station above ground in meters and must be between 10 m and 80 m. The constants a, b and c are given in Table II. The parameter ɣ is the same as the path loss exponent. For a particular terrain types the path loss exponent is defined by h_b.

Table 3.1: SUI model parameters in different environments [10]

Model parameter	**Terrain A**	**Terrain B**	**Terrain C**
a	4.6	4	3.6
b(m^{-1})	0.0075	0.0065	0.005
c(m)	12.6	17.1	20

The model's correction factors for the frequency of operation and the MS antenna height are [10]:

$$X_f = 6\log_{10}(\frac{f}{2000}) \tag{3.15}$$

and

$$X_h = -10.8\log_{10}(\frac{h_r}{2000}) \text{ for Terrain Types A and B} \tag{3.16}$$

$$X_h = -20\log_{10}(\frac{h_r}{2000}) \quad \text{for Terrain Type C} \tag{3.17}$$

Where, f is frequency in MHz and h_r is the BS antenna height above ground in meters.

The following simulated graphs shows how SUI path loss model performs to the variation of different parameters like distance, base station height and frequency.

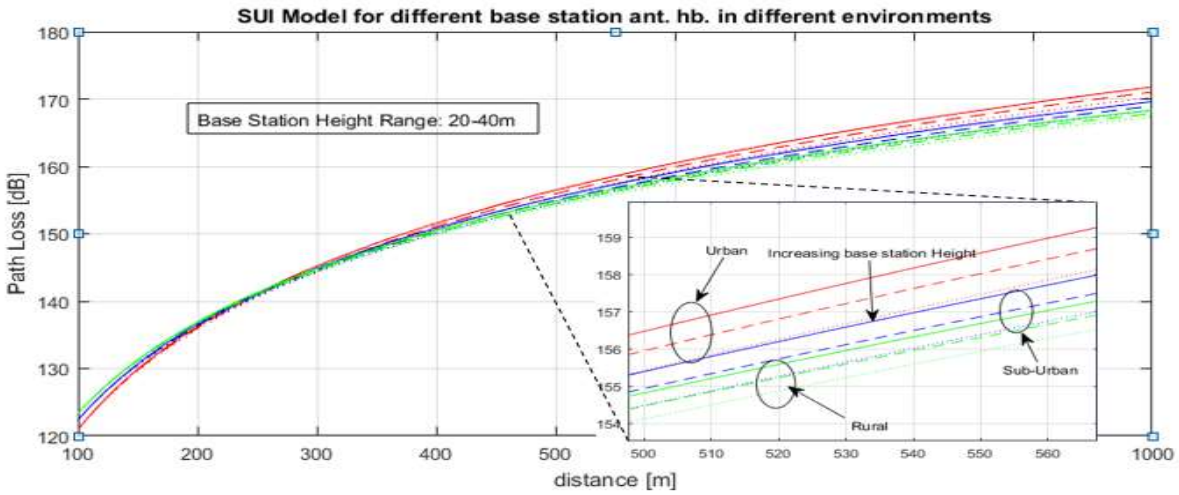

Figure 3.8 SUI model path loss performance with the variation of base station height

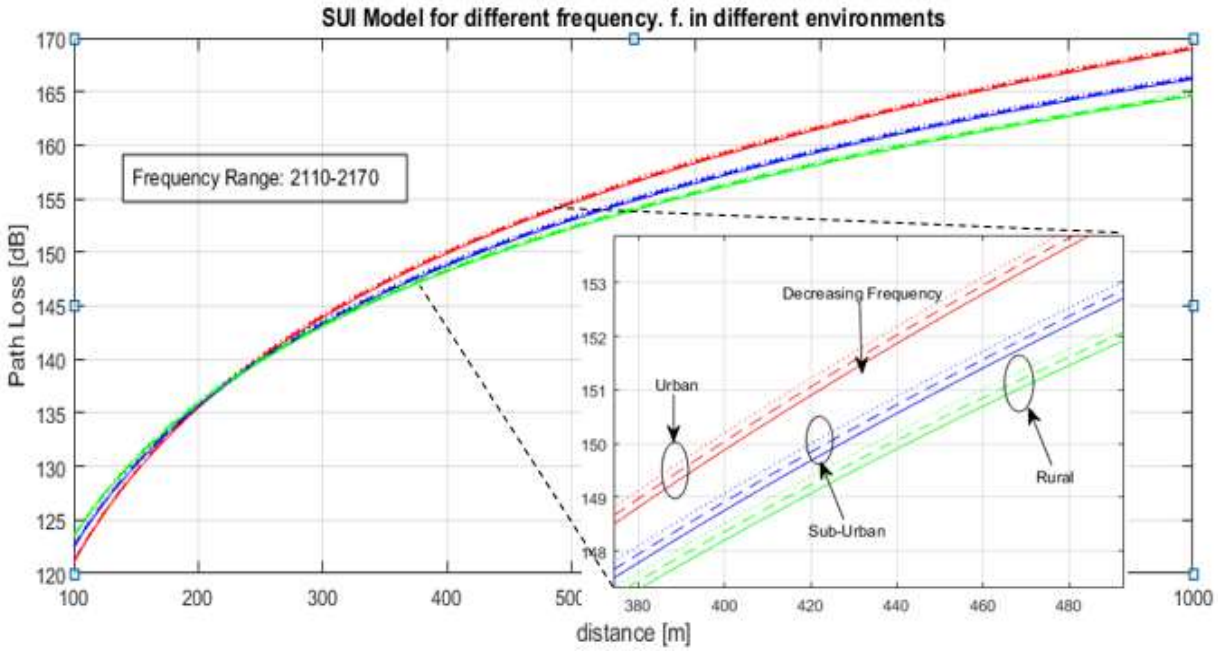

Figure 3.9 SUI model path loss performance with the variation of frequency

The above two figures show the characteristics of SUI path loss model with respect to distance. As shown in both graph the path loss nearby the base station increases as we go from rural areas to Urban areas. And as expected the path loss also increases as we go far from the base station. Figure 3.8 displays how the path loss responds when we vary base station heights in all area types. And as the base station height increase the path loss decreases. Similarly, figure 3.9 shows the relation between SUI path loss model and frequency where path loss decreases with decreasing operational frequency.

3.3.4 Hata Model

Hata model, also known as Okumura–Hata model, is among the most frequently used model to estimate the radio signal reduction in a macro cell environment. Since the model is developed using field measurements data, it is considered as an empirical model. The field measurements were executed in Tokyo-Japan, and the acquired result was issued in the form of graphs and put into equations. The model is valid for quasi-smooth terrain in urban areas. For some other terrain types correction factors are used. The ranges of the used parameters for this model are shown in the following table [6].

Table 3.2 Range parameters of Hata Model [6]

Parameter	Symbol	Range
Frequency range	f	150–1500 MHz
Frequency Extension		1500–2000 MHz
Distance between BTS and MS	d	1–20 km
Transmitter antenna height	h_b	3–200 m
Receiver antenna height	h_m	1–10 m

The Okumura–Hata model for path loss estimation in Urban areas can be expressed as

$$L = A + B\log_{10} f - 13.82\log_{10} h_b - a_{hm} + (44.9 - 6.55\log_{10} h_b)\log_{10} d \quad (3.18)$$

While: - f - frequency (Mhz). h_b - BS antenna height (m), h_m - the MS antenna height (m), a_{hm} - mobile antenna correction factor and d - distant between the BTS and MS (km). For small or medium sized cities, the correction factor of MS antenna height is formulated as shown below:

$$a_{hm} = (1.1\log_{10} f - 0.7)h_m - (1.56\log_{10} f - 0.8) \quad (3.19)$$

and for large city:

$$a_{hm} = 8.29\,(\log_{10} 1.54h_m)^2 - 1.1 \quad \text{for } f < 200 \text{ MHz} \quad (3.20)$$

$$3.2\,(\log_{10} 11.75h_m)^2 - 4.97 \quad \text{for } f \geq 400 \text{ MHz} \quad (3.21)$$

The parameters A and B are reliant on the frequency as shown below [6]:

A= 69.55 $150 < f < 1500$ MHz (3.22)

46.30 $1500 < f < 2000$ MHz (3.23)

B= 26.16 $150 < f < 1500$ MHz (3.24)

33.9 $1500 < f < 2000$ MHz (3.25)

For sub urban area

$$L = L_{urban} - 2\,[\log_{10}(\tfrac{f}{28})]^2 - 5.4 \quad (3.26)$$

For rural areas

$$L = L_{urban} - 4.78\,[\log_{10}(\frac{f}{28})]^2 + 18.33\log_{10} f - 40.94 \qquad (3.27)$$

Hata model is not appropriate for micro-cell planning where antenna is below roof-height.

The following simulated graphs shows how Hata path loss model performs to the variation of different parameters like distance, base station height and frequency.

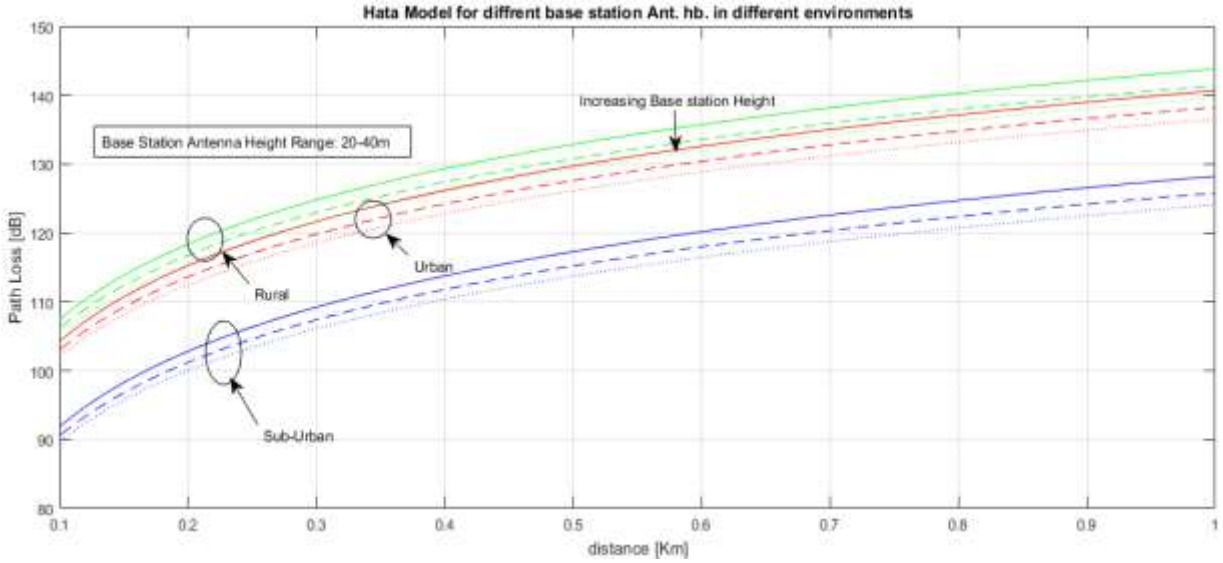

Figure 3.10 Hata model path loss performance with the variation of base station height

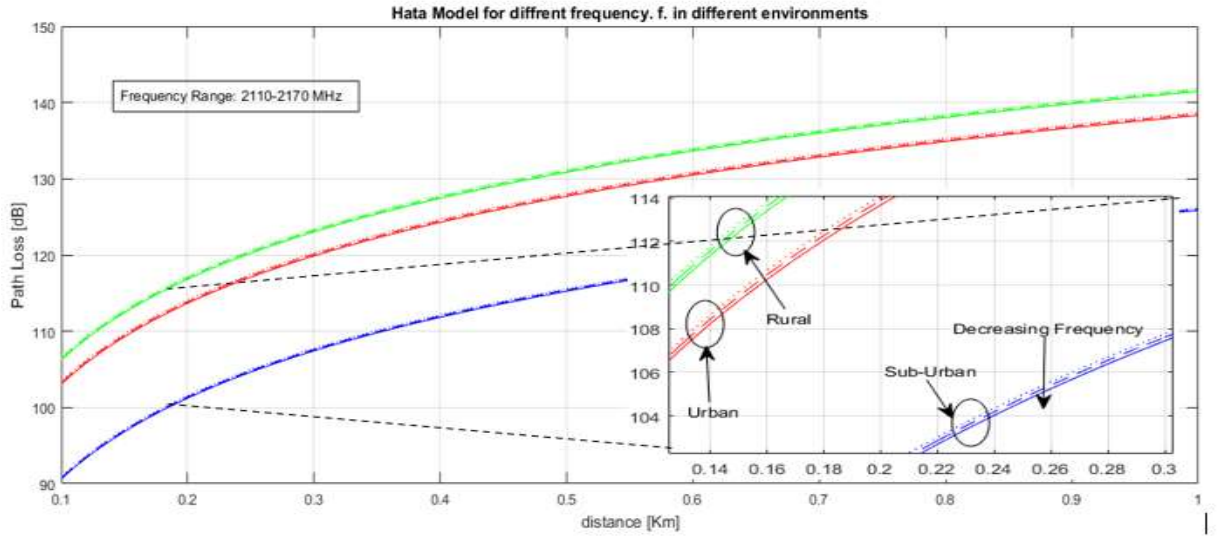

Figure 3.11 Hata model path loss performance with the variation of frequency

The above two figures show the characteristics of Hata path loss model with respect to distance. As shown in both graph the path loss nearby the base station is higher in rural areas whereas lower in sub-urban areas. And as expected the path loss also increases as we go further away from the base station. Figure 3.10 displays how the path loss responds when we vary base station heights in all area types. And as we increase the base station height the path loss decreases. Similarly, figure 3.11 shows the relation between Hata path loss model and frequency where path loss decreases with decreasing operational frequency.

3.3.5 Ericsson Model

A model where network planning engineers use a software delivered by Ericsson company to estimate a path loss is called Ericsson model. The model also relies on the reformed Okumura-Hata model so that there is a room to change parameters in accordance with the propagation environment. According to Ericsson model we can define the path loss as [10].

$$L = a_0 + a_1 \log_{10} d + a_2 \log_{10} h_b + a_3 \log_{10}(h_b) \log_{10}(d) - 3.2(\log_{10}(11.75h_r)^2) + g(f) \quad (3.28)$$

where $g(f)$is defined by [10].

$$g(f) = 44.49 \log_{10}(f) - 4.78(\log_{10}(f))^2 \quad (3.29)$$

Where, f is frequency in (MHz), h_b is the base station antenna height in (m), h_r is the MS antenna height (m).The default values of these parameters $(a_0, a_1, a_2 \; and \; a_3)$ for different terrains are provided in the table below

Table 3.3 Values of parameters for Ericsson model [10]

Environment	**a_0**	**a_1**	**a_2**	**a_3**
Urban	36.2	30.2	12	0.1
Suburban	43.2*	68.93*	12	0.1
Rural	45.95*	100.6*	12	0.1

*The value of parameter a_0 and a_1 in sub-urban and rural areas are computed using Least Square (LS) method in [17].

The following simulated graphs shows how Ericsson path loss model performs to the variation of different parameters like distance, base station height and frequency.

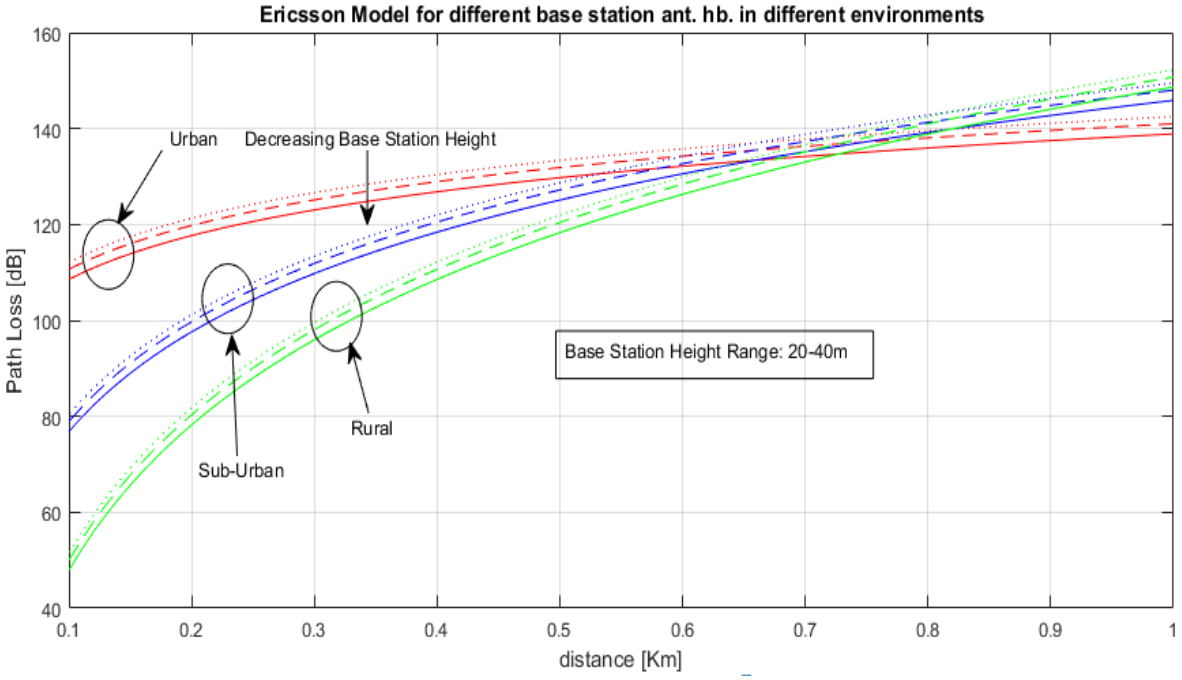

Figure 3.12 Ericsson model path loss performance with the variation of base station height

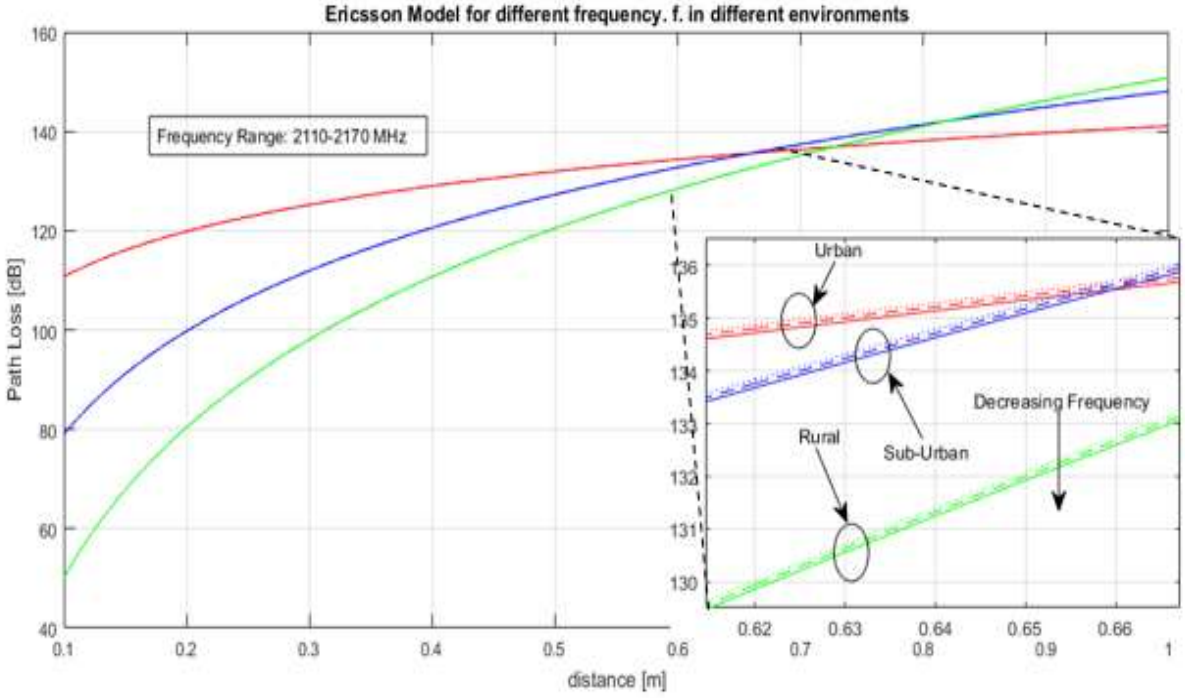

Figure 3.13 Ericsson model path loss performance with the variation of frequency

The above two figures show the characteristics of Ericsson path loss model with respect to distance. As shown in both graph the path loss near to the base station increases as we go from rural areas to Urban areas. And as expected the path loss also increases as we go further away from the base station. Figure 3.12 displays how the path loss responds when we vary base station heights in all area types. And as we decrease the base station height the path loss also decreases. Similarly, figure 3.13 shows the relation between frequency and Ericsson path loss model where path loss increases with increasing operational frequency.

Chapter Four

4. Data Collection and Path Loss Measurement

4.1 Measurement Methodology

After studying the available propagation path loss models and deciding the appropriate models for the target city or area, field measurement will be the most crucial step for path loss model tuning project. The success of the project hangs on the accuracy of the measured data. Regardless of that wrong data measurement may happen due to various reasons. Selection of proper sample site which can represent the whole city and choice of the right measurement tools are the two main factors. And a wrong field data measurement will result in a wrongly tuned path loss model.

Field data measurement tools use different hardware and software elements. And these tools have to be selected carefully and should be calibrated (configured) properly, so that the right data measurement which reflect the effect of the area in focus can be collected. And it has to be known that when base station antennas are used for measurement, the coverage area of the sector should first be determined before taking the measurement.

Despite following all procedures appropriately, measurements can be biased by many factors. Some of the challenges are the speed of the drive when the measurement was taken, Consistency of using the same measurement tools, weather condition, traffic movement, road limitation, time of measurement, etc. Since The measured data can be affected by weather condition and time of measurement, I have tried to perform the measurement at different times and on different weather condition but that is also not enough to declare the collected data perfect. So, these challenges are taken as limitations of this thesis.

4.1.1 Measurement Tools and Equipment Setup

Table 4.1 Measurement Tools

No	Tool	Version	Model	License
1	Nemo Outdoor		-	License on flash
2	ACTIX Analyzer		-	No License
3	Samsung mobile Phone (Nemo router installed)		SAMSUNG Galaxy S8	License Activated
4	Samsung mobile phone with Nemo Handy		SAMSUNG Galaxy S5	License Activated
5	GPS			No License
6	Laptop		Lenovo Core i7	No License

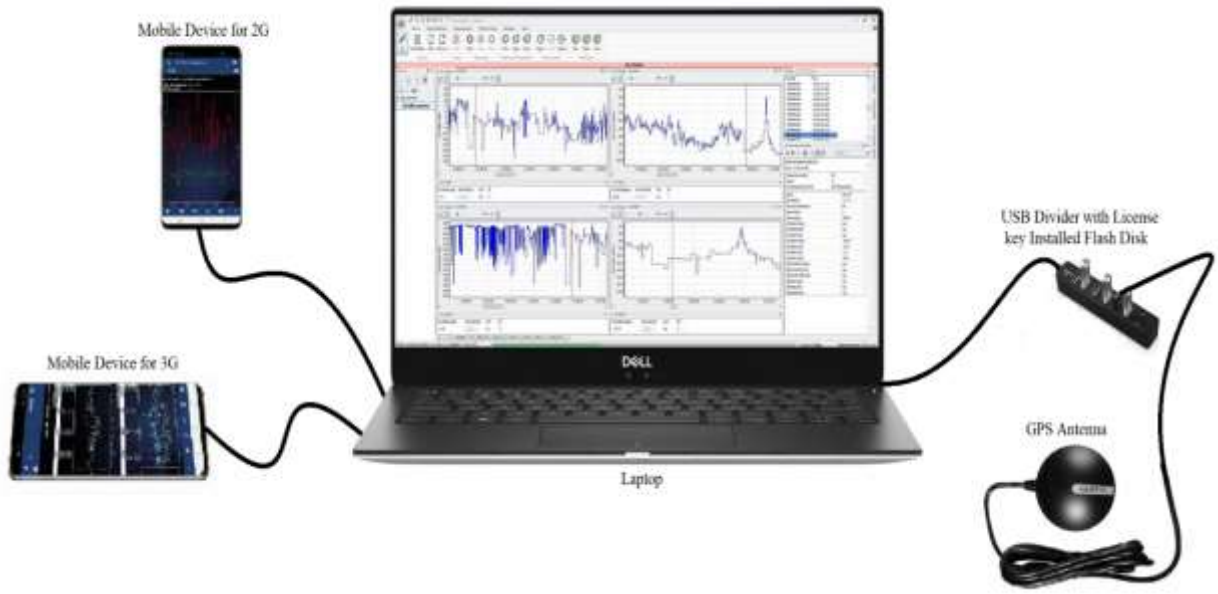

Figure 4.1 Drive Test Measurement Equipment's Setup

4.2 Site Selection

In this Thesis the whole Hawassa city is set to be the target area. Hawassa City has different area types. The city area was divided into different area types according to their morphology which depends on population density, building height and plant density. Some areas have high density

of buildings, more traffic. Other areas have some buildings, some traffic flow, living houses and dense plant coverage. There are also areas having open spaces and only some living houses. From this we can see that Hawassa city has urban, suburban and open area morphologies. Before the measurements, planning was done to decide where the measurements should be taken. A google earth assisted and physical observation planning was done on the entire city so that the best sites which can represent all the morphology types, open areas, suburban areas and urban areas of Hawassa, can be selected. There are a total of 44 sites which are dispersed around Hawassa city [14]. All the sites were installed so that they could cover the entire city based on population density and geographical structure. From these 44 sites I selected 14 sites which can represent all morphology types. In this Thesis, a sector is considered as a site because a sector facing to one side of an area and the other to the another side of an area actually represents different areas. Base stations of 2G and 3G technologies (GSM and UMTS) were used for measurement.

Figure 4.2 Total Sites in Hawassa City

The above figure shows all the 44 sites in Hawassa. As seen in the google earth image the sites are dispersed in the total area justly. The below table shows the list of the sites on the image:

Table 4.2 List of Sites in Hawassa City [14]

No.	Site ID	Town	Latitude	Longitude	Antenna Height
1	222082	Hawassa	7.0275	38.4848	35
2	222084	Hawassa	7.02883	38.47149	34
3	222089	Hawassa	7.03561	38.48378	29
4	222092	Hawassa	7.04027	38.4751	34
5	222095	Hawassa	7.0451	38.46526	32
6	222096	Hawassa	7.0452	38.482	27
7	222097	Hawassa	7.04591	38.490708	33
8	222105	Hawassa	7.05248	38.470555	37
9	222088	Hawassa	7.03823	38.50561	34
10	222101	Hawassa	7.05038	38.51297	38
11	222107	Hawassa	7.05487	38.48494	34
12	222109	Hawassa	7.05955	38.50117	34
13	222110	Hawassa	7.0597	38.4744	34
14	222113	Hawassa	7.06187	38.48696	34
15	222116	Hawassa	7.07088	38.47975	34
16	222117	Hawassa	7.0736	38.4899	27
17	222118	Hawassa	7.07464	38.50618	30
18	222080	Hawassa	7.0227	38.5008	27
19	222087	Hawassa	7.0345	38.4946	37
20	222120	Hawassa	7.08375	38.4898	35
21	222102	Hawassa	7.04801	38.47805	29
22	222076	Hawassa	7.01212	38.50313	30
23	222077	Hawassa	7.0197	38.49193	29
24	222078	Hawassa	7.0199	38.47249	29
25	222079	Hawassa	7.0203	38.48114	29
26	222083	Hawassa	7.02586	38.49523	30
27	222085	Hawassa	7.03275	38.47745	29
28	222086	Hawassa	7.02877	38.46454	29
29	222093	Hawassa	7.04087	38.48233	30
30	222094	Hawassa	7.04333	38.49763	29
31	222098	Hawassa	7.04434	38.47359	29
32	222099	Hawassa	7.04356	38.45952	30
33	222100	Hawassa	7.04953	38.49397	29
34	222091	Hawassa	7.04016	38.51438	30
35	222103	Hawassa	7.0504	38.48244	29
36	222104	Hawassa	7.05173	38.48813	30

37	222106	Hawasa	7.05328	38.4782	29
38	222108	Hawasa	7.05462	38.49331	30
39	222111	Hawasa	7.059	38.47998	28
40	222112	Hawasa	7.05313	38.50423	30
41	222114	Hawasa	7.06537	38.47574	30
42	222115	Hawasa	7.06729	38.48467	30
43	222121	Hawasa	7.07722	38.48367	29
44	222090	Hawasa	7.03922	38.48975	29

From the above listed sites the following 14, which are thought to represent all topologies and urban structure of the city, were selected:

Table 4.3 Selected Sites [14]

No.	Site ID	Specific Location	Latitude	Longitude	Antenna Height
1	222078	Baleweld Church	7.0199	38.47249	29
2	222080	New Market	7.0227	38.5008	27
3	222082	Nigist Fura	7.0275	38.4848	35
4	222089	Liz Sefer	7.03561	38.48378	29
5	222096	Behind St. Gebriel church	7.0452	38.482	27
6	222097	Pay Station	7.045912	38.490708	33
7	222101	Chefe Genet Church	7.05038	38.51297	38
8	222102	Beza Collage	7.04801	38.47805	29
9	222105	Tele Branch	7.052475	38.470555	37
10	222110	Old Market	7.0597	38.4744	34
11	222112	Hawassa University(Techno)	7.05313	38.50423	30
12	222116	Debub Ez Condominium	7.07088	38.47975	34
13	222118	Industry Park	7.07464	38.50618	30
14	222120	Dato	7.08375	38.4898	35

Figure 4.3 Selected Sites

4.3 Measurement Procedures

As mentioned above the crucial part of this work was data measurement since all the analysis and conclusions made at the end relies on the collected data. And since Drive Test Methodology is used by many telecom industries as the best possible solution to collect signal strength, mobile network latency, voice call KPIs and optimization, it is also adopted in this work for data collection process. For the Drive test measurement process, I have used different high quality and commercially licensed hardware and software tools. The tools used for drive test measurements were Nemo handy, Nemo outdoor, GPS, mobile phones, laptop, ACTIX software for data analysis and a vehicle. Nemo Handy is an Android-based application which is used for measuring and monitoring the air interface of LTE/ LTE Cat 6, HSPA+, HSUPA, HSDPA, WCDMA, EVDO, CDMA, GSM, and Wi-Fi wireless networks, and QoS/QoE of mobile application. Whereas, Nemo Outdoor is a laptop-based drive test tool which can support more than 280 terminals and scanning receivers from different vendors. And It is a powerful software platform which work for any technology and various protocol and application testing preferences. And ACTIX Analyzer is a software tool which offers a cutting-edge drive test survey analysis and support network

calibration, network acceptance and confirmation. It is used in 2G, 3G, LTE, VoLTE and 5G rollouts. The data measurement procedure starts by connecting all the devices, two Samsung S8 mobile phones (one for 2G and the other for 3G), GPS antenna and flash disks with license key to the laptop. After connecting and powering up all the devices the NEMO outdoor Software on the laptop and Nemo router on the phones will be launched. And then, Nemo outdoor software will be configured so that it could be able to measure the signal strength of BCCH (Broadcast control channel) in GSM and PSC (Pilot Scrambling Code) in WCDMA. Finally, the System will be ready for measurement after enabling carrier and channel locking to GSM and UMTS.

The measurement was conducted by initiating calls at each test point till the call is setup and then the signal strength data transmitted through air interface between the BS and the MS were read. Then the drive test is carried out by setting the tools in a car and driving along the coverage area of the site. For all sites, received signal strength was measured at a reference distant of 100m from the BS and at continuous intervals of 100m up to 1000m.

In the measurement process there were challenges that may have impacted the accuracy of the collected data. The first problem was since the drive test was performed was since the drive test was performed following the available road route it was difficult to get the signal properties of a site up to the required range. Following the road route will take us out of the coverage area of the required site and we were unable to find enough data for some sites. And the other challenge was the closeness of sites in Hawassa city. There are many sites in the city and the antennas of each sites are tilted down not to intrude into the coverage areas of other sites. Thus, the signal range of some sites are somehow shorter and measurements were unable to be taken up to the required range.

Table 4.4 Sample Path Loss Measured data of a single site at 2100Mhz

No.	Site ID	Sector	Distance from the BTS(m)	Average Signal Level(dBm)
1	222080	A	18.29	-52.4
2	222080	A	101.02	-70.5
3	222080	A	150.84	-62.6
4	222080	A	198.34	-57.4
5	222080	A	249.2	-71.45

6	222080	A	300.33	-74.2
7	222080	A	349	-75.2
8	222080	A	400.79	-71.8
9	222080	A	452.6	-69.6
10	222080	A	500.16	-82.6
11	222080	A	550.14	-95.9
12	222080	A	599.63	-98.45
13	222080	A	653.5	-95.15
14	222080	A	701.74	-99.55
15	222080	A	751.83	-99.95
16	222080	A	797.17	-99.85
17	222080	A	850.81	-68.85
18	222080	A	902.7	-74.1
19	222080	A	1001.86	-83.85

Figure 4.4 Sample drive test of 1800 MHz displayed on google earth

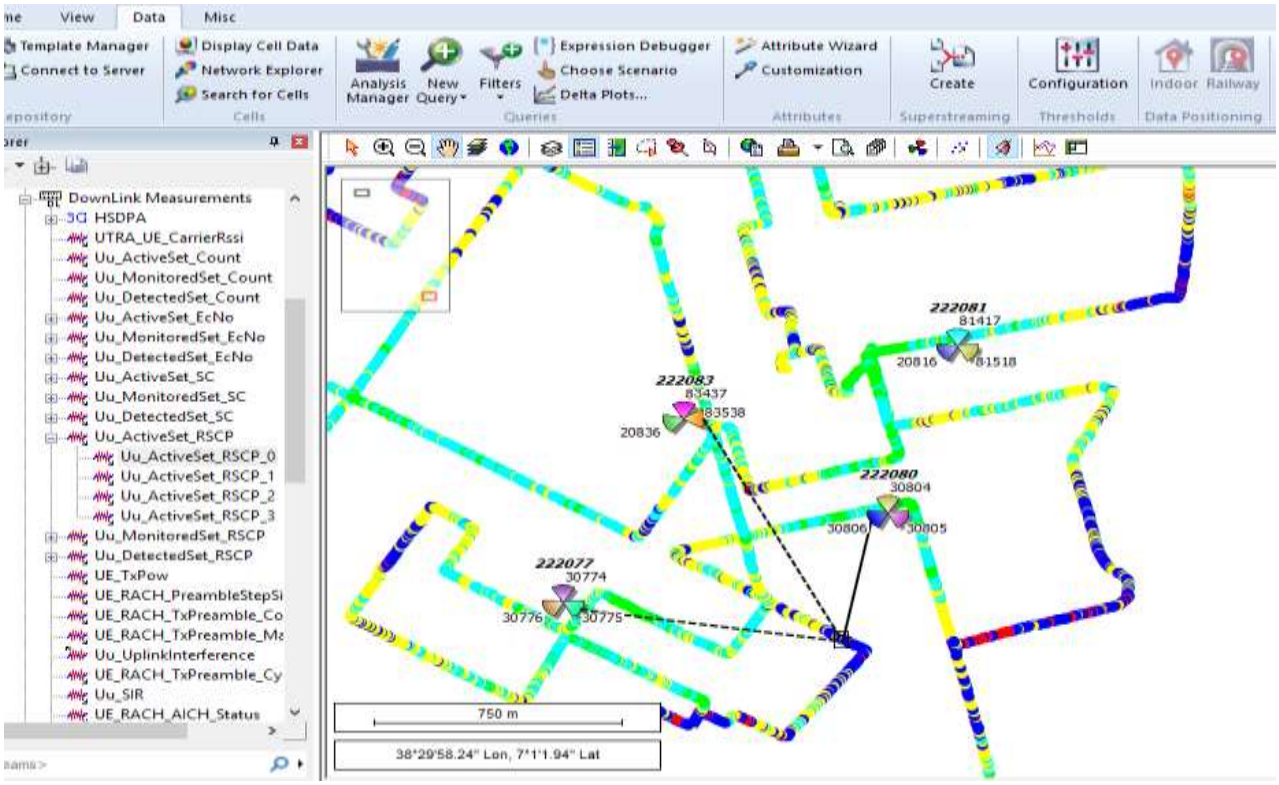

Figure 4.5 Sample drive test analysis of 2100 MHz on ACTIX analyzer

Chapter Five

5. Data Analysis and Discussion of Results

5.1 Error Measurement and Optimization Algorithm

This sub-chapter discusses the error measurement techniques used in this thesis to compare the measured and calculated data. It also discusses the model tuning algorithm used.

5.1.1 Error Measurement

Error measurement was done to evaluate the closeness of the predicted path loss by the path loss model with the measured path loss on the field. To do this four types of error measurement techniques were implemented in this Thesis. These are, Root Mean Square Error (RMSE), Mean Absolute Percentage Error (MAPE), Standard Deviation (SD) and Mean Absolute Error (MAE).

5.1.1.1 RMSE

Root mean square error measures the average dispersion of a set of data predicted by a model from an observed data. It is the most used techniques in most thesis that are done on performance comparison. In this thesis also RMSE is mainly used to compare the calculated and measured path loss. And it is calculated with the following formula:

$$RMSE = \sqrt{\frac{1}{n}(\sum_{1}^{n}(PL_m - PL_P)^2} \quad (5.1)$$

Where,

PL_m- is the measured path loss

PL_P- is the calculated path loss

n - is the number of measured data

5.1.1.2 MAPE

The mean absolute percentage error (MAPE) is a statistical measure of the precision of an estimation model. It calculates this precision as a percentage, and can be calculated as the average absolute percent error for each time period minus measured values divided by measured values.

$$MAPE = \frac{1}{n}\sum_{1}^{n}\left|\frac{(PL_m - PL_P}{PL_m}\right| \quad (5.2)$$

Where PL_m is the actual value and PL_P is the predicted value.

MAPE is the most common measure used to estimate error, and it work best if there are no extremes to the data (and no zeros).

5.1.1.3 SD

Standard deviation (SD) measures how much a data is spread out around the mean or average. And it is calculated as follows:

$$SD = \sqrt{\frac{\sum_{1}^{n}((PL_m - PL_P) - MAE)^2}{n-1}} \quad (5.3)$$

Where ME is mean error.

5.1.1.4 MAE

The Mean Absolute Error (MAE) is used to measure the closeness of the predicted values to the actually measured values. And it is calculated as follows:

$$\text{MAE} = \frac{1}{n}\sum_{1}^{n}|PL_m - PL_P| \quad (5.4)$$

5.1.2 Model Optimization Algorithm

In this part of the thesis we will discuss the crucial analysis part of the Thesis. As mentioned in different parts of the thesis the main purpose of the Thesis is to tune the pre-existing path loss model toward the measured data which represent the available environmental status. And to do that model

tuning algorithms are essential. There are different path loss optimization algorithms available but out of all the available methods Linear Least Square method is the most commonly used. And this thesis has also used LLSM for model tuning.

5.1.2.1 Linear Least Square method

Linear Least Square method is by far the most broadly used modeling method. Not only it is the most widely used method but it also has a vital underlying role in various different modeling methods, including: weighted least squares regression, non-linear least squares regression, and LOESS. This method is a form of mathematical regression analysis which is used to define the line of best fit for a set of data, providing a pictorial illustration of the correlation among the data points. LLSM is an arithmetic tuning approach where all environmental influences are considered. The key idea of LLSM is to reduce the variance between the measured and estimated data in a way of mean square error function. Therefore, its simplicity and easy implementation was the main reason to choose LLSM for mode optimization process on this case study. The following equation shows the mathematical representation of LLSM:

$$E\ (a, b, c, \dots) = \sum_1^n [yi - PR, i(xi, a, b, c)]^2 \qquad (5.5)$$

Where,

yi = measured path loss values at distant xi

$PR, i = (xi, a, b, c)$ = model calculated path loss values at distant xi

a, b and c are the model parameters, n represents number of experiment data.

Path loss model is considered calibrated at the values of a and b where the equation bring minimum value of $E\ (a, b, c, \dots)$. To see the tuning process let us for instance take cost 231 path loss equations as an example. And we can rearrange the formula as follows.

$$E_0 = 46.3 + C_k \tag{5.6}$$

$$E_{sys} = 33.9 \log_{10} f - 13.82 \log_{10} h_b - a_{hm} \tag{5.7}$$

$$B_{sys} = 44.9 - 6.55\ (\log_{10} h_b) \tag{5.8}$$

Where, E_0 is Initial offset parameter, E_{sys} is Initial system design parameter and B_{sys} is the slope of the model curve.

We can then write the total cost 231 path loss as:

$$P_L(cost_{231}) = E_0 + E_{sys} + B_{sys} \log_{10} d \tag{5.9}$$

The Above equation can be written as:

$$P_{L\ pridicted}(cost_{231}) = a + bx$$

Where,

$$a = E_0 + E_{sys}$$

$$b = B_{sys}$$

$x = \log_{10} d$, a simplified logarithmic base

As mentioned earlier the basic principle of LLSM is to reduce the variance between the measured and estimated data in a way of mean square error function so that best fit condition could be satisfied. And to ensure this, all partial differentials of error function have to be zero.

$$E\ (a, b, c, \dots) = \sum_1^n [y_i - PR, i(x_i, a, b, c)]^2 \tag{5.10}$$

Which means:

$$\frac{\partial E}{\partial a} = 0, \qquad \frac{\partial E}{\partial b} = 0, \qquad \frac{\partial E}{\partial c} = 0$$

The partial differential of error function with respect to parameter a will be

$\frac{\partial E}{\partial a} = 0,$

$\frac{\partial}{\partial a}(\sum_1^n [y_i - (a + bx_i)]^2) = 0$

After derivation, the detail is attached in the Appendix, with respect to 'a' the equation can be written as:

$na + b\sum_1^n x_i = \sum_1^n y_i$

And from this equation 'a' can be expressed in terms of 'b' as following:

$na = \sum_1^n y_i - b\sum_1^n x_i$

$$a = \frac{\sum_1^n y_i - b\sum_1^n x_i}{n} \tag{5.11}$$

After derivation of the error function with respect to parameter b and rewriting the equation we will get the following:

$a\sum_1^n x_i + b\sum_1^n (x_i)^2 = \sum_1^n y_i x_i$

And from this equation 'b' can be expressed in terms of 'a' as following:

$$b\sum_1^n (x_i)^2 = \sum_1^n y_i x_i - a\sum_1^n x_i$$

$$b = \frac{\sum_1^n y_i x_i - a\sum_1^n x_i}{\sum_1^n (x_i)^2} \tag{5.12}$$

We can find the tuned parameters $\tilde{a}$ and $\tilde{b}$ by substituting the variables a and b in equation

$$\tilde{a} = \frac{\sum_1^n (x_i)^2 . \sum_1^n y_i - \sum_1^n y_i x_i . \sum_1^n x_i}{n\sum_1^n (x_i)^2 - (\sum_1^n x_i)^2} \tag{5.13}$$

$$\tilde{b} = \frac{n\sum_1^n y_i x_i - \sum_1^n y_i . \sum_1^n x_i}{n\sum_1^n (x_i)^2 - (\sum_1^n x_i)^2} \tag{5.14}$$

Finally, we can find the tuned cost 231 Hata path loss model by substituting the tuned parameters $\tilde{a}$ and $\tilde{b}$ into the original cost 231 Hata path loss model that we begin the process with. To do that we first find the initial offset parameter and slope of the model.

$a = E_0 + E_{sys}$

Then, E_0 becomes

$E_0 = a - E_{sys}$

Then, by replacing a with $\tilde{a}$ we can find $\widetilde{E_0}$:

$$\widetilde{E_0} = \tilde{a}\text{-}E_{sys} \quad (5.15)$$

And since $b = B_{sys}$ there should be a tuning factor $\widetilde{B_{sys}}$ to get $\tilde{b}$

$$\tilde{b} = \widetilde{B_{sys}} B_{sys} \quad (5.16)$$

$$\widetilde{B_{sys}} = \frac{\tilde{b}}{B_{sys}}$$

$$\widetilde{B_{sys}} = \frac{\tilde{b}}{44.9 - 6.55\,(\log_{10} h_b)} \quad (5.17)$$

5.2 Collected Data Trend and Analysis

As mentioned in the site selection sub-chapter for this thesis I have selected 14 sites. And drive test data was tried to be collected from all sites for 900 MHz, 1800 MHz and 2100 MHz frequencies. But since most sites in the city are working on 1800 MHZ and 2100 MHz frequencies and those working on 900 MHZ are installed to cover far areas I was unable to collect enough 900 MHZ data for analysis. Therefore, the data analysis was done for 1800 MHz and 2100 MHz frequencies only. Data measurement was done up to 1000 meter from the sites. But since the drive test was done via a vehicle and the coverage area of some selected sites were out of the available road route, some sites data was not in the required range.

After collecting the data and getting the received power, P_{rx}, at the required ranges, Path Loss calculation was done to find the selected sites path loss trend. Path loss was calculated with the equation, $P_L = P_t - P_r$. Based on the data I got from Ethio-telecom, all sites are configuered with transmission power of 43 dBm [14]. Hence, 43 dBm is used for path loss calculation for all 1800

MHZ frequency. whereas for 2100 MHz,3G, 10% out of the total transmission power allocated for the BS (43dBm) is used for PCPICH. So, 33dBm is used for path loss calculation for all 2100 MHZ frequency.

In the site selection process, even if sites were selected to represent all area types as much as possible it was necessary to categorize the selected sites to each area by using error measurement techniques. Therefore, the four error measurement techniques (Root mean square error, Mean Absolute Percentage Error, Standard Deviation and Mean Absolute Error) were used to compare the measured path loss values with the estimated path loss values of all models. And sites were classified in the area where the measured path loss was closer to the estimated values of variant models of that area type.

5.2.1 Collected Data Trend

Here are the data samples collected from each selected sites. The graphs show the path loss of each site in dBm versus distance in meter.

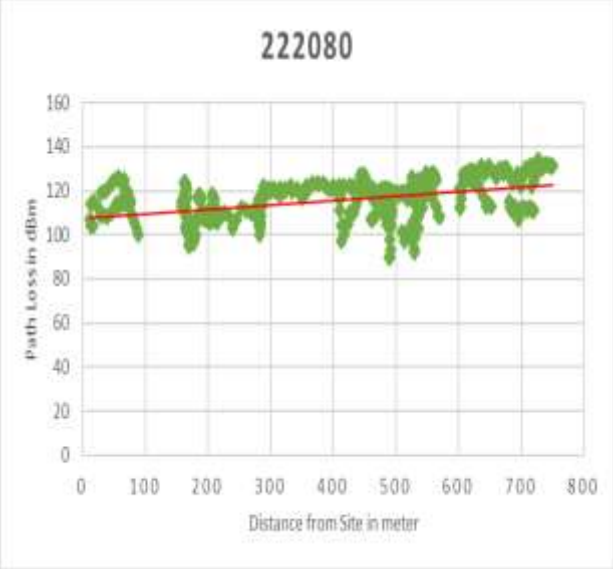

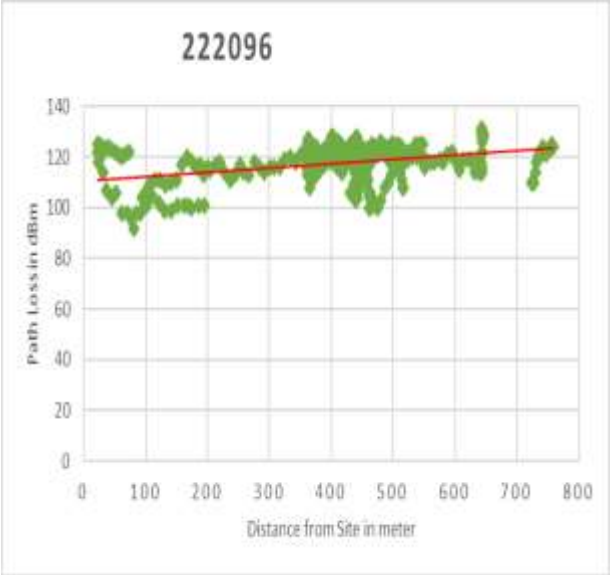
222096
Path Loss in dBm
Distance from Site in meter

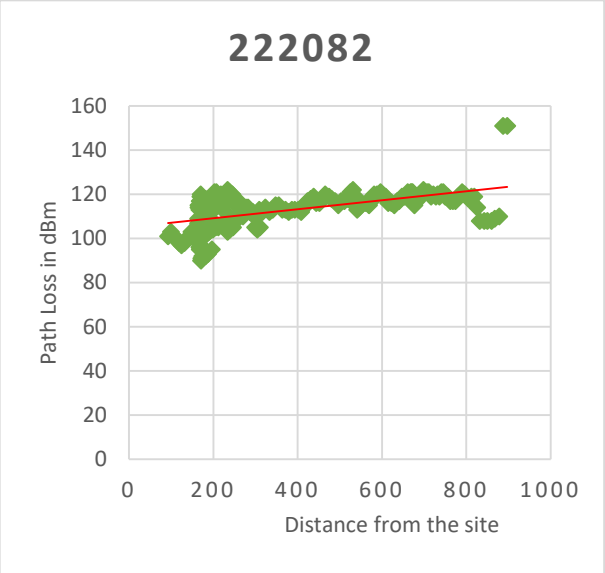
222082
Path Loss in dBm
Distance from the site

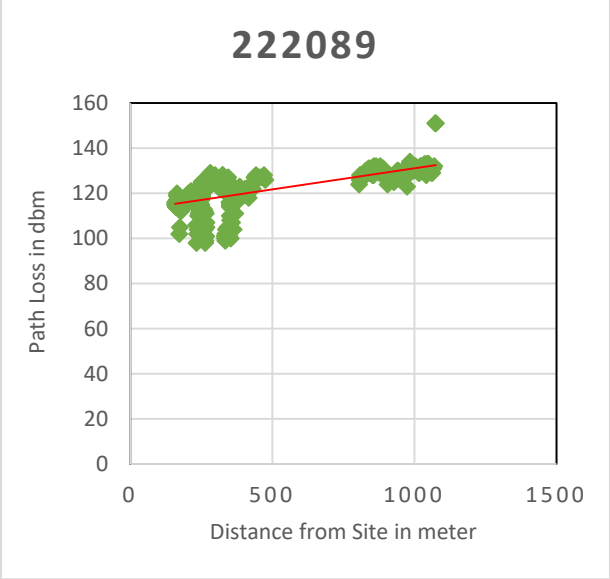
222089
Path Loss in dbm
Distance from Site in meter

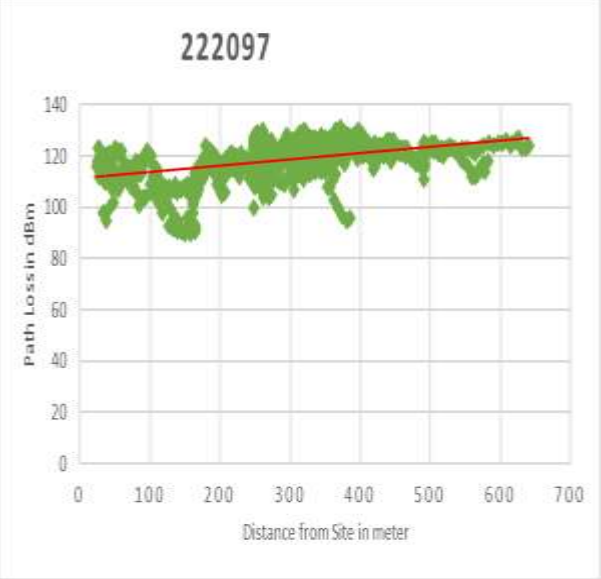
222097
Path Loss in dBm
Distance from Site in meter

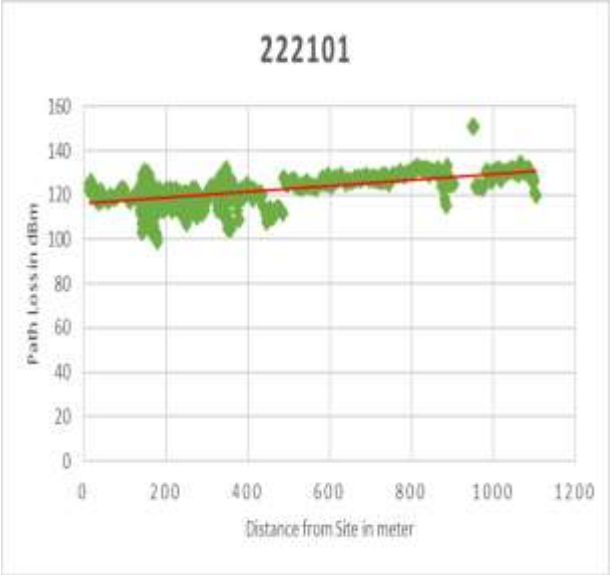
222101
Path Loss in dBm
Distance from Site in meter


222102
Path Loss in dBm
Distance from Site in meter

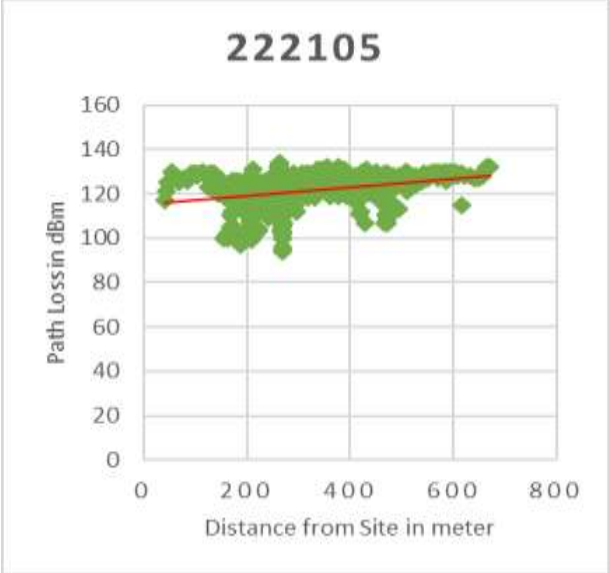
222105
Path Loss in dBm
Distance from Site in meter

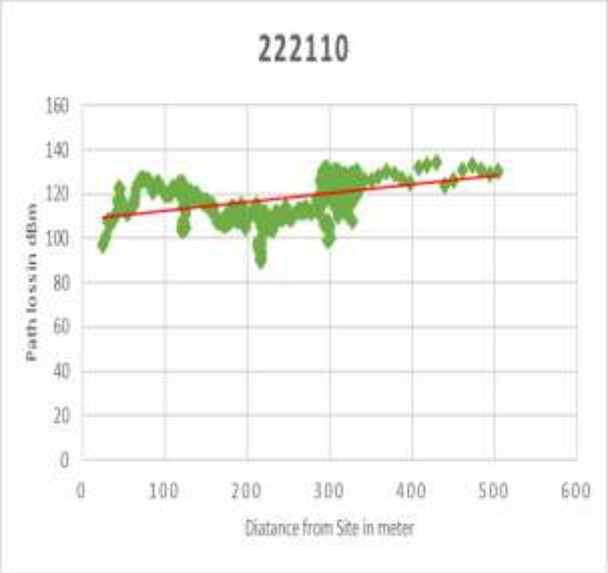
222110
Path loss in dBm
Diatance from Site in meter

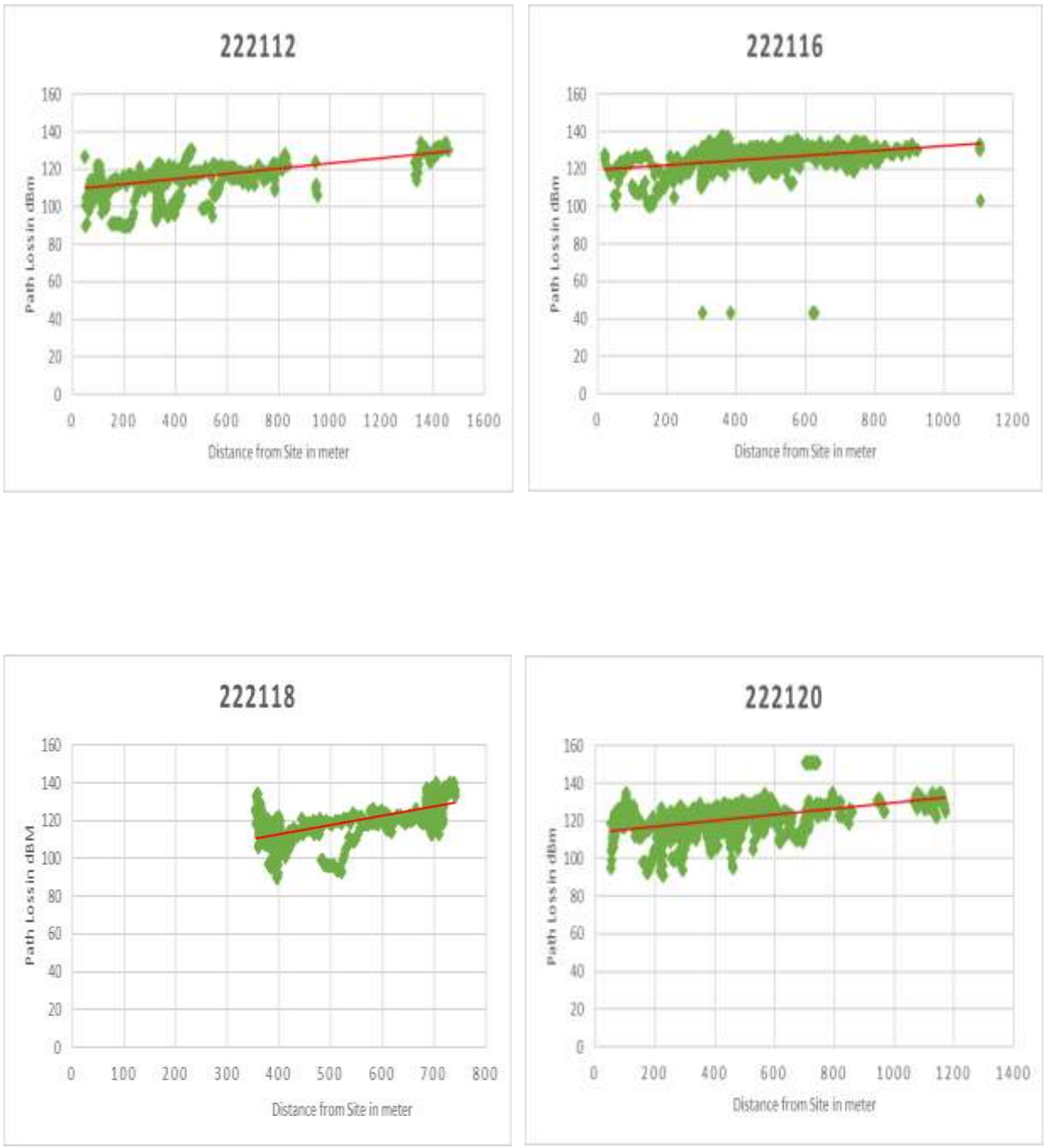

Figure 5.1 Collected Data Trend of selected sites at 1800 MHz

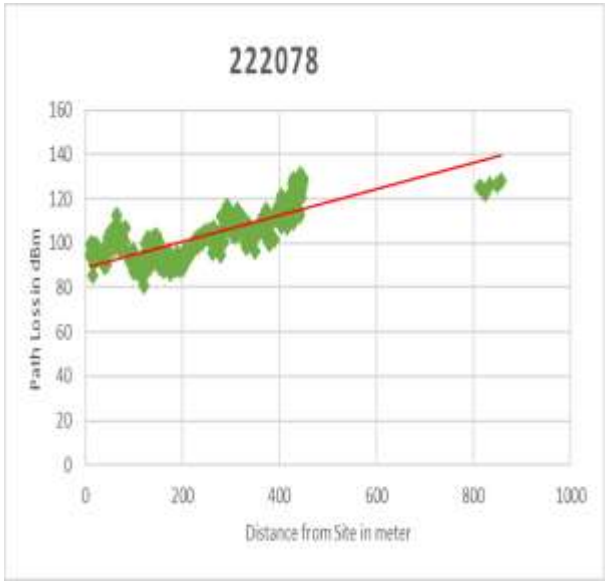
222078
Path Loss in dBm
Distance from Site in meter

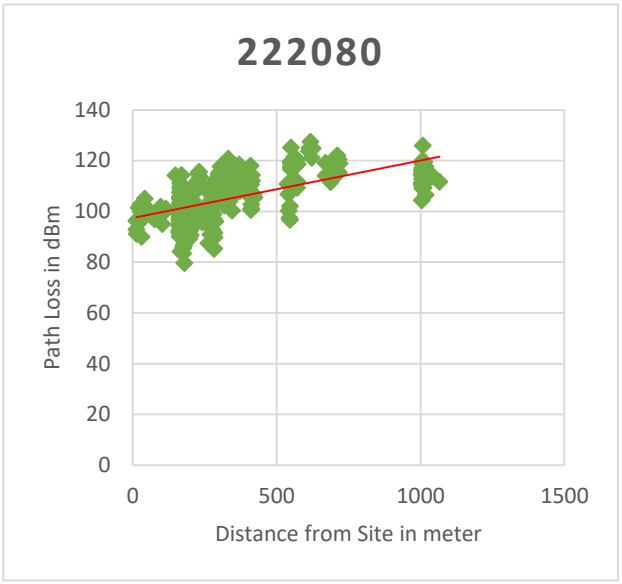
222080
Path Loss in dBm
Distance from Site in meter

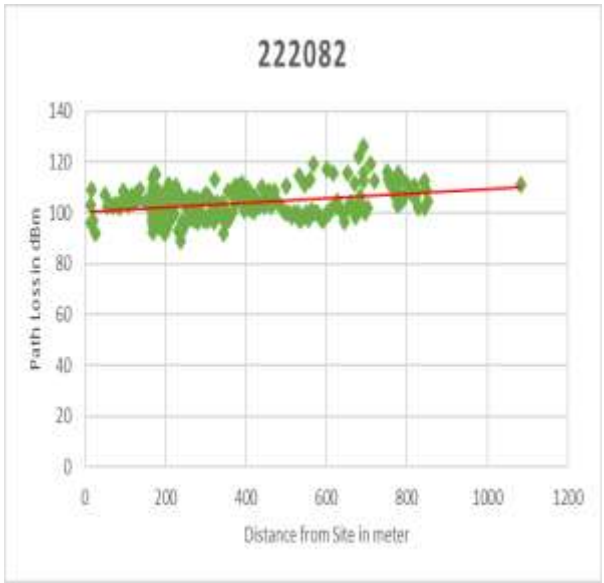
222082
Path Loss in dBm
Distance from Site in meter

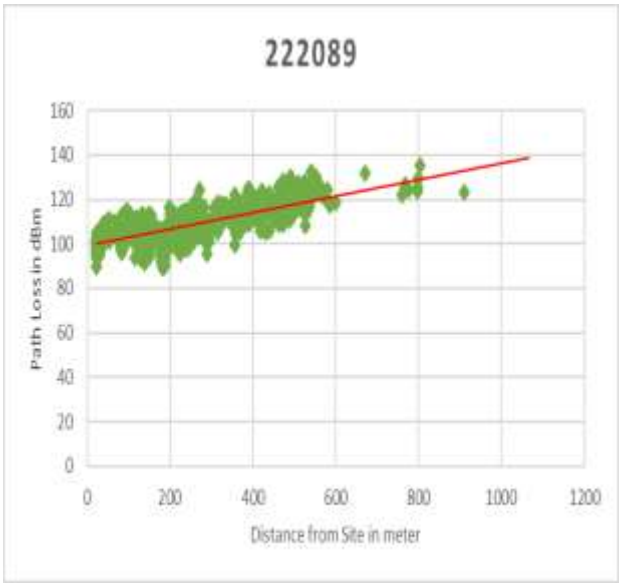
222089
Path Loss in dBm
Distance from Site in meter

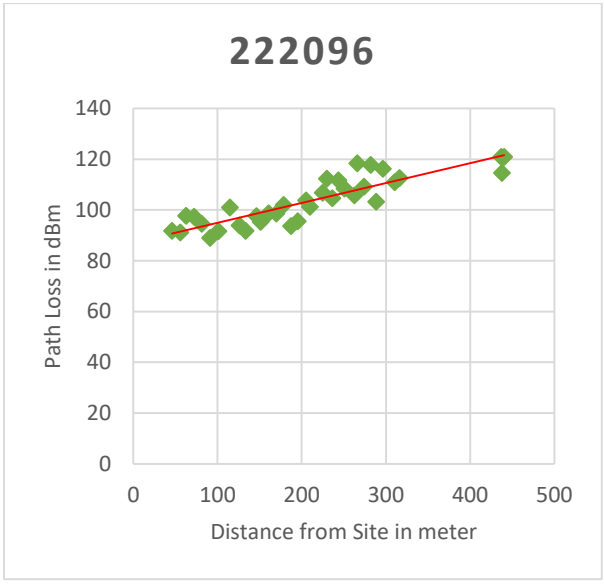
222096
Path Loss in dBm
Distance from Site in meter
0
20
40
60
80
100
120
140
0
100
200
300
400
500

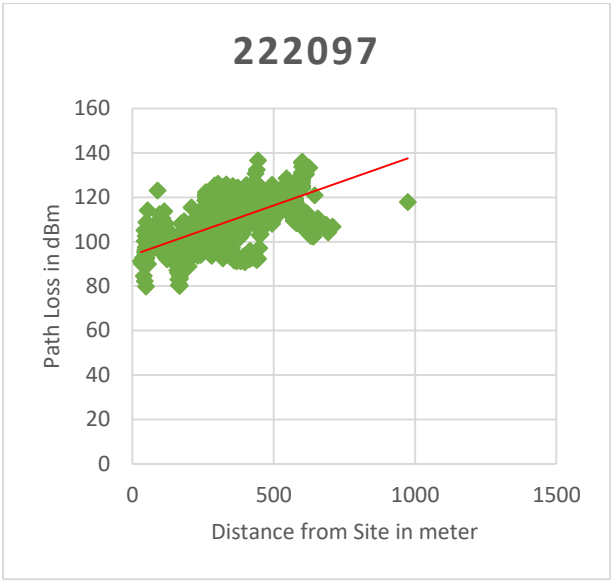
222097
Path Loss in dBm
Distance from Site in meter
0
20
40
60
80
100
120
140
160
0
500
1000
1500

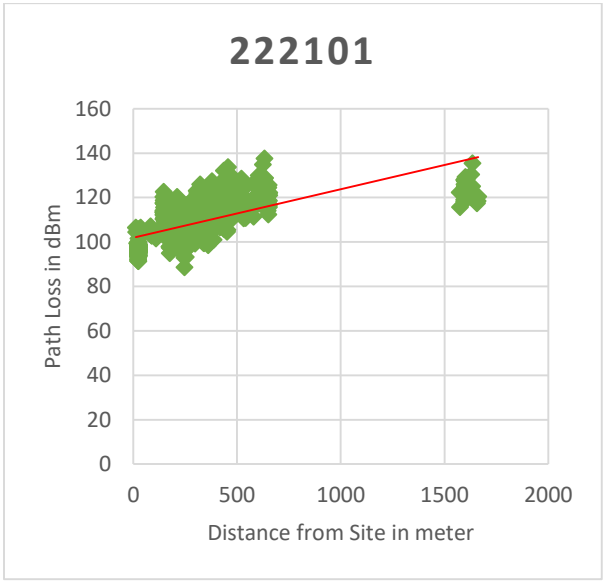
222101
Path Loss in dBm
Distance from Site in meter
0
20
40
60
80
100
120
140
160
0
500
1000
1500
2000

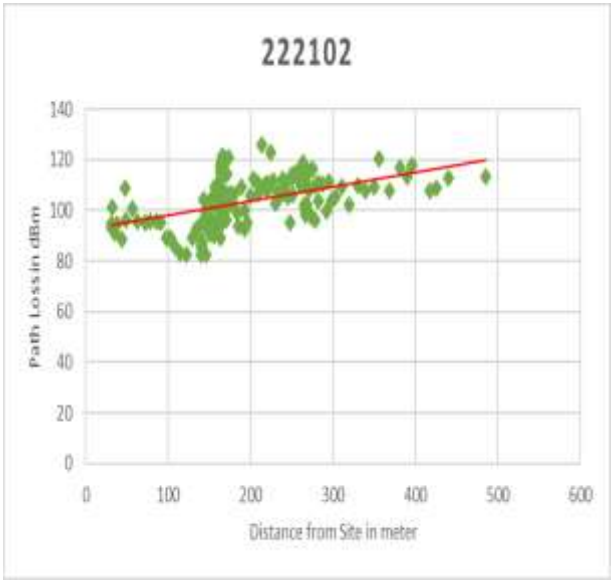
222102
Path Loss in dBm
Distance from Site in meter
0
20
40
60
80
100
120
140
0
100
200
300
400
500
600

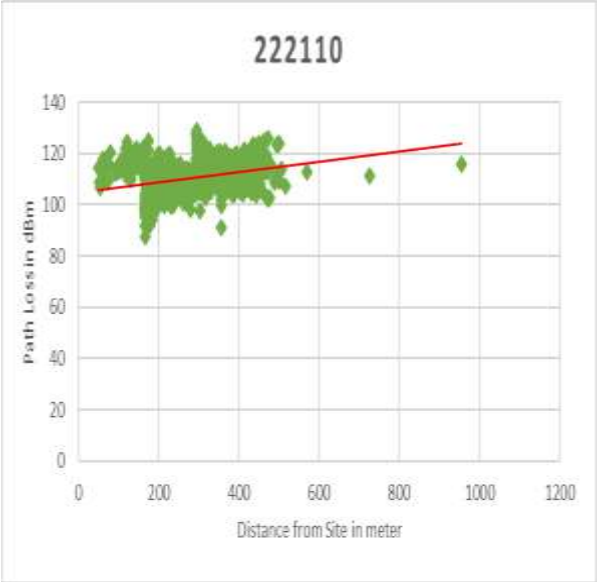
222110
Path Loss in dBm
Distance from Site in meter

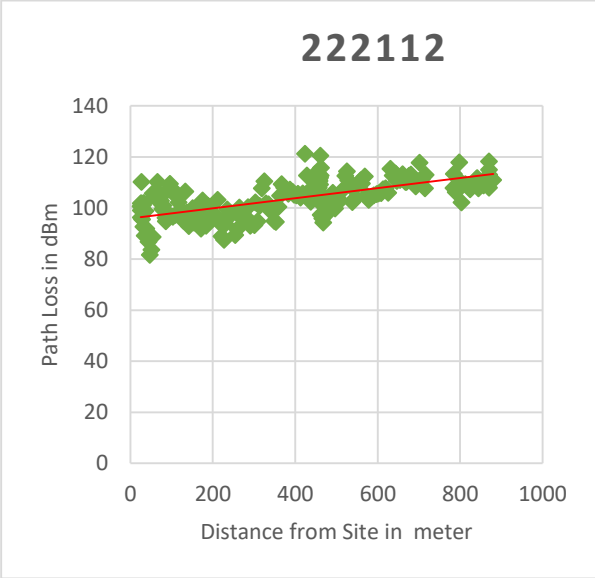
222112
Path Loss in dBm
Distance from Site in meter

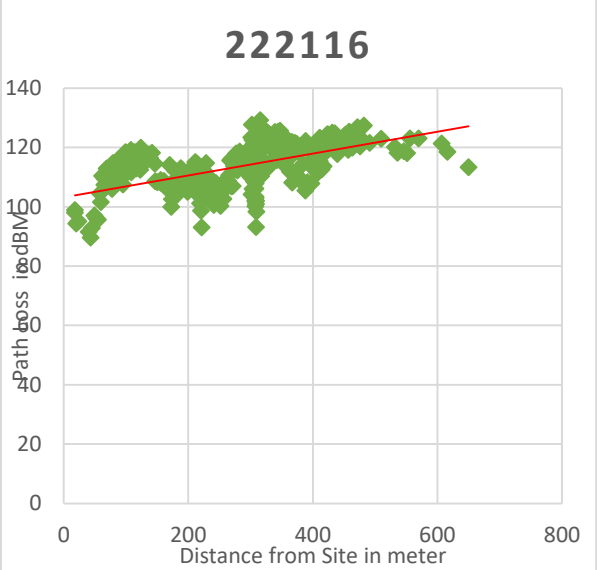
222116
Path Loss in dBm
Distance from Site in meter

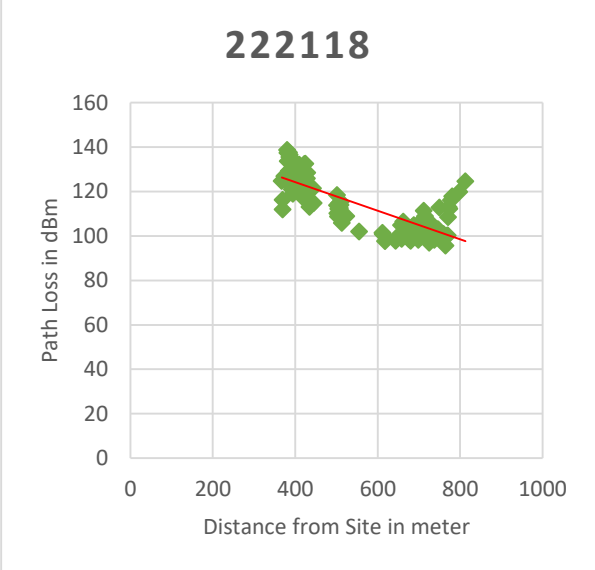
222118
Path Loss in dBm
Distance from Site in meter

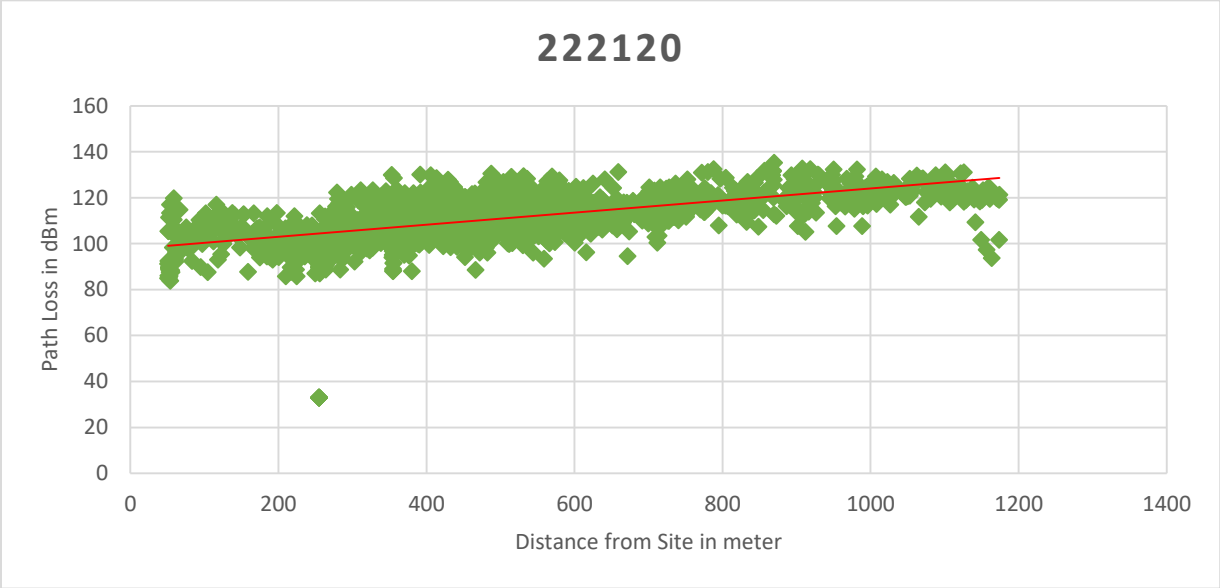

Figure 5.2 Collected Data Trend of selected sites at 2100 MHz

From the above general trend of the collected data samples we can observe that the path loss increases as the mobile station goes farther away from the base station. And this is expected characteristics of any propagation medium. But beyond that, we can observe how the samples are dispersed up and down in the path loss vs distance graph. Even if the average path loss is increasing vs distance, individual records runs up and down, at points where path loss is expected to be high it is low and vice versa. This is because of blockage and scattering of signals in the propagation and it is the main reason why we need to tune the path loss model according to the existing environment.

5.3 Site Classification based on Error Measurement

In this part of the Thesis sites are classified by comparing their measured path loss values with the forecasted path loss values of all models using the four error measurement techniques (Root mean square error (RMSE), Mean Absolute Percentage Error (MAPE), Standard Deviation (SD) and Mean Absolute Error (MAE)).

The following table shows the error measurement between estimated and measured path loss values at 1800 MHz frequency on each sites using all the five path loss models.

Table 5.1 Sites and PL models performance classification based on Error measurement (1800)

Area Type	PL Model	BS ID / Error Model	222078	222080	222082	222089	222096	222097	222101	222102	222105	222110	222112	222116	222118	222120
URBAN	COST-231	RMSE	15.66	8.42	12.45	7.00	10.52	9.66	9.47	7.52	11.43	8.24	15.09	7.40	12.95	8.90
		MAPE	12.65	5.66	9.53	4.79	6.34	5.42	6.11	4.99	5.33	5.40	11.59	0.47	8.36	6.08
		MAE	13.15	6.53	11.13	6.02	7.59	6.47	7.63	5.88	6.68	6.18	13.17	5.74	7.48	7.32
		SD	8.48	5.31	5.57	3.58	7.28	7.18	5.60	4.69	9.28	5.45	7.36	4.67	9.32	4.95
	SUI	RMSE	34.66	29.18	33.85	29.41	28.08	25.47	28.64	14.60	22.46	22.77	38.49	27.02	34.15	30.82
		MAPE	30.67	23.89	27.95	22.32	22.53	20.68	21.17	10.62	17.37	17.73	31.98	2.07	27.93	23.68
		MAE	33.32	28.08	32.21	27.99	26.80	24.65	26.44	12.59	21.56	20.72	36.96	25.79	26.74	29.07
		SD	9.56	7.94	10.41	9.01	8.36	6.39	11.00	7.39	7.80	9.45	10.75	8.06	11.57	10.11
	ECC-33	RMSE	13.61	6.46	9.63	3.83	6.72	6.79	8.20	6.82	9.70	7.58	11.12	6.25	10.76	5.83
		MAPE	10.86	4.20	7.01	2.43	3.81	3.42	4.43	4.47	4.97	5.83	8.00	0.38	6.96	3.94
		MAE	11.05	4.71	8.27	3.03	4.53	4.04	5.59	5.38	6.25	6.84	8.89	4.67	6.32	4.67
		SD	7.94	4.42	4.95	2.34	4.97	5.46	6.00	4.19	7.07	3.25	6.68	4.16	7.63	3.20
	ERICSSON	RMSE	17.42	9.75	15.57	7.61	10.23	9.96	10.74	4.97	9.46	9.03	16.76	8.46	14.51	11.06
		MAPE	14.51	7.08	12.55	5.18	7.25	7.24	7.71	3.38	5.84	6.15	13.28	0.58	9.50	8.01
		MAE	15.02	8.11	14.47	6.52	8.63	8.60	9.58	4.05	19.70	19.96	15.05	7.06	8.53	9.69
		SD	8.82	5.42	5.74	3.93	5.49	5.03	4.85	2.89	6.92	8.85	7.37	4.67	10.27	5.24
	HATA	RMSE	13.94	6.60	10.53	5.82	10.03	9.89	9.39	9.89	12.80	8.88	12.66	7.36	11.29	7.65
		MAPE	10.77	3.77	7.76	3.96	5.51	4.74	5.27	7.14	5.83	6.03	9.53	0.42	7.39	5.24
		MAE	11.19	4.30	9.14	4.95	6.55	5.67	6.60	8.39	7.31	7.08	10.77	5.20	6.66	6.27
		SD	8.31	5.01	5.22	3.07	7.60	8.11	6.68	5.24	9.56	5.35	6.65	5.22	7.96	4.21
SUB-URBAN	COST-231	RMSE	13,93	6.59	10.52	5.82	10.03	9.90	9.39	9.91	12.81	8.88	12.65	7.37	11.29	7.64
		MAPE	10.76	3.76	7.75	3.95	5.51	4.74	5.26	7.15	5.84	6.03	9.52	0.42	7.38	5.24
		MAE	11.18	4.29	9.13	4.94	6.55	5.67	6.60	8.40	7.32	7.09	10.76	5.20	6.66	6.27
		SD	8.31	5.00	5.22	3.07	7.60	8.11	6.68	5.24	9.56	5.35	6.65	5.22	7.96	4.21
	SUI	RMSE	33.68	28.19	32.36	27.68	26.99	24.38	26.66	14.62	21.16	22.10	36.71	25.35	32.57	28.94
		MAPE	29.78	23.25	26.84	21.17	21.78	19.91	19.72	11.09	16.40	17.22	30.69	1.95	26.57	22.40

		MAE	32.21	27.26	30.87	26.53	25.87	23.69	24.59	13.06	20.34	20.09	35.38	24.22	25.38	27.45
		SD	20.46	7.18	9.72	7.92	7.69	5.77	10.29	6.57	7.18	9.20	9.77	7.48	11.43	9.06
	ECC-33	RMSE	28.27	22.34	24.65	18.63	20.70	18.30	17.34	14.80	14.12	17.44	27.71	16.92	23.98	19.77
		MAPE	24.65	18.76	20.67	14.66	16.76	14.99	12.70	12.13	10.90	13.75	23.56	1.29	18.91	15.56
		MAE	26.00	21.68	23.56	18.23	19.73	17.62	15.72	13.82	13.43	15.87	26.84	15.89	17.78	18.90
		SD	11.08	5.38	7.26	3.83	6.29	4.95	7.34	5.30	4.67	7.24	6.90	5.80	10.88	5.68
	ERICSSON	RMSE	18.87	12.69	15.96	14.69	21.60	21.52	17.73	27.05	24.52	17.19	19.57	15.31	12.28	16.63
		MAPE	11.76	8.64	11.68	10.80	12.59	11.68	11.54	21.15	12.22	10.02	14.42	0.96	8.18	11.32
		MAE	13.01	9.72	13.39	13.40	14.72	13.76	14.35	24.08	15.16	11.84	16.85	11.94	7.44	13.81
		SD	13.67	8.16	8.70	6.02	15.81	16.55	10.41	12.32	16.04	12.47	9.96	9.58	8.41	9.15
	HATA	RMSE	13.02	10.64	10.65	12.32	15.47	17.15	16.15	20.99	21.78	17.34	8.37	15.18	12.07	12.43
		MAPE	8.86	8.53	6.40	8.89	9.98	11.94	10.73	17.37	15.26	12.61	5.71	1.07	8.88	8.32
		MAE	10.06	10.01	7.60	10.91	11.77	14.18	13.60	20.33	18.98	15.26	6.41	13.35	8.73	10.18
		SD	8.26	3.61	7.46	5.73	10.03	9.63	8.70	5.24	9.57	8.23	5.39	7.23	5.96	7.05
RULAR	COST-231	RMSE	13,93	6.59	10.52	5.82	10.03	9.90	9.39	9.91	12.81	8.88	12.65	7.37	11.29	7.64
		MAPE	10.76	3.76	7.75	3.95	5.51	4.74	5.26	7.15	5.84	6.03	9.52	0.42	7.38	5.24
		MAE	11.18	4.29	9.13	4.94	6.55	5.67	6.60	8.40	7.32	7.09	10.76	5.20	6.66	6.27
		SD	8.31	5.00	5.22	3.07	7.60	8.11	6.68	5.24	9.56	5.35	6.65	5.22	7.96	4.21
	SUI	RMSE	33.23	27.72	31.62	26.76	26.45	23.87	25.63	14.80	20.50	21.83	35.76	24.48	31.74	27.95
		MAPE	29.33	22.96	26.30	20.58	21.41	19.55	18.97	11.50	15.90	17.13	30.01	1.88	25.85	21.74
		MAE	31.64	26.89	30.21	25.76	25.40	23.22	23.63	13.48	19.70	19.96	34.56	23.39	24.66	26.62
		SD	10.14	6.76	9.35	7.26	7.36	5.50	9.92	6.11	6.92	8.85	9.21	7.22	11.36	8.45
	ERICSSON	RMSE	30.35	24.70	22.83	24.14	36.95	37.68	26.67	50.31	40.75	32.61	25.99	25.51	11.39	25.25
		MAPE	15.81	16.93	15.78	17.93	21.85	21.83	15.84	40.39	22.34	21.98	18.90	1.52	6.81	16.33
		MAE	17.30	18.83	17.64	21.98	25.36	25.35	19.61	45.90	27.54	25.92	21.75	18.59	6.25	19.73
		SD	24.94	15.99	14.49	9.98	26.86	27.88	18.07	20.59	26.21	19.78	14.21	17.46	8.57	15.71
	HATA	RMSE	15.73	8.49	12.52	7.06	10.55	9.67	9.48	7.45	11.39	8.24	15.18	7.42	13.02	8.95
		MAPE	12.72	5.74	9.60	4.83	6.37	5.45	6.15	4.95	5.33	5.40	11.66	0.47	8.40	6.13
		MAE	13.23	6.62	11.21	6.08	7.64	6.51	7.68	5.83	6.68	6.16	13.25	6.11	9.18	7.38
		SD	8.49	5.32	5.58	3.60	7.28	7.15	5.56	4.63	8.19	5.46	7.39	4.68	9.23	4.97

As shown in the above table the RMSE, MAPE, MAE and SD between the measured and the estimated path loss are calculated to all sites. And based on the closeness of the estimated path loss to the measured one, sites are classified to the three area types (Urban, Sub-urban and rural). Since RMSE and MAPE calculates closeness better than the other tools, they are mainly used to classify the sites. Thus, according to the error measurement tools the least values shows the highest closeness of the path loss models to the measured data. In addition to classifying the area type of the sites, the table also shows which path loss model predict that area best.

Therefore, out of the evaluated 14 sites, 11 sites are classified under Urban area type whereas the remaining 3 sites have fallen into Sub-Urban area type. And as can be seen on the highlighted cells of the table, among the sites classified in the urban type ECC-33 has performed best in 10 of them which is 91 % of the urban sites. When we see the RMSE, the minimum it has scored is 3.83. Ericsson model has performed best in the remaining 1 site of the urban sites which is 9 % of the total urban sites.

Out of the 3 sites which have fallen under Sub-Urban area type Hata path loss model has performed best in 2 of them, which means 67% of the total Sub-Urban type area. When we see their RMSE, the minimum value scored is 8.37. And in the remaining 1 site of Sub-urban area COST-231 model performed better. This means 33% of the total Sub-Urban type area.

The following table shows each sites and the area they are categorized in:

Table 5.2 1800 Mhz Sites and the area type they categorized into

No.	Site ID	Antenna Height	Best Fit Model	Area Type
1	222082	35	ECC-33	Urban
2	222089	29	ECC-33	Urban
3	222096	27	ECC-33	Urban
4	222097	33	ECC-33	Urban
5	222101	38	ECC-33	Urban
6	222102	29	Ericsson	Urban
7	222105	37	ECC-33	Urban
8	222110	34	ECC-33	Urban
9	222116	34	ECC-33	Urban

10	222118	30	ECC-33	Urban
11	222120	35	ECC-33	Urban
12	222078	29	Hata	Sub-Urban
13	222080	27	Cost-231	Sub-Urban
14	222112	30	Hata	Sub-Urban

The following table shows the error measurement between estimated and measured path loss values at 2100 MHz frequency on each sites using all the five path loss models.

Table 5.3 Sites and PL models performance classification based on Error measurement (2100)

Area Type	PL Model	BS ID / Error Model	222078	222080	222082	222089	222096	222097	222101	222102	222110	222112	222116	222118	222120
URBAN	COST-231	RMSE	18.30	17.32	23.13	13.14	12.15	15.79	45.23	13.17	13.42	23.90	11.26	24.92	18.66
		MAPE	16.40	14.60	19.28	10.51	10.97	10.46	30.38	12.17	10.01	21.24	8.51	21.28	16.01
		MAE	16.50	16.15	21.31	11.87	11.18	15.84	57.71	12.77	11.42	22.16	9.67	22.47	17.52
		SD	7.90	6.16	8.99	5.63	4.78	7.75	6.17	3.22	7.05	8.95	5.77	10.77	6.36
	SUI	RMSE	38.23	39.19	47.33	34.75	29.44	34.61	29.09	35.08	33.09	46.20	30.35	48.12	40.81
		MAPE	35.88	34.05	41.19	29.46	27.61	24.15	19.45	32.74	25.87	42.50	24.54	43.42	34.70
		MAE	37.48	37.96	45.62	33.90	28.65	37.92	32.07	34.84	29.82	44.69	28.06	31.26	38.50
		SD	7.53	9.21	12.62	7.64	6.78	9.89	8.31	4.03	14.33	11.72	11.57	19.36	13.50
	ECC-33	RMSE	17.09	14.27	18.16	10.39	13.56	12.15	7.16	13.81	9.45	20.13	8.53	20.43	14.57
		MAPE	15.17	12.04	15.31	8.16	12.55	7.74	4.53	12.76	6.47	18.19	6.62	16.89	12.18
		MAE	14.97	13.12	16.83	9.05	12.40	12.67	7.70	13.26	7.38	18.83	7.40	11.64	13.13
		SD	8.23	5.56	6.81	5.10	5.47	6.87	4.39	3.84	5.91	7.09	4.24	11.87	6.24
	ERICSSON	RMSE	65.28	17.45	24.89	14.07	14.23	17.00	12.78	17.03	14.71	24.87	13.16	25.43	20.75
		MAPE	60.41	14.89	21.45	11.39	13.30	11.45	8.27	15.95	10.94	22.59	10.53	21.92	17.70
		MAE	64.73	16.36	23.63	12.79	13.42	18.36	14.12	16.75	12.56	23.51	11.91	15.38	19.31
		SD	8.47	6.05	7.82	5.86	4.73	7.19	5.74	3.05	7.67	8.10	5.60	13.03	7.54
	H	RMSE	13.73	12.65	18.39	8.79	7.60	12.03	6.79	9.95	10.83	19.11	9.56	22.25	16.18

		MAPE	12.07	10.55	14.94	7.00	6.60	7.47	4.30	9.05	7.50	17.32	7.06	18.54	13.76
		MAE	12.09	11.69	16.49	7.86	6.59	10.68	6.92	9.52	8.46	18.04	8.00	12.83	15.02
		SD	6.52	4.64	8.13	3.95	3.78	7.60	3.67	2.89	6.76	6.32	5.23	12.65	5.95
SUB-URBAN	COST-231	RMSE	15.72	14.51	20.48	10.64	9.36	13.53	6.78	12.02	11.77	21.13	9.55	22.24	16.17
		MAPE	13.94	12.20	16.70	8.40	8.01	8.69	4.29	11.08	8.44	18.99	7.05	18.52	13.75
		MAE	13.97	13.51	18.46	9.43	8.12	12.71	6.91	11.67	9.57	19.79	7.99	12.82	15.00
		SD	7.20	5.13	8.86	4.93	4.65	7.75	3.66	2.89	6.85	7.41	5.23	12.65	5.95
	SUI	RMSE	37.55	38.00	45.17	33.55	29.69	33.14	27.60	34.64	31.79	44.80	29.40	46.35	39.15
		MAPE	35.37	33.23	39.55	28.59	28.14	23.14	18.50	32.45	25.22	41.42	24.11	41.82	33.66
		MAE	36.81	36.98	43.74	32.82	29.08	36.85	31.03	34.47	29.05	43.49	27.50	30.09	37.24
		SD	7.46	8.38	11.28	6.97	5.95	9.07	7.39	3.47	12.90	10.74	10.41	18.71	12.05
	ECC-33	RMSE	34.14	29.76	35.97	27.67	31.37	26.15	20.88	31.98	25.72	37.99	24.84	37.60	32.00
		MAPE	32.22	26.58	32.09	23.87	30.53	18.22	13.97	30.20	21.56	35.75	21.28	33.78	28.57
		MAE	32.86	29.20	35.32	27.03	30.89	31.16	25.40	31.75	24.72	37.32	23.96	24.21	31.20
		SD	9.24	5.57	6.81	5.91	5.47	6.87	5.54	3.84	7.10	7.09	6.55	15.74	7.06
	ERICSSON	RMSE	11.66	17.00	28.82	12.78	15.06	16.08	11.81	7.98	14.71	23.22	18.27	24.48	24.07
		MAPE	9.90	11.87	22.64	8.55	10.11	9.72	6.48	6.70	10.94	20.37	12.24	19.94	19.80
		MAE	10.46	13.49	25.22	9.88	9.64	12.96	12.21	7.05	28.73	21.71	13.58	13.77	22.02
		SD	5.16	10.32	13.95	8.10	11.57	11.23	7.70	3.74	12.03	8.24	12.22	14.54	9.66
	HATA	RMSE	7.93	6.96	9.88	8.19	7.70	6.26	6.29	3.77	13.43	10.23	11.66	12.87	9.78
		MAPE	5.56	4.75	7.18	4.98	5.91	3.58	2.97	2.51	10.03	8.47	7.94	9.86	6.98
		MAE	5.94	5.32	7.79	5.88	6.17	6.63	7.28	2.72	11.38	8.75	9.04	6.67	7.43
		SD	5.26	4.48	6.09	5.69	4.60	4.25	5.98	2.61	7.14	5.30	7.36	8.54	6.28
RULAR	COST-231	RMSE	15.72	14.51	20.48	10.64	9.36	13.53	6.78	12.02	11.77	21.13	9.55	22.24	16.17
		MAPE	13.94	12.20	16.70	8.40	8.01	8.69	4.29	11.08	8.44	18.99	7.05	18.52	13.75
		MAE	13.97	13.51	18.46	9.43	8.12	12.71	6.91	11.67	9.57	19.79	7.99	12.82	15.00
		SD	7.20	5.13	8.86	4.93	4.65	7.75	3.66	2.89	6.85	7.41	5.23	12.65	5.95
	SUI	RMSE	37.29	37.40	44.02	32.96	29.99	32.37	26.84	34.52	31.15	44.09	28.99	45.40	38.32
		MAPE	35.18	32.85	38.69	28.17	28.60	22.60	18.00	32.40	24.95	40.89	23.98	40.96	33.17
		MAE	36.53	36.50	42.76	32.29	29.48	36.35	30.56	34.37	28.73	42.90	27.30	29.47	36.62

		SD	7.51	7.89	10.48	6.62	5.51	8.61	6.90	3.20	12.03	10.17	9.73	18.35	11.22
	ERICSSON	RMSE	19.07	24.82	34.27	20.88	37.06	14.74	12.81	19.93	35.11	26.11	33.06	22.34	33.80
		MAPE	15.14	18.57	26.62	13.81	31.27	8.17	5.33	15.39	23.14	19.33	21.34	17.72	23.74
		MAE	15.57	20.49	29.48	15.33	30.40	18.33	17.79	15.44	25.89	20.68	23.32	12.22	26.16
		SD	11.01	12.36	17.48	14.17	21.20	13.24	16.21	12.60	23.72	15.93	23.44	13.87	21.38
	HATA	RMSE	16.37	15.36	21.15	11.26	10.20	14.21	8.82	12.95	12.15	21.90	11.36	25.06	18.79
		MAPE	14.53	12.93	17.31	8.89	8.86	9.23	5.64	11.98	8.77	19.62	8.60	21.42	16.12
		MAE	14.57	14.32	19.14	9.99	9.01	13.67	8.48	12.62	9.97	20.45	9.78	14.98	17.64
		SD	7.46	5.41	8.99	5.19	4.78	7.75	5.39	2.89	6.93	7.84	5.79	13.20	6.39

The Same as 1800 Mhz sites analysis the above table also presents the performance the path loss models in each 2100 Mhz sites. Therefore, out of observed 13 sites, 2 sites are classified under Urban area type whereas the remaining 11 sites falls under Sub-Urban area type. The highlighted parts of the table show the minimum values scored under each sites and minimum value means that Path loss model prediction is closer to the measured value. And based on that, among the sites classified in the urban type ECC-33 has performed best in all of them which is 100 % of the urban sites. When we see the RMSE, the minimum it has scored is 8.53.

And out of the 11 sites which have fallen under Sub-Urban area type Hata path loss model has performed best in all of them, which means 100% of the total Sub-Urban type area. When we see their RMSE, the minimum value scored is 6.26.

The following table shows each sites and the area they are categorized in:

Table 5.4 2100 MHz Sites and the area type they categorized into

No.	Site ID	Antenna Height	Best Fit Model	Area Type
1	222110	30	ECC-33	Urban
2	222116	34	ECC-33	Urban
3	222078	29	Hata	Sub-Urban
4	222080	27	Hata	Sub-Urban
5	222082	35	Hata	Sub-Urban
6	222089	29	Hata	Sub-Urban

7	222096	27	Hata	Sub-Urban
8	222097	33	Hata	Sub-Urban
9	222101	38	Hata	Sub-Urban
10	222102	29	Hata	Sub-Urban
11	222112	30	Hata	Sub-Urban
12	222118	30	Hata	Sub-Urban
13	222120	35	Hata	Sub-Urban

After categorizing the sites into the area type where they behave the nearest, now we can see the measured path loss trend of each sites in their respective area.

The following graph shows the measured path loss trend of sites classified under Urban area type at 1800 Mhz frequency.

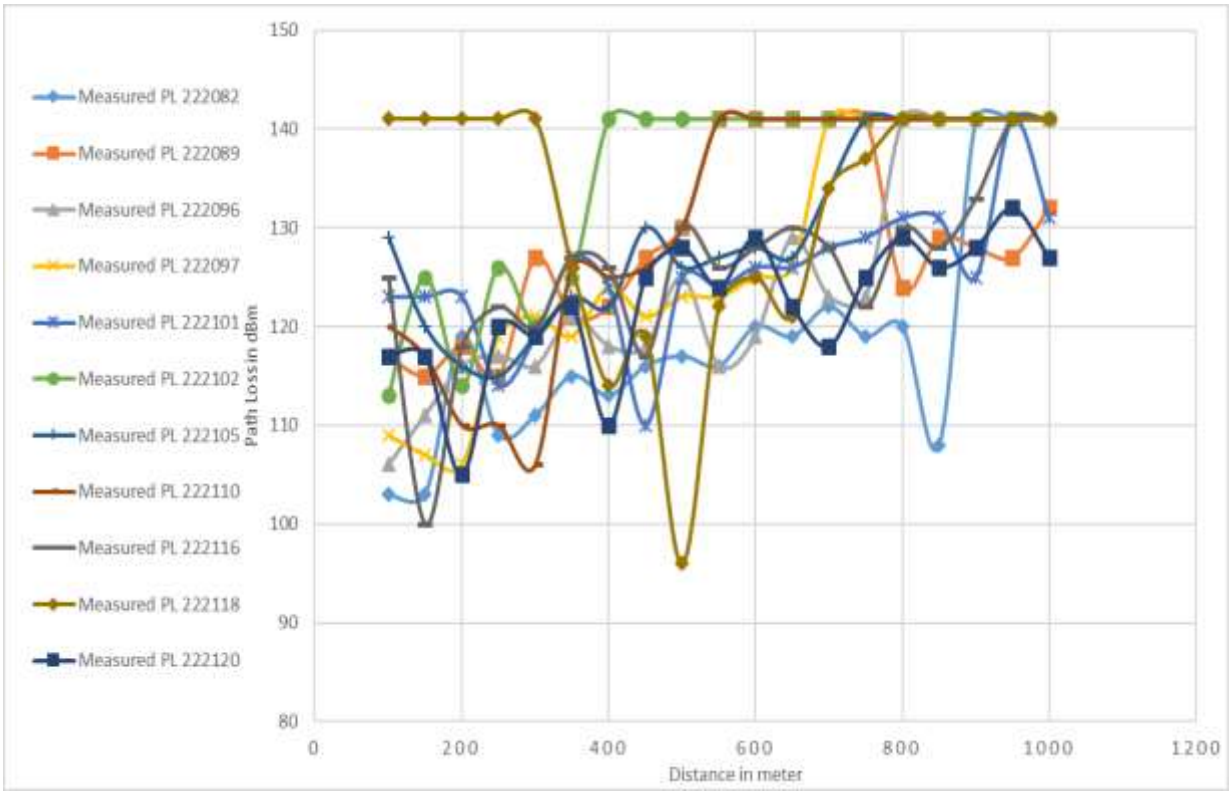

Figure 5.3 Measured Path Loss trend of Sites in Urban area type at 1800 Mhz

Whereas, the next graph shows the measured path loss trend of sites classified under Sub-Urban area type at 1800 Mhz frequency.

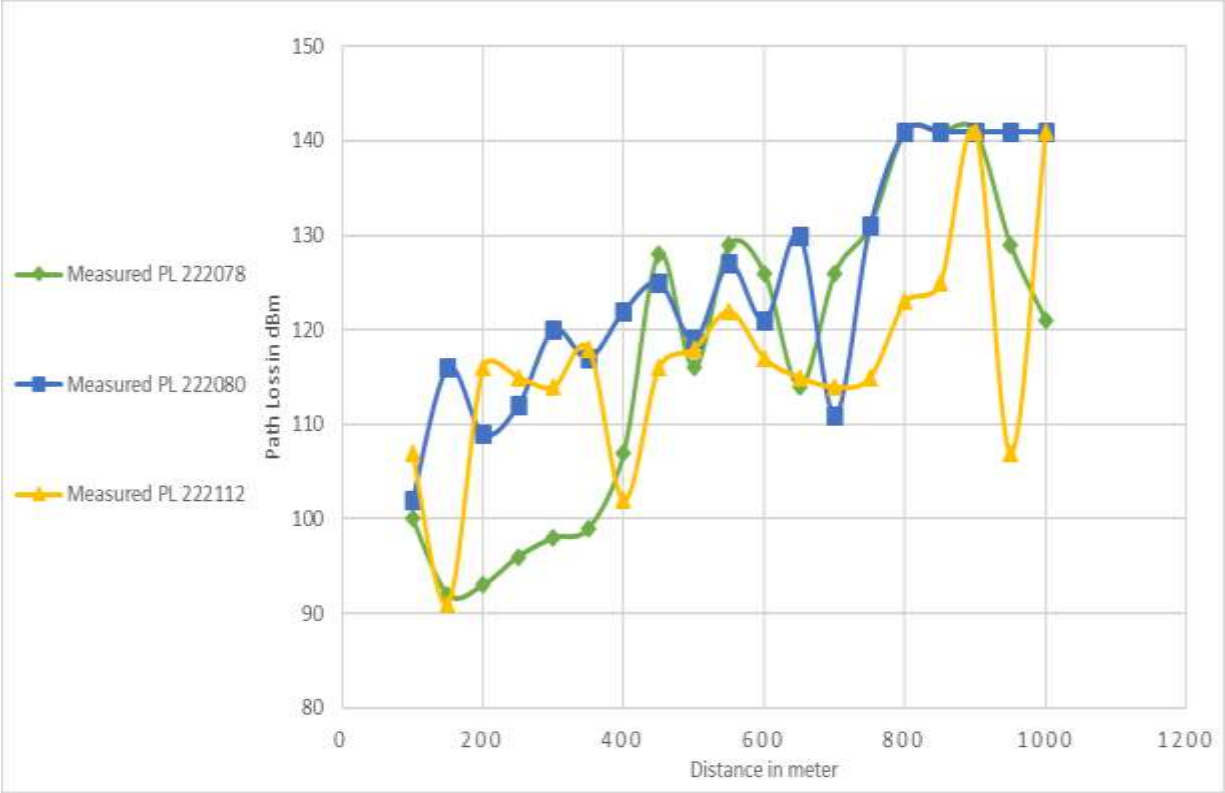

Figure 5.4 Measured Path Loss trend of Sites in Sub-Urban area type at 1800 Mhz

The above two figures show the measured path loss characteristics of selected 1800 Mhz sites versus distance in Urban and Sub-urban area types respectively. As shown in the figures each sites are represented by different colors. The graph is plotted using path loss records taken at 100m interval. Even if the path loss runs up and down unpredictably, we can see that the average path loss is increasing vs distance.

After categorizing the sites in their area types and observing the measured path loss trend of each sites. I have calculated the average measured path loss of both area types and evaluated it against all path loss models so that I can determine which path loss model predict each area type best. And as shown in the below table, for Urban area type ECC-33 scores the least value when compared to the other models with RMSE of 4.18. ECC-33 was also the best model (in 91 % of the total Urban sites) in urban areas when each sites were analyzed separately. And for Sub-urban area type HATA scores the least value when compared to the other models with RMSE of 7.86.

Table 5.5 Urban area type Average measured path loss performance at 1800 MHz

RMSE					MAPE					MAE				
Cost-231	SUI	Ericsson	ECC-33	Hata	Cost-231	SUI	Ericsson	ECC-33	Hata	Cost-231	SUI	Ericsson	ECC-33	Hata
4.26	25.18	4.45	4.18	4.96	2.39	18.8	3.16	2.64	2.41	3.12	25.45	4.18	3.56	3.1

Table 5.6 Sub-Urban area type Average measured path loss performance at 1800 MHz

RMSE					MAPE					MAE				
Cost-231	SUI	Ericsson	ECC-33	Hata	Cost-231	SUI	Ericsson	ECC-33	Hata	Cost-231	SUI	Ericsson	ECC-33	Hata
7.95	31.75	12.12	24.15	7.86	5.92	26.45	8.3	20.28	5.15	6.88	31.2	9.7	23.49	6.24

The following graphs shows the average measured path loss of Urban and Sub-Urban areas in comparison with the best fit path loss prediction model in that area.

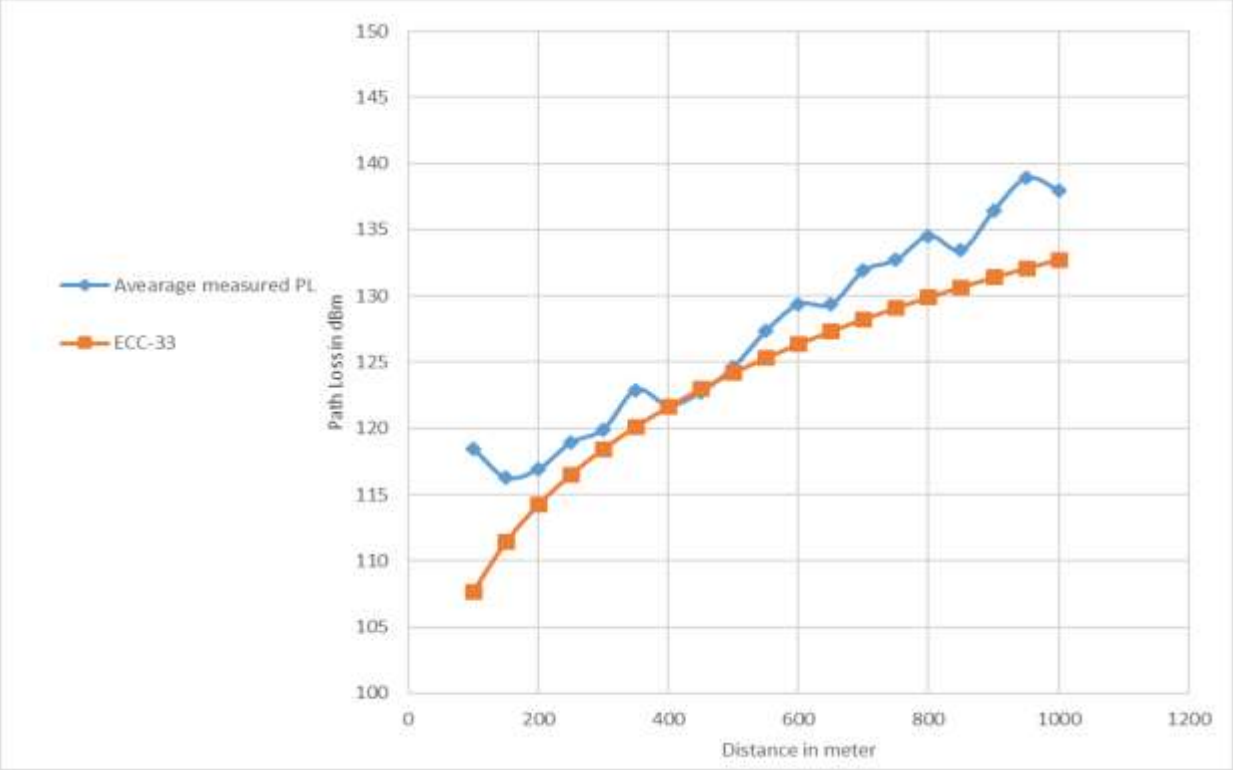

Figure 5.5 Urban area type average measured path loss and ECC-33 model for 1800 MHz

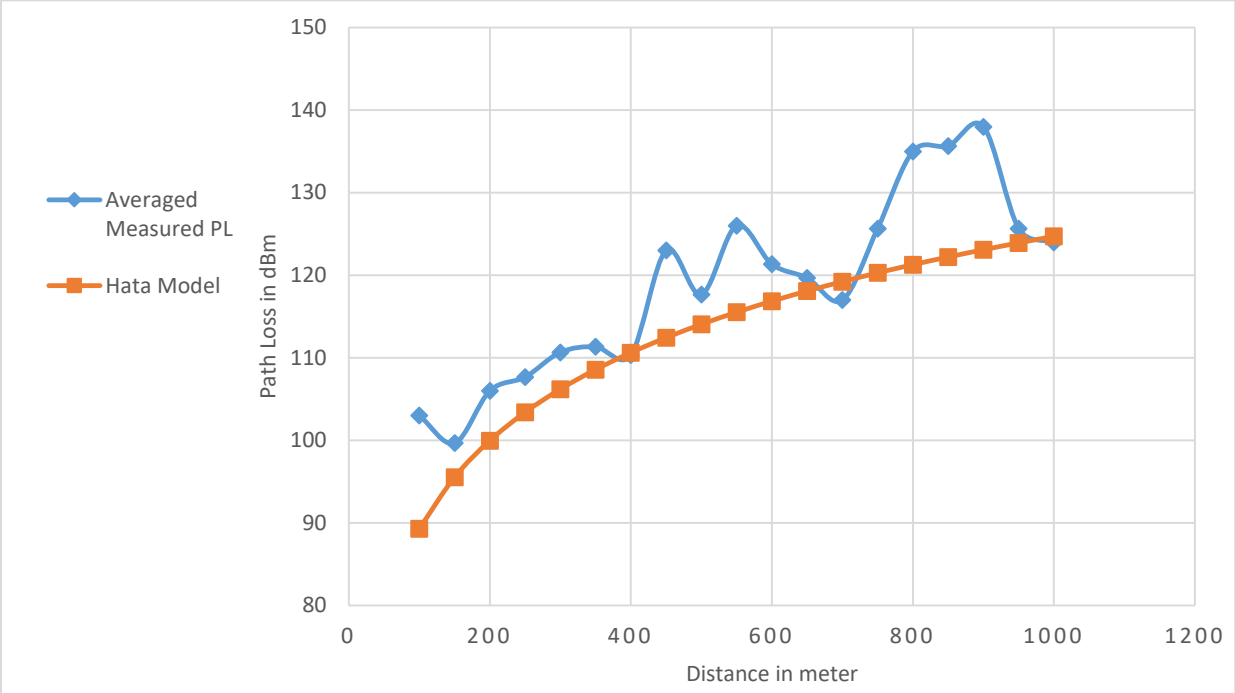

Figure 5.6 Sub Urban area type average measured path loss and Hata model for 1800

The above two figures compare selected sites averaged path loss characteristics in both urban and Sub urban areas with the best fit path loss model determined in that respective area type. As can be seen on the figure the averaged path loss trend of urban areas and sub-urban areas trace ECC-33 and Hata path loss models respectively.

Similar to the analysis at 1800 MHz frequency, the below graphs and tables explain the collected path loss data of 2100 MHz and its analysis.

The following graph shows the measured path loss trend of sites classified under Urban area type at 2100 Mhz frequency.

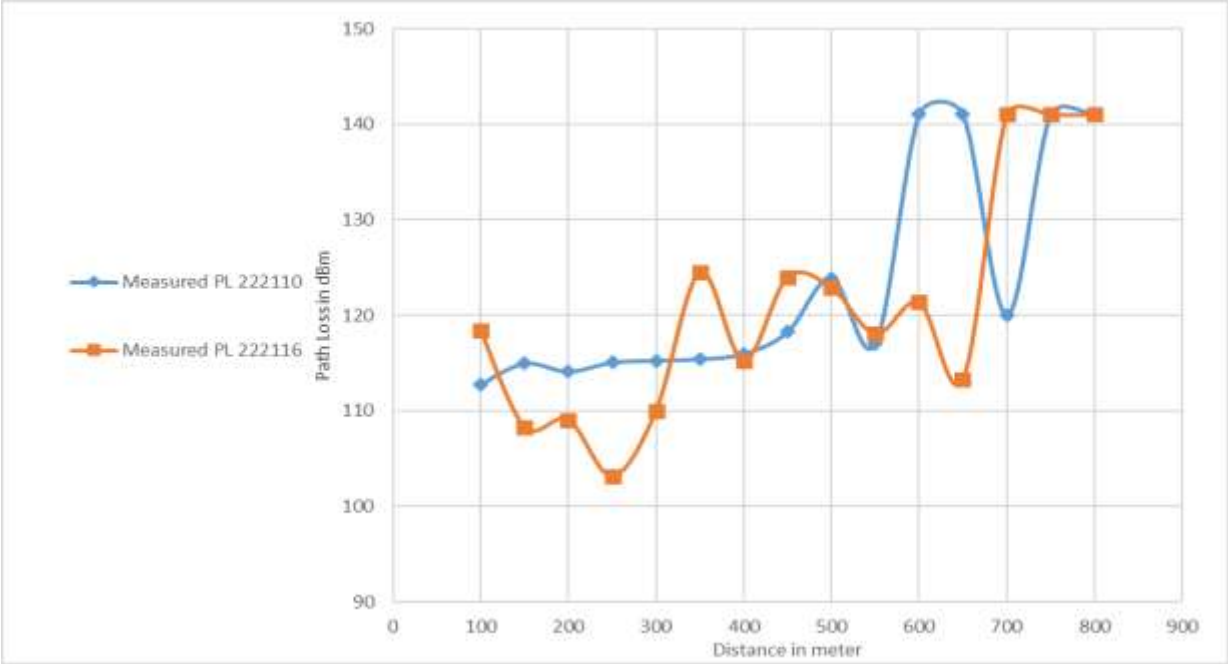

Figure 5.7 Measured Path Loss trend of Sites in Urban area type at 2100 Mhz

Whereas, the next graph shows the measured path loss trend of sites classified under Sub-Urban area type at 2100 Mhz frequency.

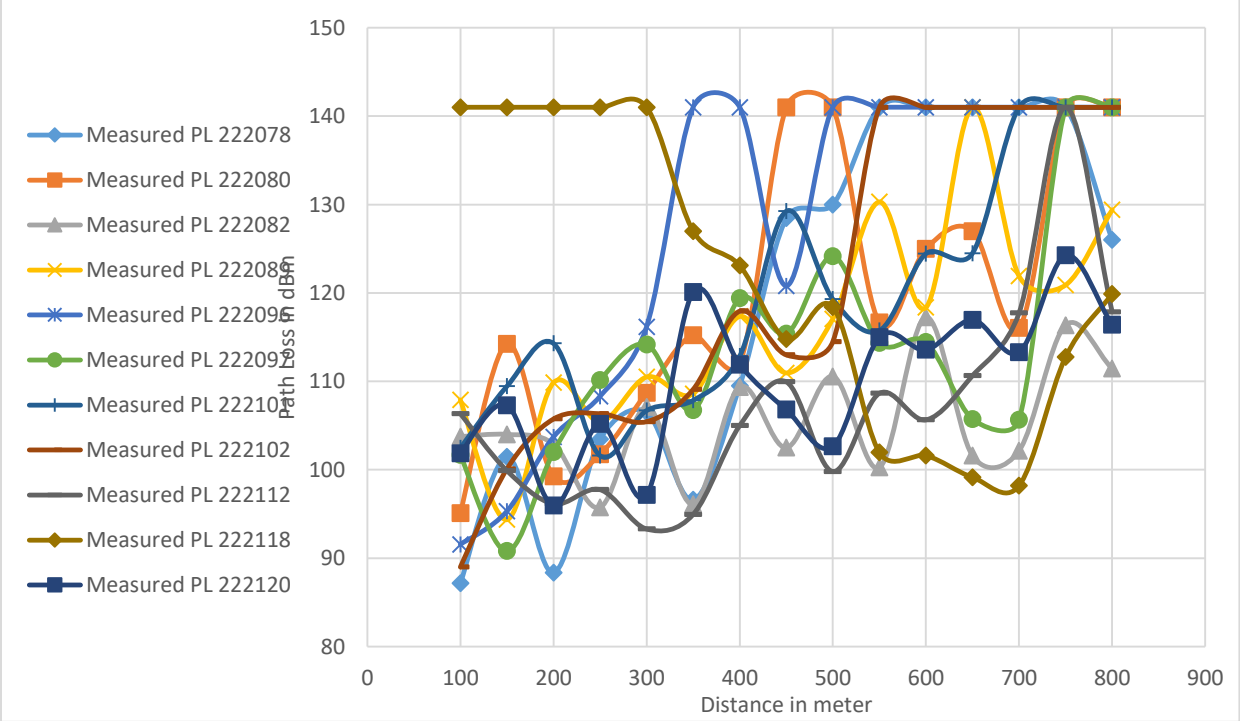

Figure 5.8 Measured Path Loss trend of Sites in Sub-Urban area type at 2100 Mhz

Similarly, the above two figures also show the measured path loss characteristic of selected 2100 Mhz sites versus distance in Urban and Sub-urban area types respectively. As shown in the figures each sites are represented by different colors. The graph is plotted using path loss records taken at 100m interval. Even if the path loss runs up and down unpredictably, we can see that the average path loss is increasing vs distance.

As done in 1800 MHz data, here the average measured path loss of 2100 MHz sites in both area types is calculated and evaluated against all path loss models. And as shown in the below table, for Urban area type ECC-33 scores the least value when compared to the other models with RMSE of 6.15. ECC-33 was also the best model in all urban areas when each sites were analyzed separately. And for Sub-urban area type HATA scores the least value when compared to the other models with RMSE of 6.11.

Table 5.7 Urban area type Average measured path loss performance at 2100 MHz

RMSE					MAPE					MAE				
Cost-231	SUI	Ericsson	ECC-33	Hata	Cost-231	SUI	Ericsson	ECC-33	Hata	Cost-231	SUI	Ericsson	ECC-33	Hata
7.73	27.8	9.49	6.15	6.5	5.72	22.06	7.17	4.26	4.59	6.81	26.71	8.48	5.18	5.51

Table 5.8 Sub-Urban area type Average measured path loss performance at 2100 MHz

RMSE					MAPE					MAE				
Cost-231	SUI	Ericsson	ECC-33	Hata	Cost-231	SUI	Ericsson	ECC-33	Hata	Cost-231	SUI	Ericsson	ECC-33	Hata
7.87	31.62	10.85	25.62	6.11	6.23	26.98	8.03	22.13	4.51	7.2	31.34	9.28	25.4	5.22

Similar to the 1800 MHz analysis, the following graphs shows the average measured path loss of Urban and Sub-Urban area in comparison with the best fit path loss prediction model in that area.

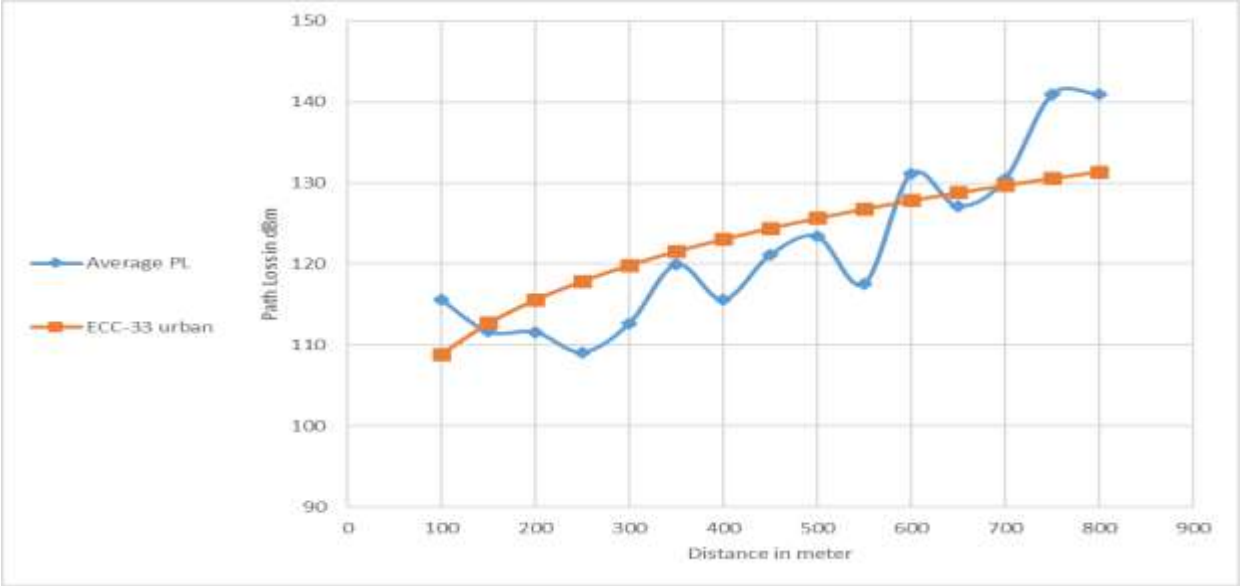

Figure 5.9 Urban area type average measured path loss and ECC-33 model for 2100 MHz

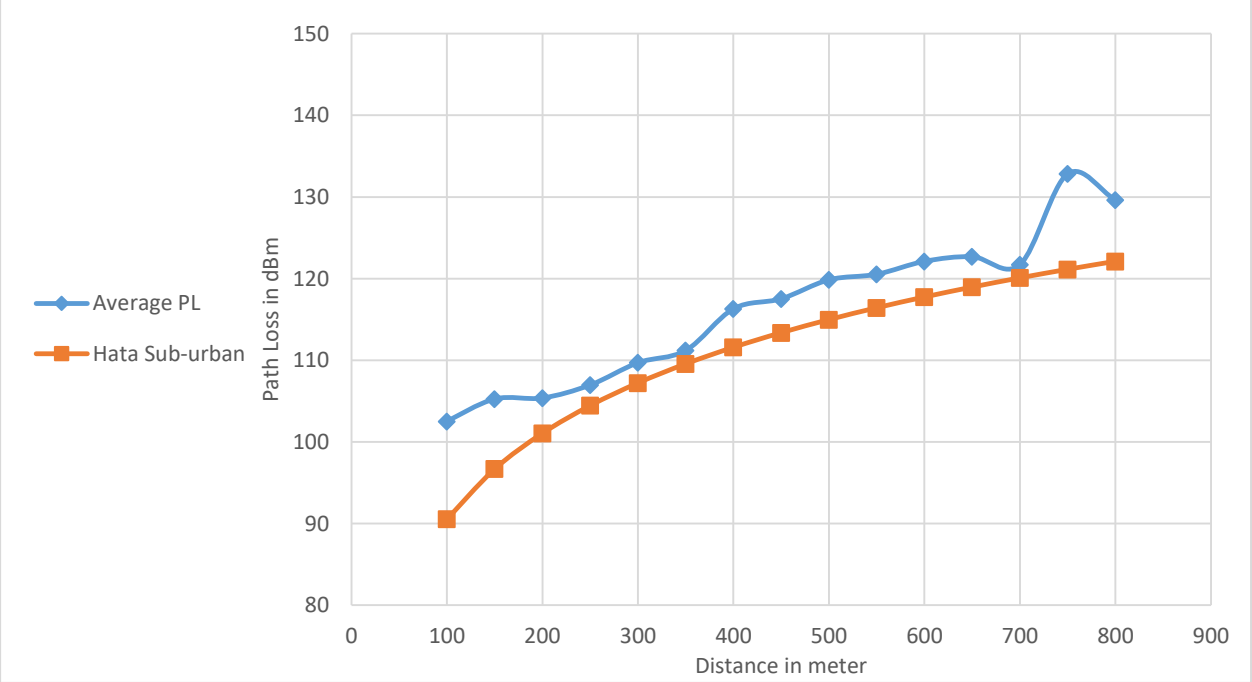

Figure 5.10 Sub-Urban area type average measured path loss and Hata model for 2100 MHZ

The above two figures compare selected 2100 Mhz sites averaged path loss characteristic in both urban and Sub urban area with the best fit path loss model determined in that respective area type. As can be seen on the figure the averaged path loss trend of urban areas and sub-urban areas trace ECC-33 and Hata path loss models respectively.

5.4 Model Optimization

As briefly shown in the collected data analysis part, the best measured path loss data estimating models have been selected. So based on the analysis, ECC-33 is the best estimating model for urban areas where Hata model is selected to be the best method in Sub-Urban areas at both 1800 MHz and 2100MHz frequencies. And after selecting the best estimating models, in this section the model optimization will be done for both area types. The model optimization is done using Linear Least Square method (LLSM). Once the optimized path loss model is found the RMSE values are calculated to see how close the model is tuned to the measured data.

In the model tuning process the average height of 1800 Mhz base station antennas in urban areas and Sub Urban area is rounded to 30m and 28m respectively. Whereas, the average height of 2100 Mhz base station antennas in urban areas and Sub Urban area is rounded to 34m and 33m respectively.

5.4.1 Correction Factors and Parameters after Calibration for 1800MHZ

The following tables shows the calibrated parameters of the models based on the calculations presented in the appendix and the RMSE values of the optimized models.

For Urban area types:

Table 5.9 Tuned parameters of ECC-33 model for Urban area

C1	Tuned slope value of $A_{bm,}$C2	Tuned offset value of $A_{bm,}$K1	K2
135.575	28.187	23.207	8.187

Then, the calibrated ECC-33 model equation for Urban area types will be:

$$PL_{ECC-33} = A_{fs} + \widetilde{A_{bm}} - G_b - G_r \quad (5.18)$$

where,

$$A_{fs} = 92.4 + 20\log_{10} d + 20\log_{10} f \quad (5.19)$$

$$\widetilde{A_{bm}} = 23.21 + 8.19\log_{10} d + 7.894\log_{10} f + 9.56[\log_{10} f]^2 \quad (5.20)$$

$$G_b = \log_{10}(\frac{h_b}{200})\{13.958 + 5.8[\log_{10} d]^2\} \quad (5.21)$$

$$G_r = 0.759h_r - 1.862 \quad (5.22)$$

The performance of the calibrated ECC-33 model for Urban area will be:

Table 5.10 Performance of Tuned ECC-33 after for urban area

RMSE	MAPE	MAE	SD
2.46	1.54	2.04	1.53

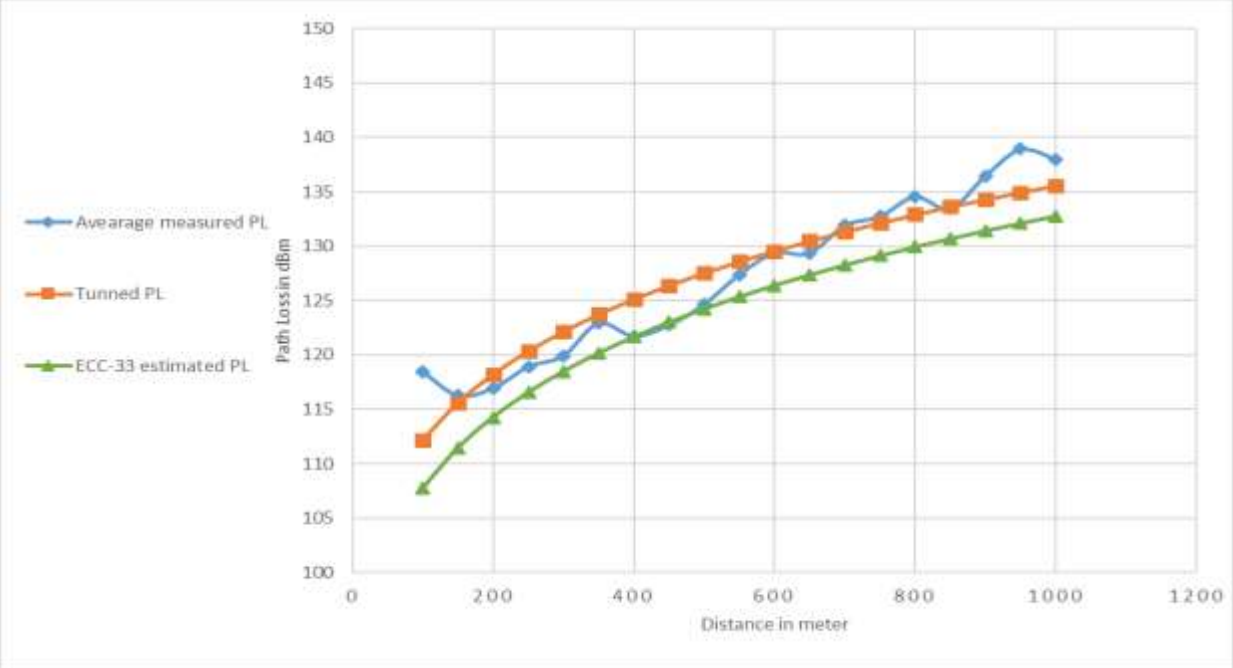

Figure 5.11 Urban area Calibrated ECC-33 model Vs measured PL and original ECC-33 (1800)

The above figure shows the comparison of Urban area tuned path loss model characteristics versus selected sites averaged path loss characteristics and ECC-33 (Urban area best fit model) path loss characteristics at 1800 Mhz. And as shown on the graphs trend the tuned path loss model is closer to the measured Path Loss than the original model, which means it can estimate hawassa's Urban areas propagation environment (at 180 MHz) better than the original model, and it have also optimized the sinusoidal feature of the averaged measured path loss model to linearly increasing path loss versus distance. Therefore, we can say that calibrated ECC-33 model can finely represent Urban area types of Hawassa city.

For Sub-Urban area types:

Table 5.11 Tuned parameters of Hata model for Sub-Urban area

Tuned parameter $\tilde{a}$	Tuned parameter $\tilde{b}$	Esys	Bsys	Original Eo	Tuned Eo	Slope Correction factor, $\widetilde{B_{sys}}$
130.135	33.982	83.772	35.421		46.362	0.959

Then, the calibrated Hata model equation for Sub-Urban area types will be:

$$\mathbf{PL_{Hata} = 46.36 + 33.9\log_{10} f - 13.82\log_{10} h_b - a_{hm} + (43.06 - 6.28\log_{10} h_b)\log_{10} d - 2\left[\log_{10}\left(\frac{f}{28}\right)\right]^2} \quad (5.23)$$

Where,

$$a_{hm} = (1.1\log_{10} f - 0.7)h_m - (1.56\log_{10} f - 0.8) \quad (5.24)$$

The performance of the calibrated Hata model for Sub-Urban area will be:

Table 5.12 Performance of Tuned Hata model for Sub-Urban area

RMSE	MAPE	MAE	SD
5.18	3.63	4.63	2.76

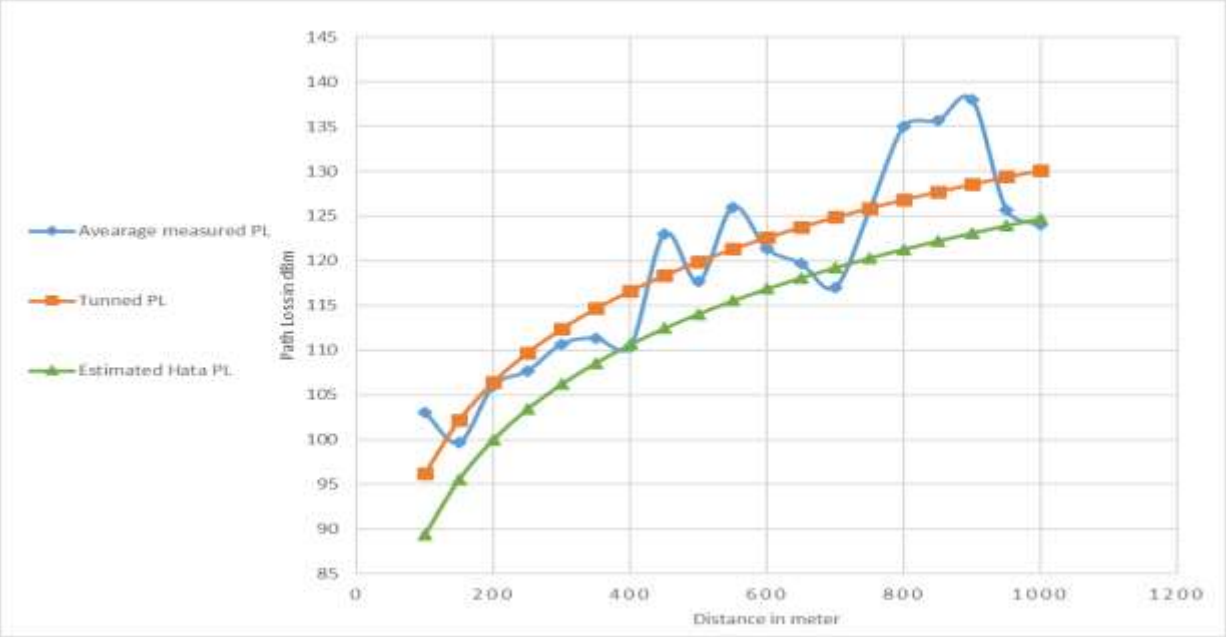

Figure 5.12 Sub-Urban Area Calibrated Hata model Vs measured PL and original Hata (1800)

The above figure shows the comparison of Sub-Urban area tuned path loss model characteristics versus selected sites averaged path loss characteristics and Hata (Sub-Urban area best fit model) path loss characteristics at 1800 Mhz. And as shown in the graphs trend the tuned path loss model is closer to the measured Path Loss than the original model, which means it can estimate hawassa's Sub-Urban areas propagation environment (at 1800 MHz) better than the original model, and it have also optimized the sinusoidal feature of the averaged measured path loss model to linearly increasing path loss versus distance. Therefore, we can say that calibrated Hata model can finely represent Sub-Urban area types of Hawassa city.

5.4.2 Correction Factors and Parameters after Calibration for 2100 MHz

The following tables shows the calibrated parameters of the models based on the calculations presented in the appendix and the RMSE values of the optimized models.

For Urban area types:

Table 5.13 Tuned parameters of ECC-33 model for Urban area

C1	Tuned slope value of A_{bm},C2	Tuned offset value of A_{bm},K1	K2
135.063	34.38	0.808	14.38

Then, the calibrated ECC-33 model equation for Urban area types will be:

$$PL_{ECC-33} = A_{fS} + \widetilde{A_{bm}} - G_b - G_r \quad (5.25)$$

where,

$$A_{fS} = 92.4 + 20\log_{10} d + 20\log_{10} f \quad (5.26)$$

$$\widetilde{A_{bm}} = 0.81 + 14.38\log_{10} d + 7.894\log_{10} f + 9.56[\log_{10} f]^2 \quad (5.27)$$

$$G_b = \log_{10}(\frac{h_b}{200})\{13.958 + 5.8[\log_{10} d]^2\} \quad (5.28)$$

$$G_r = 0.759h_r - 1.862 \quad (5.29)$$

The performance of the calibrated ECC-33 model for Urban area will be:

Table 5.14 Performance of Tuned ECC-33 after for urban area

RMSE	MAPE	MAE	SD
5.28	3.09	4.78	3.83

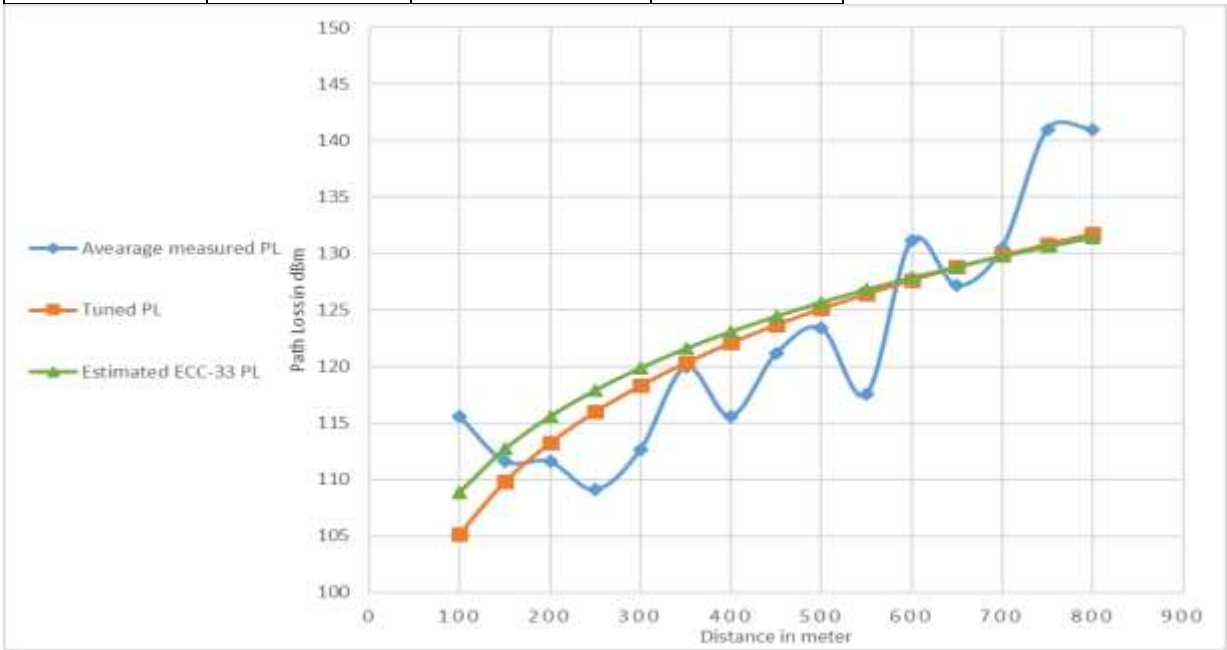

Figure 5.13 Urban area Calibrated ECC-33 model Vs measured PL and original ECC-33 (2100)

Similarly, the above figure shows the comparison of Urban area tuned path loss model characteristics versus selected sites averaged path loss characteristics and ECC-33 (Urban area best fit model) path loss characteristics at 2100 Mhz. And as shown in the graphs trend the tuned path loss model is closer to the measured Path Loss than the original model, which means it can estimate hawassa's Urban areas propagation environment (at 2100 MHz) better than the original model, and it have also optimized the sinusoidal feature of the averaged measured path loss model to linearly increasing path loss versus distance. Therefore, we can say that calibrated ECC-33 model can finely represent Urban area types of Hawassa city.

For Sub-Urban area types:

Table 5.15 Tuned parameters of Hata model for Sub-Urban areas

Tuned parameter $\tilde{a}$	Tuned parameter $\tilde{b}$	Esys	Bsys	Original Eo	Tuned Eo	Slope Correction factor, $\widetilde{B_{sys}}$
129.419	31.796	84.557	34.954		44.862	0.91

Then, the calibrated Hata model equation for Sub-Urban area types will be:

$$\mathbf{PL_{Hata} = 44.86 + 33.9\log_{10} f - 13.82\log_{10} h_b - a_{hm} + (40.84 - 5.96\log_{10} h_b)\log_{10} d - 2\left[\log_{10}\left(\frac{f}{28}\right)\right]^2} \quad (5.30)$$

Where,

$$a_{hm} = (1.1\log_{10} f - 0.7)h_m - (1.56\log_{10} f - 0.8) \quad (5.31)$$

The performance of the calibrated Hata model for Sub-Urban area will be:

Table 5.16 Performance of Tuned Hata model for Sub-Urban area

RMSE	MAPE	MAE	SD
2.86	1.79	2.63	2.04

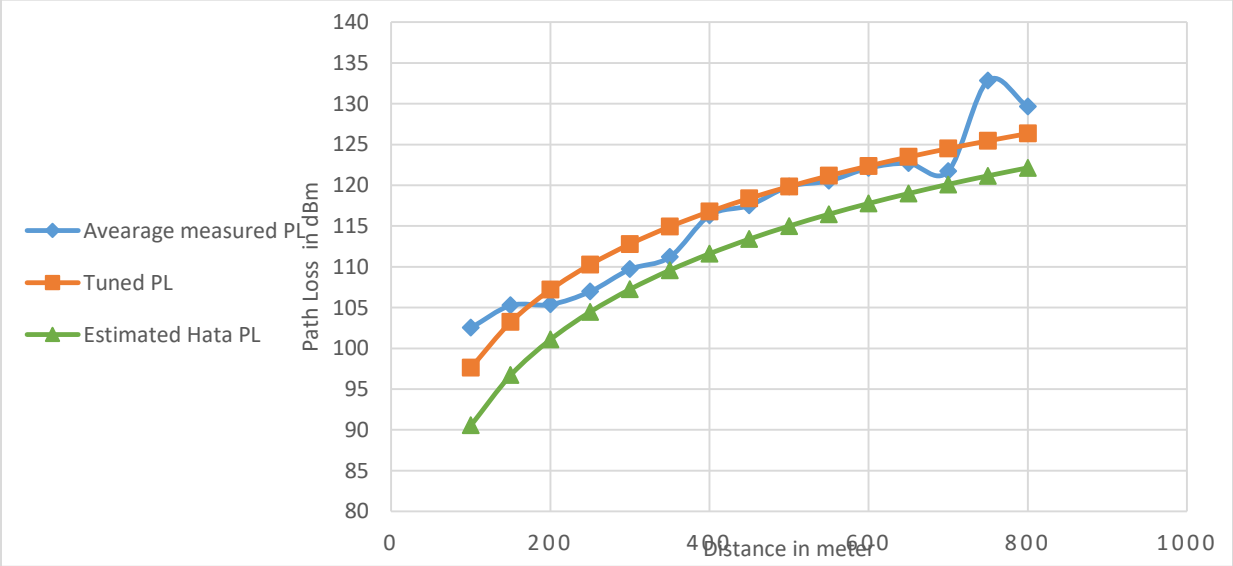

Figure 5.14 Sub-Urban Area Calibrated Hata model Vs measured PL and original Hata (2100)

The above figure also shows the comparison of Sub-Urban area tuned path loss model characteristics versus selected sites averaged path loss characteristics and Hata (Urban area best fit model) path loss characteristics at 2100 Mhz. And shown in the graphs trend the tuned path loss model is closer to the measured Path Loss than the original model, which means it can estimate hawassa's Sub-Urban areas propagation environment (at 2100 MHz) better than the original model, and it have also optimized the sinusoidal feature of the averaged measured path loss model to linearly increasing path loss versus distance. Therefore, we can say that calibrated Hata model can finely represent Urban area types of Hawassa city.

Chapter Six

6. Conclusion

As described in the abstract part, the goal of this Thesis was to compare the performance of five empirical path loss models named COST-231, ECC-33, Hata, SUI, and Ericsson models for different selected areas of Hawassa city at 1800 and 2100 MHz and tune the best performing models so that they could fit the terrain, propagation medium and environmental aspects of the city. The performance analysis was done based on the measured path loss data and theoretically calculated values. Data was collected from 14 selected sites which nearly represent all area types (Urban, Sub-Urban and Rural) in Hawassa city. The four error measuring tools, RMSE, MAPE, SUI and MAE, were implemented to measure the error between predicted path loss values and the measured values. After the performance investigation Least Square Algorithm was used to tune the best fit models. Based upon the investigation done, the following results are obtained.

At 1800 MHz, ECC-33 performed best under 10 sites out of 11 sites which classified as Urban area type. This means in 91% sites with Urban area type behavior ECC-33 was found to be the best. This was again confirmed by calculating the average measured path loss of both area types and evaluating it against all path loss models, again ECC-33 scores the list RMSE value which is 4.18 db. And calibrating the model improved the RMSE from 4.18 to 2.46 dB. Whereas, Hata path loss model was found to be the best fit model in Sub-Urban areas by performing best in 2 sites out of 3 sites categorized as Sub-Urban. And when the average measured path loss value was evaluated, Hata model again found to be the best fit model in Sub-Urban sites by scoring minimum RMSE value of 7.86. And calibrating the model improved the RMSE from 7.86 to 5.18 dB.

At 2100 MHz, ECC-33 path loss model once again performed best under 2 sites out of 2 sites classified as Urban area type. This means in 100% sites with Urban area type behavior ECC-33 was found to be the best. This was again evaluated by calculating the average measured path loss of both area types and evaluating it against all path loss models, again ECC-33 scores the list RMSE value which is 6.15 dB. And tuning the model improved the RMSE from 6.15 to 5.28 dB. Whereas, Hata path loss model was found to be the best fit model in Sub-Urban areas by

performing best in 11 sites out of 11 sites categorized as Sub-Urban. And when the average measured path loss value was calculated, Hata path loss model was again found to be the best fit model in Sub-Urban sites by scoring minimum RMSE value of 6.11. And calibrating the model improved the RMSE from 6.11 to 2.86 dB.

Therefore, at the end of this Thesis I have established that at 1800 MHz ECC-33 is the most suitable path loss model in Urban area type sites. And Hata path loss model best represent Sub-Urban area type sites. Similarly, at 2100 Mhz ECC-33 is the most suitable path loss model in Urban area type sites once and Hata path loss model is the best path loss model for Sub-Urban areas.

Appendix A

Tuning SUI model

$$PL_{SUI} = A + 10\gamma \log_{10}(\frac{d}{d_o}) + X_f + X_h + s \text{ for } d > d_o \quad (1)$$

Where,

$$A = 20 \log_{10}(\frac{4\pi d_o}{\lambda}) \quad (2)$$

$$\gamma = a - bh_b + \frac{c}{h_b} \quad (3)$$

$$X_f = 6 \log_{10}(\frac{f}{2000}) \quad (4)$$

and

$$X_h = -10.8 \log_{10}(\frac{h_r}{2000}) \text{ for Terrain types A and B} \quad (5)$$

$$X_h = -20 \log_{10}(\frac{h_r}{2000}) \quad \text{for Terrain Type C} \quad (6)$$

d is the distant between the AP and MS in meters, $d_o = 100m$, s is a log normally distributed factor (8.2 dB and 10.6dB), h_r is the mobile station height and h_b is the base station height (10 m and 80 m).

We can rewrite the equation as:

$PL_{SUI} = k_1 + k_2 B$

Where, $k_1 = A + X_f + X_h + s$

$k_2 = \gamma$

$B = 10 \log_{10}(\frac{d}{d_o})$

Since the basic principle of LLSM is to reduce the difference between the measured and estimated data in a way of mean square error, the partial differentials of the below error function have to be zero. Where y is the measured path loss.

$$E(k_1, k_2) = \sum_1^n [y_i - PL_{SUI} i(k1, k2)]^2 \quad (7)$$

Which means:

$\frac{\partial E}{\partial k1} = 0$ and $\frac{\partial E}{\partial k2} = 0$

The partial differential of error function with respect to parameter k1 will be

$\frac{\partial E}{\partial k1} = 0,$

$\frac{\partial}{\partial k1}(\sum_1^n [y_i - PL_{SUI}i(k1, k2)]^2) = 0$

$\sum_1^n [y_i - PL_{SUI}i]\,[0 - \frac{\partial}{\partial k1}(PL_{SUI}i(k1, k2)] = 0$

$\sum_1^n [y_i - PL_{SUI}i]\,[0 - \frac{\partial}{\partial k1}(\mathrm{k_1} + \mathrm{k_2B})] = 0$

$\sum_1^n [y_i - PL_{SUI}i]\,[-1] = 0$

$nk1 + k2\sum_1^n B_i = \sum_1^n y_i$ (8)

Whereas, the partial differential of error function with respect to parameter k2 will be

$\frac{\partial E}{\partial k2} = 0,$

$\frac{\partial}{\partial k2}(\sum_1^n [y_i - PL_{SUI}i(k1, k2)]^2) = 0$

$\sum_1^n [y_i - PL_{SUI}i]\,[0 - \frac{\partial}{\partial k2}(PL_{SUI}i(k1, k2)] = 0$

$\sum_1^n [y_i - PL_{SUI}i]\,[0 - \frac{\partial}{\partial k2}(\mathrm{k_1} + \mathrm{k_2B_i})] = 0$

$\sum_1^n [y_i - PL_{SUI}i]\,[-\mathrm{B_i}] = 0$

$\sum_1^n [y_i - \mathrm{k_1} - \mathrm{k_2B_i}][-\mathrm{B_i}] = 0 = \sum_1^n [y_i\mathrm{B_i} - \mathrm{k_1B_i} - \mathrm{k_2B_i}^2]$

$\sum_1^n y_i\mathrm{B_i} - k1\sum_1^n \mathrm{B_i} - k2\sum_1^n \mathrm{B_i}^2 = 0$ (9)

From equation

$k1 = \frac{1}{n}(\sum_1^n y_i - k2\sum_1^n B_i)$ (10)

Replacing equation 10 into equation 9 we will get

$\sum_1^n y_i\mathrm{B_i} - (\frac{1}{n}(\sum_1^n y_i - k2\sum_1^n B_i))\sum_1^n \mathrm{B_i} - k2\sum_1^n \mathrm{B_i}^2 = 0$

$$\sum_1^n y_i \mathrm{B}_i - \frac{1}{n}\left(\sum_1^n y_i \sum_1^n \mathrm{B}_i\right) + \frac{k2}{n}\left(\sum_1^n B_i\right)^2 - k2\sum_1^n {\mathrm{B}_i}^2 = 0$$

$$k2\left(\frac{1}{n}\left(\sum_1^n B_i\right)^2 - \sum_1^n {\mathrm{B}_i}^2\right) = \frac{1}{n}\left(\sum_1^n y_i \sum_1^n \mathrm{B}_i\right) - \sum_1^n y_i \mathrm{B}_i$$

$$k2 = \frac{\left(\sum_1^n y_i \sum_1^n \mathrm{B}_i\right) - n\sum_1^n y_i \mathrm{B}_i}{\left(\sum_1^n B_i\right)^2 - n\sum_1^n {\mathrm{B}_i}^2} \tag{11}$$

Then, k1 will be calculated by inserting equation 11 into equation 10

$$k1 = \frac{1}{n}\left(\sum_1^n y_i - \left(\frac{\left(\sum_1^n y_i \sum_1^n \mathrm{B}_i\right) - n\sum_1^n y_i \mathrm{B}_i}{\left(\sum_1^n B_i\right)^2 - n\sum_1^n {\mathrm{B}_i}^2}\right)\sum_1^n B_i\right)$$

$$k1 = \frac{\frac{1}{n}\sum_1^n y_i \left(\sum_1^n B_i\right)^2 - \sum_1^n {\mathrm{B}_i}^2 \sum_1^n y_i - \frac{1}{n}\left(\sum_1^n y_i \left(\sum_1^n \mathrm{B}_i\right)^2\right) + \sum_1^n y_i \mathrm{B}_i \sum_1^n B_i)}{\left(\sum_1^n B_i\right)^2 - n\sum_1^n {\mathrm{B}_i}^2}$$

$$k1 = \frac{\sum_1^n y_i \mathrm{B}_i \sum_1^n B_i) - \sum_1^n {\mathrm{B}_i}^2 \sum_1^n y_i}{\left(\sum_1^n B_i\right)^2 - n\sum_1^n {\mathrm{B}_i}^2} \tag{12}$$

Appendix B

Tuning ECC-33

$$PL_{ECC-33} = A_{fS} + A_{bm} - G_b - G_r \quad (13)$$

where, A_{fS}, A_{bm} , G_b and G_r are free space attenuation, basic median path loss, BS height gain factor and receiver height gain factor.

$$A_{fS} = 92.4 + 20\log_{10} d + 20\log_{10} f \quad (14)$$

$$A_{bm} = 20.41 + 9.83\log_{10} d + 7.894\log_{10} f + 9.56[\log_{10} f]^2 \quad (15)$$

$$G_b = \log_{10}(\frac{h_b}{200})\{13.958 + 5.8[\log_{10} d]^2\} \quad (16)$$

for medium city environments.

$$G_r = [42.57 + 13.7\log_{10} f][\log_{10} h_r - 0.585] \quad (17)$$

and for the large city.

$$G_r = 0.759h_r - 1.862 \quad (18)$$

where, f is the frequency in GHz, d is the distant between BS and MS antenna in km, h_b is the BS antenna height in meters and h_r is the MS antenna height in meters.

We can rewrite equation 1 as:

$$PL_{ECC-33} = c1 + c2\log_{10} d + c3\,(\log_{10} d)^2$$

$PL_{ECC-33} = c1 + c2x_i + c3(x_i)^2$,where $x_i = \log_{10} d_i$

Where, $c1 = 92.4 + 20\log_{10} f + 20.41 + 7.894\log_{10} f + 9.56[\log_{10} f]^2 - 13.958\log_{10}(\frac{h_b}{200}) - 0.759h_r + 1.862 + k1$. k1 is the tuned offset value of A_{bm}.

$c2 = k2 + 20$, the tuned slope value of the d-term in A_{bm}.

$c3 = -5.8\log_{10}(\frac{h_b}{200})$

Then, the minimum error can be calculated by setting the following error function to zero.

$$E\ (c_1, c_2) = \sum_1^n [y_i - PL_{ECC} i(k1, k2)]^2 \quad (19)$$

Which means:

$\frac{\partial E}{\partial c1} = 0$ and $\frac{\partial E}{\partial c2} = 0$

The partial differential of error function with respect to parameter c1 will be

$\frac{\partial E}{\partial c1} = 0,$

$\frac{\partial}{\partial c1}(\sum_1^n [y_i - c1 - c2x_i - c3(x_i)^2]^2) = 0$

$\sum_1^n [y_i - c1 - c2x_i - c3(x_i)^2]\,[-1] = 0$

$nc1 + c2\sum_1^n x_i = \sum_1^n y_i - c3\sum_1^n (x_i)^2$

$c1 = \frac{1}{n}\sum_1^n y_i - \frac{c2}{n}\sum_1^n x_i - \frac{c3}{n}\sum_1^n (x_i)^2 \quad (20)$

The partial differential of error function with respect to parameter c2 will be

$\frac{\partial E}{\partial c2} = 0,$

$\frac{\partial}{\partial c2}(\sum_1^n [y_i - c1 - c2x_i - c3(x_i)^2]^2) = 0$

$\sum_1^n [y_i - c1 - c2x_i - c3(x_i)^2][-x_i] = 0$

$\sum_1^n y_i\, x_i - c1\sum_1^n x_i - c2\sum_1^n (x_i)^2 - c3\sum_1^n (x_i)^3 = 0$

$c1\sum_1^n x_i + c2\sum_1^n (x_i)^2 = \sum_1^n y_i\, x_i - c3\sum_1^n (x_i)^3 \quad (21)$

Inserting equation 20 into equation 21

$\frac{1}{n}\sum_1^n y_i \sum_1^n x_i - \frac{c2}{n}(\sum_1^n x_i)^2 - \frac{c3}{n}\sum_1^n x_i \sum_1^n (x_i)^2 + c2\sum_1^n (x_i)^2 = \sum_1^n y_i\, x_i - c3\sum_1^n (x_i)^3$

$c2\left[\sum_1^n (x_i)^2 - \frac{1}{n}(\sum_1^n x_i)^2\right] = \frac{c3}{n}\sum_1^n x_i \sum_1^n (x_i)^2 + \sum_1^n y_i\, x_i - c3\sum_1^n (x_i)^3 - \frac{1}{n}\sum_1^n y_i \sum_1^n x_i$

$c2 = \frac{c3\sum_1^n x_i \sum_1^n (x_i)^2 + n\sum_1^n y_i x_i - nc3\sum_1^n (x_i)^3 - \sum_1^n y_i \sum_1^n x_i}{n\sum_1^n (x_i)^2 - (\sum_1^n x_i)^2} \quad (22)$

$$c1 = \frac{1}{n}\sum_1^n y_i - \frac{\frac{c3\sum_1^n x_i \sum_1^n (x_i)^2 + n\sum_1^n y_i x_i - nc3\sum_1^n (x_i)^3 - \sum_1^n y_i \sum_1^n x_i}{n\sum_1^n (x_i)^2 - \left(\sum_1^n x_i\right)^2}}{n}\sum_1^n x_i - \frac{c3}{n}\sum_1^n (x_i)^2$$

$$c1 = \frac{1}{n}\sum_1^n y_i - \frac{\frac{c3}{n}\sum_1^n x_i \sum_1^n (x_i)^2 + \sum_1^n y_i x_i - c3\sum_1^n (x_i)^3 - \frac{1}{n}\sum_1^n y_i \sum_1^n x_i}{n\sum_1^n (x_i)^2 - (\sum_1^n x_i)^2}\sum_1^n x_i - \frac{c3}{n}\sum_1^n (x_i)^2$$

$c1 =$

$$\frac{\sum_1^n y_i \sum_1^n (x_i)^2 - \frac{1}{n}\sum_1^n y_i (\sum_1^n x_i)^2 - \frac{c3}{n}(\sum_1^n x_i)^2 \sum_1^n (x_i)^2 - \sum_1^n x_i \sum_1^n y_i x_i + c3\sum_1^n x_i \sum_1^n (x_i)^3 + \frac{1}{n}\sum_1^n y_i (\sum_1^n x_i)^2 - c3(\sum_1^n (x_i)^2)^2 + \frac{c3}{n}\sum_1^n (x_i)^2 (\sum_1^n x_i)^2}{n\sum_1^n (x_i)^2 - (\sum_1^n x_i)^2}$$

$$\boldsymbol{c1 = \frac{n\sum_1^n y_i \sum_1^n (x_i)^2 - c3(\sum_1^n x_i)^2 \sum_1^n (x_i)^2 - n\sum_1^n x_i \sum_1^n y_i x_i + nc3\sum_1^n x_i \sum_1^n (x_i)^3 - nc3(\sum_1^n (x_i)^2)^2 + c3\sum_1^n (x_i)^2 (\sum_1^n x_i)^2}{n^2\sum_1^n (x_i)^2 - n(\sum_1^n x_i)^2}} \quad (23)$$

Appendix C

Tuning Hata model

$$PL_{Hata} = A + B\log_{10} f - 13.82\log_{10} h_b - a_{hm} + (44.9 - 6.55\log_{10} h_b)\log_{10} d \quad (24)$$

Where: - f is the frequency (MHz). h_b is BS antenna height (m), h_b is the MS antenna height (m), a_{hm} is the MS antenna correction factor d is the distant between the BTS and MS (km). The correction factor for the MS antenna height is represented as follows, for a small or medium sized city:

$$a_{hm} = (1.1\log_{10} f - 0.7)h_m - (1.56\log_{10} f - 0.8) \quad (25)$$

and for large city:

$a_{hm} =$

$$8.29\,(\log_{10} 1.54h_m)^2 - 1.1 \quad \text{for } f < 200 \text{ MHz} \quad (26)$$

$$3.2\,(\log_{10} 11.75h_m)^2 - 4.97 \quad \text{for } f \geq 400 \text{ MHz} \quad (27)$$

The parameters A and B are dependent on the frequency as follows:

A= 69.55 $150 < f < 1500$ MHz (28)

46.30 $1500 < f < 2000$ MHz (29)

B= 26.16 $150 < f < 1500$ MHz (30)

33.9 $1500 < f < 2000$ MHz (31)

For sub urban area

$$PL_{Hata} = PL_{Urban} - 2\,[\log_{10}(\tfrac{f}{28})]^2 - 5.4 \quad (32)$$

For rural areas

$$L = L_{urban} - 4.78\,[\log_{10}(\tfrac{f}{28})]^2 + 18.33\log_{10} f - 40.94 \quad (33)$$

Now for urban areas we can rearrange the urban path loss formula as follows.

$E_0 = A$

$E_{sys} = B \log_{10} f - 13.82 \log_{10} h_b - a_{hm}$

$B_{sys} = 44.9 - 6.55 (\log_{10} h_b)$

And for Sub-urban areas we can rearrange the sub-urban path loss formula as follows.

$E_0 = A - 5.4$

$E_{sys} = B \log_{10} f - 13.82 \log_{10} h_b - a_{hm} - 2 [\log_{10}(\frac{f}{28})]^2$

$B_{sys} = 44.9 - 6.55 (\log_{10} h_b)$

Where, E_0 is Initial offset parameter, E_{sys} is Initial system design parameter and B_{sys} is the slope of the model curve.

We can then write the total Hata path loss as:

$P_L(Hata) = E_0 + E_{sys} + B_{sys} \log_{10} d$

The Above equation can be written as:

$P_{L\,pridicted}(Hata) = a + bx$

Where,

$a = E_0 + E_{sys}$

$b = B_{sys}$

$x = \log_{10} d$, a simplified logarithmic base

Then, the minimum error can be calculated by setting the partial differentials of the following error function to zero.

$E\ (a, b, c, \dots) = \sum_1^n [y_i - PL_{Hata} i(x_i, a, b, c)]^2$ (33)

Which means:

$\frac{\partial E}{\partial a} = 0, \quad \frac{\partial E}{\partial b} = 0, \quad \frac{\partial E}{\partial c} = 0$

The partial differential of error function with respect to parameter a will be

$\frac{\partial E}{\partial a} = 0,$

$\frac{\partial}{\partial a}(\sum_1^n [y_i - (a + bx_i)]^2) = 0$

$\sum_1^n [y_i - (a + bx_i)][0 - \frac{\partial}{\partial a}(a + bx_i)] = 0$

$\sum_1^n [y_i - (a + bx_i)][0 - 1] = 0$

$na + b\sum_1^n x_i = \sum_1^n y_i$

And from this equation 'a' can be expressed in terms of 'b' as the following:

$na = \sum_1^n y_i - b\sum_1^n x_i$

$$a = \frac{\sum_1^n y_i - b\sum_1^n x_i}{n} \quad (34)$$

The partial differential of error function with respect to parameter a will be

$\frac{\partial E}{\partial b} = 0,$

$\frac{\partial}{\partial b}(\sum_1^n [y_i - (a + bx_i)]^2) = 0$

$\sum_1^n [y_i - (a + bx_i)][0 - \frac{\partial}{\partial b}(a + bx_i)] = 0$

$\sum_1^n [y_i - (a + bx_i)][0 - x_i] = 0$

$a\sum_1^n x_i + b\sum_1^n (x_i)^2 = \sum_1^n y_i x_i$

And from this equation 'b' can be expressed in terms of 'a' as following:

$b\sum_1^n (x_i)^2 = \sum_1^n y_i x_i - a\sum_1^n x_i$

$$b = \frac{\sum_1^n y_i x_i - a\sum_1^n x_i}{\sum_1^n (x_i)^2} \quad (35)$$

We can find the tuned parameters $\tilde{a}$ and $\tilde{b}$ by substituting the variables a and b in equation

$$\tilde{a} = \frac{\sum_1^n (x_i)^2 . \sum_1^n y_i - \sum_1^n y_i x_i . \sum_1^n x_i}{n \sum_1^n (x_i)^2 - \left(\sum_1^n x_i\right)^2} \quad (36)$$

$$\tilde{b} = \frac{n \sum_1^n y_i x_i - \sum_1^n y_i . \sum_1^n x_i}{n \sum_1^n (x_i)^2 - \left(\sum_1^n x_i\right)^2} \quad (37)$$

Then we find the tuned Hata path loss model by substituting the tuned parameters $\tilde{a}$ and $\tilde{b}$ into the original Hata path loss model that we begin the process with

$a = E_0 + E_{sys}$

Then, E_0 becomes

$E_0 = a - E_{sys}$

Then, by replacing a with $\tilde{a}$ we can find $\widetilde{E_0}$:

$$\widetilde{E_0} = \tilde{a} - E_{sys} \quad (38)$$

And since $b = B_{sys}$ there should be a tuning factor $\widetilde{B_{sys}}$ to get $\tilde{b}$

$$\tilde{b} = \widetilde{B_{sys}} B_{sys} \quad (39)$$

$$\widetilde{B_{sys}} = \frac{\tilde{b}}{B_{sys}} \quad (40)$$

$$\widetilde{B_{sys}} = \frac{\tilde{b}}{44.9 - 6.55 \left(\log_{10} h_b\right)} \quad (41)$$

References

[1] Anthony, O. N., & Okonkwo Obikwelu, R., "Characterization of Signal Attenuation using Path loss Exponent in South-South Nigeria", International Journal of Emerging Trends & Technology in Computer Science (IJETTCS), 100-104.

[2] Andrusenko, J., Burbank, J., & Ward, J. (2009), "Modeling and simulation for RF propagation", The Jonhs Hopkins University Design & Developers Fourm IEEE Globecom.

[3] Andreas F. Molisch, "Wireless Communications, Second Edition", 2011.

[4] A.O. Akande, F.A. Semire and Z. K. Adeyemo "Performance Analysis and Optimization of Cost 231-Hata Model for Mobile Communication in Nigeria", International Journal of Computer Applications Volume 173 – No.6, September 2017.

[5] R. Mardeni and K. F. Kwan, "OPTIMIZATION OF HATA PROPAGATION PREDICTION MODEL IN SUBURBAN AREA IN MALAYSIA", Progress In Electromagnetics Research C, Vol. 13, 91–106, 2010.

[6] "Propagation path loss model for great Tripoli area for Almadar mobile network in frequency bands (900-1800-2100) MHz"

[7] Esayas Andarge, "Comparison and Fine Tuning Empirical Path loss Models at 1800MHZ and 2100MHZ Bands for Addis Ababa, Ethiopia" October, 2018. Chhaya Dalela, M V S N Prasad, P K Dalela "Tuning of COST-231 Hata model for Radio Wave Propagation Prediction"

[8] H. K. Hoomod, I. Al-Mejibli and A. I. Jabboory "Analyzing Study of Path Loss Propagation Models in Wireless Communications at 0.8 GHz", IOP Conf. Series: Journal of Physics: Conf. Series 1003 (2018) 012028.

[9] Michael S. Mollel Dr. Michael Kisangiri "Comparison of Empirical Propagation Path Loss Models for Mobile Communication", Computer Engineering and Intelligent Systems ISSN 2222-2863 (Online) Vol.5, No.9, 2014.

[10] Sujeet Kumar Jha ,Rupa Rokaya, Amit Bhagat ,Ahmed Raja Khan ,Laxman Aryal, "LTE NETWORK : COVERAGE AND CAPACITY PLANNING 4G cellular Network planning around Banepa", IEEE, 2017.

[11] Azar Taufique, Mona Jaber, Ali Imran, Zaher Dawy, Elias Yacoub, “Planning Wireless Cellular Networks of Future: Outlook, Challenges and Opportunities”, IEEE, 2017.

[12] “The High Level Design for RF LOT1 Addis Ababa Swap and Build” ethiotelecom, 2013.

[13] Florian Letourneux, Sylvain Guivarch, Yves Lostanlen “Propagation Models for Heterogeneous Networks”,7th European conference on antennas and propagation (EUCAP 2013).

[14] “Ericsson Ethiopia Physical data 10.38” ethiotelecom,2015.

[15] T.S Rappaport, Wireless communications –Principles and practice, 2nd Edition, Prentice Hall, 2001.

[16] I. SIMI, I. STANI, and B. ZIRNI, “Minimax LS Algorithm for Automatic Propagation Model Tuning”, in Proceeding of the 9th Telecommunications Forum (TELFOR 2001), Belgrade, 2001.

[17] Y. Okumura, E. Ohmori, T. Kawano, and K. Fukuda, “Field strength and its variability in VHF and UHF land-mobile radio service," Rev. Elec. Commun. Lab, vol. 16, pp. 825-73, 1968.

[18] S. R. Saunders, "Antennas and propagation for wireless communication systems, 1999," ed: John Wiley & Sons Ltd, England.

[19] Isabona Joseph1, Konyeha. C.C2, “Urban Area Path loss Propagation Prediction and Optimisation Using Hata Model at 800MHz”, IOSR Journal of Applied Physics (IOSR-JAP) e-ISSN: 2278-4861. Volume 3, Issue 4 (Mar. - Apr. 2013), PP 08-18

[20] Kaveh Pahlavan; Prashant Krishnamurthy, *Principles of Wireless Networks: A Unified Approach*, Illustrate. New Jersey: Prentice Hall PTR, 2002 - Technology & Engineering, 2002.

[21] Simon R. Saunders and Alejandro Aragon Zavala,” Antenna and Propagation for Wireless Communication Systems, Second Edition”, Wiley, 2007

[22] Rhattoy, A. and A. Zatni, “The Impact of Radio Propagation Models on Ad Hoc Networks Performances” Journal of Computer Science 8 (5): 752-760, 2012 ISSN 1549-3636

[23] E. Ostlin, "On radio wave propagation measurments and modeling for cellular mobile radio networks," Blekinge Institute of Technology, Sweden, July 2009

[24] Raad Farhood Chisab, Member IEEE and Prof. (Dr.) C. K. Shukla, "Performance Evaluation of 4G-LTE-SCFDMA Scheme under SUI and ITU Channel Models" International Journal of Engineering & Technology IJET-IJENS Vol:14 No:01

[25] Joydeep Banerjee, Swarup Kumar Mitra, and Mrinal Kanti naskar, "Comparative Study of Radio Models for data Gathering in Wireless Sensor Network" International Journal of Computer Applications (0975 – 8887) Volume 27– No.4, August 2011